



## ANALYTICAL METHODOLOGIES BASED ON CHEMOMETRICS TO OPTIMIZE THE PHOTODEGRADATION OF DYES

Cristina Fernández Barrat

Dipòsit Legal: T. 160-2012

**ADVERTIMENT.** La consulta d'aquesta tesi queda condicionada a l'acceptació de les següents condicions d'ús: La difusió d'aquesta tesi per mitjà del servei TDX ([www.tesisenxarxa.net](http://www.tesisenxarxa.net)) ha estat autoritzada pels titulars dels drets de propietat intel·lectual únicament per a usos privats emmarcats en activitats d'investigació i docència. No s'autoritza la seva reproducció amb finalitats de lucre ni la seva difusió i posada a disposició des d'un lloc aliè al servei TDX. No s'autoritza la presentació del seu contingut en una finestra o marc aliè a TDX (framing). Aquesta reserva de drets afecta tant al resum de presentació de la tesi com als seus continguts. En la utilització o cita de parts de la tesi és obligat indicar el nom de la persona autora.

**ADVERTENCIA.** La consulta de esta tesis queda condicionada a la aceptación de las siguientes condiciones de uso: La difusión de esta tesis por medio del servicio TDR ([www.tesisenred.net](http://www.tesisenred.net)) ha sido autorizada por los titulares de los derechos de propiedad intelectual únicamente para usos privados enmarcados en actividades de investigación y docencia. No se autoriza su reproducción con finalidades de lucro ni su difusión y puesta a disposición desde un sitio ajeno al servicio TDR. No se autoriza la presentación de su contenido en una ventana o marco ajeno a TDR (framing). Esta reserva de derechos afecta tanto al resumen de presentación de la tesis como a sus contenidos. En la utilización o cita de partes de la tesis es obligado indicar el nombre de la persona autora.

**WARNING.** On having consulted this thesis you're accepting the following use conditions: Spreading this thesis by the TDX ([www.tesisenxarxa.net](http://www.tesisenxarxa.net)) service has been authorized by the titular of the intellectual property rights only for private uses placed in investigation and teaching activities. Reproduction with lucrative aims is not authorized neither its spreading and availability from a site foreign to the TDX service. Introducing its content in a window or frame foreign to the TDX service is not authorized (framing). This rights affect to the presentation summary of the thesis as well as to its contents. In the using or citation of parts of the thesis it's obliged to indicate the name of the author.

# **Analytical methodologies based on chemometrics to optimize the photodegradation of dyes**

Doctoral Thesis



UNIVERSITAT ROVIRA I VIRGILI

UNIVERSITAT ROVIRA I VIRGILI

ANALYTICAL METHODOLOGIES BASED ON CHEMOMETRICS TO OPTIMIZE THE PHOTODEGRADATION OF DYES

Cristina Fernández Barrat

DL:T. 160-2012

UNIVERSITAT ROVIRA I VIRGILI

Department of Analytical Chemistry and Organic Chemistry

Analytical methodologies based on  
chemometrics to optimize the  
photodegradation of dyes

**CRISTINA FERNÁNDEZ BARRAT**

Doctoral Thesis

Supervisors

Prof. María Pilar Callao Lasmarías

Prof. María Soledad Larrechi García

Tarragona, 2011

UNIVERSITAT ROVIRA I VIRGILI

ANALYTICAL METHODOLOGIES BASED ON CHEMOMETRICS TO OPTIMIZE THE PHOTODEGRADATION OF DYES

Cristina Fernández Barrat

DL:T. 160-2012



UNIVERSITAT  
ROVIRA I VIRGILI

DEPARTAMENT DE QUÍMICA ANALÍTICA  
I QUÍMICA ORGÀNICA

Campus Sescelades  
C/ Marcel·lí Domingo, s/n  
43007 Tarragona  
Tel. 34 977 55 97 69  
Fax 34 977 55 84 46  
e-mail: secqaqo@quimica.urv.cat

Dr. MARÍA PILAR CALLAO LASMARÍAS and Dr. MARÍA SOLEDAD LARRECHI GARCÍA, Professors of the Department of Analytical Chemistry and Organic Chemistry at the Universitat Rovira i Virgili,

CERTIFY:

The Doctoral Thesis entitled: "**Analytical methodologies based on chemometrics to optimize the photodegradation of dyes**" presented by CRISTINA FERNÁNDEZ BARRAT to receive the degree of Doctor of the Universitat Rovira i Virgili, has been carried out under our supervision, in the Department of Analytical Chemistry and Organic Chemistry at the Universitat Rovira i Virgili, and all the results presented in this thesis were obtained in experiments conducted by the above mentioned student.

Tarragona, November 2011

Dr. María Pilar Callao Lasmarías

Dr. María Soledad Larrechi García

UNIVERSITAT ROVIRA I VIRGILI

ANALYTICAL METHODOLOGIES BASED ON CHEMOMETRICS TO OPTIMIZE THE PHOTODEGRADATION OF DYES

Cristina Fernández Barrat

DL:T. 160-2012

Aquesta tesi representa el final d'una etapa de la meua vida que de ben segur, sigui quin sigui el camí que m'espera a partir d'ara, sempre em portarà molt bons records. Es tracta d'una etapa en què he crescut moltíssim personalment i professionalment. Durant tot aquest temps he conegut molta gent i de tots m'emporto alguna cosa. Gràcies perquè entre tots heu donat color a la tesi i a la meua vida.

Res del que es mostra en aquesta tesi no hauria estat possible sense l'esforç i, en especial, la confiança que van dipositar en mi ara fa quatre anys les meues directores de tesi: la Pilar Callao i la Marisol Larrechi, que no han deixat d'escoltar-me, ajudar-me i aconsellar-me en tot aquest temps.

Tampoc no em podria oblidar dels membres del grup de Quimiometria, Qualimetria i Nanosensors (F. Xavier Rius, Itziar Ruisánchez, Joan Ferré, Ricard Boqué, Jordi Riu...); ni de tots els companys doctorands que hi han passat, des de la Vero, que va introduir-me en el "meravellós" món de la quimiometria, fins a la Carolina, la Idoia i la Maribel, que m'han acompanyat durant la darrera etapa. També vull agrair, entre d'altres, al Santi, al Jaume, a la Tere i a l'Eulàlia el seu ajut i la seva predisposició a l'hora de solucionar problemes tècnics.

Durant aquests quatre anys he tingut la gran sort —i això és una de les altres coses que agrairé sempre a la Pilar i a la Marisol— de poder fer dues estades a llocs que m'han robat un trosset de cor, on he deixat bons amics i on he après moltíssimes coses a nivell professional i personal. La primera va tenir lloc a la Universitat de les Illes Balears, amb el Dr. Víctor Cerdà i el Dr. Rafel Forteza del grup de Química Analítica, Automatització i Medi Ambient, on tothom em va acollir i ajudar dins i fora del laboratori. María, Mailen, Ruth, Jessi, Irene, Ferni..., gràcies per tots els bons moments que m'heu regalat. Arran d'aquest viatge també vaig poder conèixer el Martí, que va ser la primera persona que vaig trobar quan l'avió va aterrar a Mallorca. Des d'aleshores mai no ha deixat de ser al meu costat.

En el marc de la meua segona estada, a la University of Copenhagen, he d'agradir al Dr. Rasmus Bro, al Jose i als companys que m'hagin fet sentir com a casa a més de dos mil quilòmetres de la meua pròpia. A més a més, durant aquests mesos vaig tenir la sort de coincidir amb el Dr. Santi MasPOCH, a qui també agraeixo el seu suport i els seus consells.



*Jeg vil gerne takke Dr. Rasmus Bro for at muliggøre mit ophold hos Kvalitet og Teknologi gruppen. Eskerrik asko Jose, por los conocimientos de Matlab, quimiometría y otras cosas, además de por tu capacidad para estresarme. I want to thank also my "danish" friends Maider, Sanni, Daniela, Gözde, Helene... for their friendship and for helping me in the difficult moments. Gracias a Eva por el apoyo moral y a Carlos por dejarse conocer en Copenhague.*

Desitjo agrair a l'Anna de Juan la seva predisposició a l'hora de col·laborar amb nosaltres, la seva eficiència i les seves grans qualitats humanes.

No em puc oblidar de tota la gent que m'acompanya fora del laboratori i que em dona suport i m'ànima, tot i no entendre gaire bé el que faig: la Sílvia, la Gem, la Neus, la Patri, la Laura, la Gemma..., la Lucy, que ja ha encetat aquest camí, i la Maria, que espero que algun dia ho faci —estic convençuda que serà una gran investigadora. També vull recordar aquí els que m'entenen i han patit com jo l'última etapa d'aquest camí: l'Eduard, la Irene, la Mireia i la Dolores. Gràcies a tots.

Per a qui no tinc paraules és per a les dues persones que han estat els pilars de la meua vida durant aquest temps i que espero que continuïn sent-ho, tot i saber que potser serà complicat: el Xavi i l'Eugènia. Tant de bo us pugui tenir sempre al meu costat. Gràcies per fer-me créixer. Xaf, fa vuit anys que compartim camí i experiències i en tot aquest temps no podria dir ni una sola cosa dolenta de tu. Sempre m'has ajudat, donat suport, animat..., malgrat que no sempre ha estat fàcil. Segurament per tot això ets molt més que un amic. Eugen, des del dia que et vaig conèixer res no ha tornat a ser el mateix. Gràcies per donar color a la meua vida fora de la universitat, pels bons i no tan bons moments, les excursions, els viatges, la paciència, el suport constant, els ànims, la confiança..., per tot.

Finalment vull donar les gràcies a la meua família, sense la qual tampoc no podria haver arribat fins aquí: a mon pare, als meus avis, als meus tiets, al Jordi, a l'Íngrid i sobretot a ma mare, a qui dedico aquesta tesi pel seu constant exemple d'humor, força i superació davant totes les adversitats.

Don't lose your grip on the dreams of the past  
You must fight just to keep them alive.

**Eye of the tiger – Survivor**

UNIVERSITAT ROVIRA I VIRGILI

ANALYTICAL METHODOLOGIES BASED ON CHEMOMETRICS TO OPTIMIZE THE PHOTODEGRADATION OF DYES

Cristina Fernández Barrat

DL:T. 160-2012

## TABLE OF CONTENTS

<b>Chapter 1.</b> Introduction and objectives	13
1.1. Introduction	15
1.2. Objectives	16
1.3. Structure of the thesis	17
1.4. References	18
<b>Chapter 2.</b> Theoretical aspects	19
2.1. Photodegradation	21
2.1.1. Photolysis	21
2.1.2. Heterogeneous Photocatalysis	22
2.2. Instrumental techniques	24
2.2.1. UV-visible spectroscopy	24
2.2.2. Mass spectrometry	25
2.2.3. Flow analysis and sequential injection chromatography (SIC) systems	26
2.3. Chemometric techniques	29
2.3.1. Experimental design	29
2.3.2. Multivariate data treatment	32
2.4. References	39
<b>Chapter 3.</b> Experimental part and results	41
3.1. Removing dyes	43

3.1.1. Paper. <i>An analytical overview of processes for removing organic dyes from wastewater effluents.</i> Trends Anal. Chem. 29 (2010) 1202-1211.	45
3.2. Optimization of photodegradation processes	67
3.2.1. Paper. <i>Study of the influential factors in the simultaneous photocatalytic degradation process of three textile dyes.</i> Talanta 79 (2009) 1292-1297.	69
3.2.2. Paper. <i>Modelling of the simultaneous photodegradation of Acid Red 97, Acid Orange 61 and Acid Brown 425 using factor screening and response surface strategies.</i> J. Hazard. Mater. 180 (2010) 474-480.	89
3.3. Kinetic studies	109
3.3.1. Paper. <i>Kinetic analysis of C.I. Acid Yellow 9 photooxidative decolorization by UV-visible and chemometrics.</i> J. Hazard. Mater. 190 (2011) 986-992.	111
3.3.2. Paper. <i>The evaluation of the adsorption and rate constants of the photocatalytic degradation of C.I. Acid Yellow 9 by means of HS-MCR-ALS: a study of process variables.</i> Submitted.	129
3.4. Dye determination by sequential injection chromatography (SIC)	149
3.4.1. Paper. <i>Multisyringe chromatography (MSC) using a monolithic column for the determination of sulphonated azo dyes.</i> Talanta 82 (2010) 137-142.	151
<b>Chapter 4. General conclusions</b>	169
Appendix	175



# **1. INTRODUCTION AND OBJECTIVES**

UNIVERSITAT ROVIRA I VIRGILI

ANALYTICAL METHODOLOGIES BASED ON CHEMOMETRICS TO OPTIMIZE THE PHOTODEGRADATION OF DYES

Cristina Fernández Barrat

DL:T. 160-2012

## 1.1. INTRODUCTION

This doctoral thesis tackles the problem of textile dyes, mainly azo dyes, being present in industrial waste and their subsequent release into the environment. It should be pointed out that dyeing is one of the most polluting industries in the world and it is estimated that almost  $10^9$  kg of dyes are produced annually, 70% of which are azo dyes [1]. As the demand for textile products has increased, the textile industry and its wastewaters have been increasing proportionally and it is now one of the main sources of severe pollution problems worldwide.

Ever since Paul T. Anastas coined the term green chemistry in 1991 (also called sustainable chemistry), considerable effort has been made in many different fields (chemistry, engineering, biotechnology, etc.) to develop processes that obey some of the 12 principles of green chemistry defined by the United States Environmental Protection Agency [2]. This philosophy encourages the design of products and chemical processes that minimize the use and generation of contaminating substances.

The experimental developments that shape this doctoral thesis are the consequence of the working hypothesis that efficient analytical methodologies can be designed and developed in accordance with the basic principles of sustainable chemistry.

The methodologies developed in this thesis are based on analytical determinations that do not require samples to be subject to any additional treatment, which means that savings can be made in such chemical products as reagents or solvents. The methodologies incorporate a variety of chemometric tools since the research was carried out in the context of a research group in chemometrics.



## 1.2. OBJECTIVES

The main objective of this thesis is to develop analytical methodologies to determine organic azo dyes present in textile industry wastewater and to look into the processes by which they can be removed. This main objective has given rise to other objectives:

- a) To prepare a critical overview of the processes that are currently available for removing organic dyes and of the most common techniques for monitoring these processes.
  
- b) To establish methodologies that use second order data treatment for the simultaneous analysis of more than one component throughout photodegradation processes.
  
- c) To use experimental design methodologies to study the influence of the variables in photodegradation processes and to optimize these processes.
  
- d) To establish methodologies for studying the degradation kinetics (degradation constants and/or degradation intermediates) that are based on the multivariate data obtained throughout dye photodegradation processes.
  
- e) To develop rapid methodologies based on sequential injection chromatography (SIC) for determining dyes.

### 1.3. STRUCTURE OF THE THESIS

This thesis is based on papers that have been published in international journals. These papers have been edited to give a uniform format. The contents have been structured in four chapters.

Chapter 1. **Introduction and objectives.** This chapter contains the general scope, objectives and structure of the thesis.

Chapter 2. **Theoretical aspects.** This chapter contains a brief description of the theoretical aspects that have been used during this thesis. In particular, it deals with the photodegradation procedures carried out and the instrumental techniques used. Moreover, the theoretical background to the chemometric techniques used is introduced.

Chapter 3. **Experimental part and results.** This chapter contains the bulk of the work carried out and is structured in four sections. At the beginning of each section, there is an introduction to the analytical problems that are to be looked at and an explanation of how they led to these scientific papers. Specifically, the first section provides an overview of the current developments in the removal of dyes from the environment and the analytical techniques associated with these studies. The second section deals with the optimization of the simultaneous photodegradation of three textile dyes. The third section reports kinetic studies of photodegradation processes with and without heterogeneous catalysts. Finally, the last section presents the determination of sulphonated azo dyes using low pressure chromatography with a monolithic column coupled to a flow system.

Chapter 4. **General conclusions.** This chapter contains the overall conclusions of the doctoral thesis.

The **Appendix** contains the list of papers and presentations given by the author while she was writing the thesis.

#### 1.4. REFERENCES

- [1] A.B. dos Santos, F.J. Cervantes, J.B. van Lier, *Bioresour. Techno.* 98 (2007) 2369-2385.
- [2] P.T. Anastas, J.C. Warner, *Green Chemistry: Theory and Practice*. Oxford University Press: New York, 1998.



## **2. THEORETICAL ASPECTS**

UNIVERSITAT ROVIRA I VIRGILI

ANALYTICAL METHODOLOGIES BASED ON CHEMOMETRICS TO OPTIMIZE THE PHOTODEGRADATION OF DYES

Cristina Fernández Barrat

DL:T. 160-2012

## 2.1. PHOTODEGRADATION

This section provides a brief description of the two photodegradation techniques used throughout this doctoral thesis.

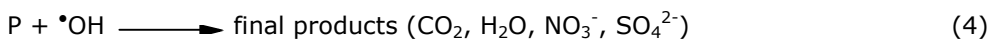
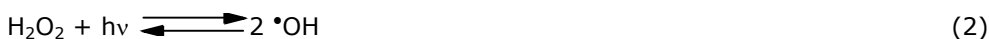
### 2.1.1. Photolysis

Photolysis is a degradation process that uses radiation with ultraviolet (UV) light to generate such reactive species as radicals, ions and excited molecules [1,2]. This process is intensified in aqueous solutions by the primary products formed from the photolysis of water.

The effect of radiation on a compound depends on the nature of the compound and the amount of energy that is transferred by the radiation. In dilute solutions the photolysis of water produces electrons ( $e_{aq}^-$ ), hydroxyl radicals ( $\bullet OH$ ) and hydrogen radicals ( $\bullet H$ ) as intermediate species that decompose the solute. The electrons and the hydrogen radicals are the main reductive species produced in irradiated aqueous solutions.

The combination of such oxidants as  $O_3$ ,  $H_2O_2$  or Fenton reagent with UV light is more effective at decolourizing dyes in wastewater than UV alone, which is why photooxidation processes are more commonly used. The hydroxyl radicals and perhydroxyl radicals ( $\bullet HO_2$ ) produced in subsequent reactions are the main oxidizing species.

Eq. (1-6) show the reactions involved throughout the process when hydrogen peroxide ( $H_2O_2$ ) is used.



$H_2O_2$  has such advantages as complete miscibility with water, stability, commercial availability, no phase transfer problems, no sludge formation, no air emissions, simplicity, low investment costs and the generation of a high-quantum yield of hydroxyl radicals. The main drawback is that  $H_2O_2$  absorption is very low in the solar UV range. [3-5].

The  $H_2O_2$ /UV process does not only decolour the dyes. The aromatic fragments formed are also degraded, as is shown in (Eq. (4)), but at a slower rate than decolorization. The formation of  $H_2O_2$  (Eq. (6)) is responsible for the constant concentration of  $H_2O_2$  during the  $H_2O_2$ /UV decomposition of dyes. The UV/ $H_2O_2$  decolorization of azo dye in wastewater could be described as two reactions taking place in parallel: a pure photolysis reaction and a  $H_2O_2$ -assisted oxidation reaction. The rate expression of this process can be assumed to be a pseudo-first-order kinetic model that takes into account these two processes [4].

### 2.1.2. Heterogeneous photocatalysis

Photocatalysis consists of a photoinduced reaction which is accelerated by the presence of a catalyst. A schematic representation of the activation of the catalyst and the generation of the reactive species is shown in Fig. 1 [6-9].

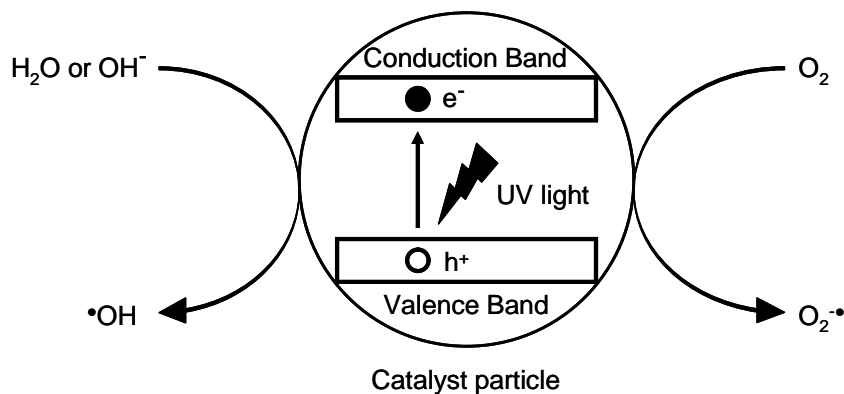


**Fig. 1.** Scheme of the activation of catalyst.

The process starts when a photon with sufficient energy (equal to or higher than the band-gap energy ( $E_{bg}$ ) of the catalyst) is absorbed. This absorption leads

---

to charge separation because an electron ( $e^-$ ) is promoted from the valence band of the catalyst to the conduction band, thus generating a hole ( $h^+$ ) in the valence band. This electron-hole pair can migrate to the catalyst surface where it can enter into a redox reaction with other species present on the surface.

Several semiconductors (e.g.  $TiO_2$ ,  $ZnO$ ,  $Fe_2O_3$ ,  $CdS$ , and  $ZnS$ ) can act as catalysts for light-induced redox-processes due to the electronic structure of their metal atoms, which is characterized by a filled valence band and an empty conduction band separated by an energy gap or band-gap. The semiconductor that is most widely used as a catalyst is  $TiO_2$  because it is chemically and biologically inert, photocatalytically stable, relatively easy to produce and use, and catalyzes reactions efficiently. It is also cheap and does not pose any risk to environment or humans [8].  $ZnO$  is also widely used.

The main problem of using heterogeneous catalysts is the undesired electron-hole recombination, which in the absence of a proper electron acceptor or donor is extremely efficient and is the major energy-wasting step. One strategy for inhibiting electron-hole recombination is to add irreversible electron acceptors to the reaction system. In this context the addition of  $H_2O_2$  is beneficial, but it can also become a scavenger of valence band holes and  $\bullet OH$  when present at high concentrations (see Eq. (7-9)),



Both  $h^+$  and  $\bullet OH$  are strong oxidants for dyes, so photocatalytic oxidation will be inhibited when the  $H_2O_2$  level gets too high.  $H_2O_2$  can also be adsorbed onto  $TiO_2$  particles to modify their surfaces and subsequently decrease their catalytic activity. An optimal dosage of  $H_2O_2$  is required if degradation is to be efficient. This means that  $H_2O_2$  has been controversial in some cases and it seems that it is dependent on the substrate type and various experimental parameters. Therefore, the usefulness of this oxidant must be checked before it is used [7,8].



## 2.2. INSTRUMENTAL TECHNIQUES

This section provides a brief description of the theoretical concepts of the instrumental techniques used in this thesis and of their common uses in dye determination or dye removal.

### 2.2.1. UV-visible spectroscopy

UV-Vis spectra are obtained by measuring the absorbance of monochromatic radiation across a range of wavelengths passing through a solution in a cell. Following Lambert Beer's law, for a given system there is a linear relationship between the absorbance and the concentration of the species that are sensitive to the radiation [10]. Fig. 2 shows the scheme of a spectrophotometer.

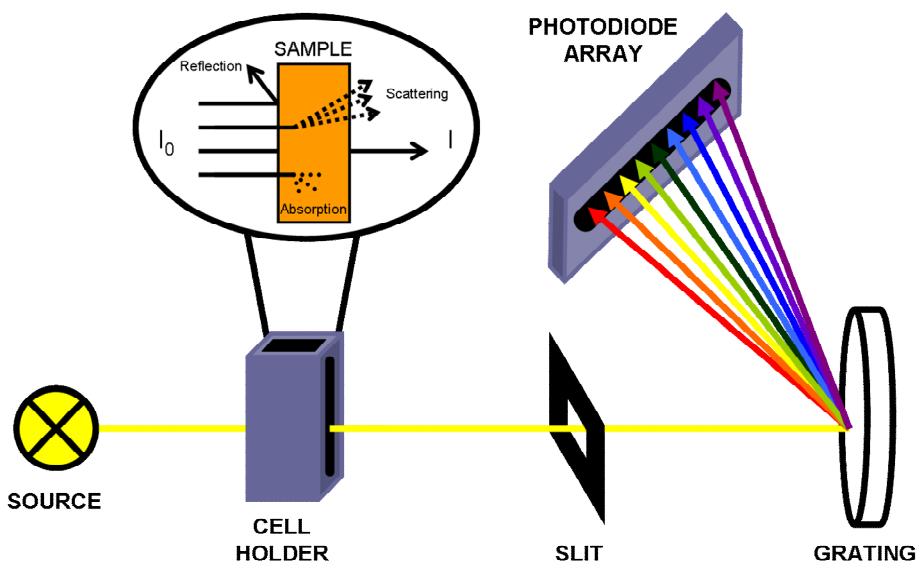


**Fig. 2.** Scheme of a UV-Vis spectrophotometer with diode array detector.

Organic azo dyes are chemical compounds with the functional group  $R-N=N-R'$  where  $R$  and  $R'$  are aryl groups. Because of the electron delocalization through the  $N=N$  and the aryl groups these compounds are naturally colored, which is why the visible spectral region (400-700 nm) is appropriate for both

qualitative and quantitative analysis. It is important that the visible range is not the only range recorded because information about the intermediates present in dye degradation processes can also be obtained from the UV range (190-400 nm).

In dye removal, UV-Vis spectroscopy is the most common technique for monitoring removal processes. The wavelength of maximum absorbance of the dye or the whole spectrum is usually monitored throughout the process, because it has been shown that in this way the removal can be understood and the various processes compared. Nevertheless it should be pointed out that UV-vis spectroscopy is not a selective technique and it can lead to erroneous results if there are intermediates (in degradation processes) that absorb at the same wavelength as the dye. Therefore, such other techniques as chromatography or chemometric treatments of multivariate data should be used if more information about the system is to be obtained.

### **2.2.2. Mass spectrometry**

Mass spectrometry (MS) generates gaseous ions from analyte molecules, separates these ions according to their mass-to-charge ( $m/z$ ) ratio, and detects and determines the abundance of these ions. The resulting mass spectrum is a plot of the (relative) abundance of the ions produced as a function of the  $m/z$  ratio [10]. A general scheme of the mass spectrometer is shown in Fig. 3.

The classical mass spectrometer configuration is directly coupled to capillary gas chromatography where the sample constituents are separated and transferred to the MS ion source as pure substances or simple mixtures in gas or vapor state. The most commonly used ionization source is electron impact which is highly energetic and makes it difficult to obtain the molecular ion. This classical configuration has several limitations if organic azo dyes are to be analyzed by MS because only volatile analytes are amenable to GC-MS analysis, ionization is limited to compounds with sufficient vapour pressure and stability, and the high fragmentation can prevent the molecular mass being obtained in less stable compounds.

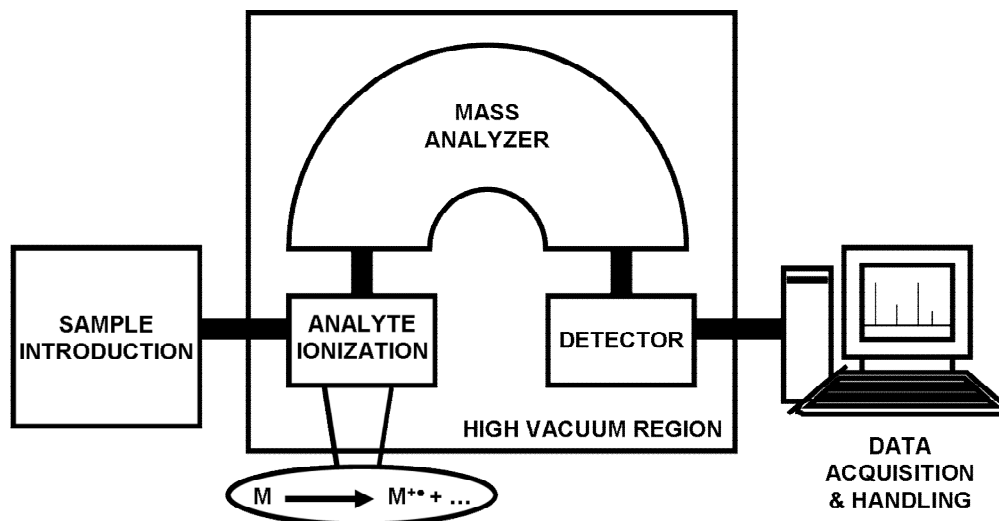


Fig. 3. Scheme of a mass spectrometer.

In order to overcome these limitations a number of other approaches to sample introduction, analyte ionization and mass analysis have been developed. One way of analyzing organic azo dyes with MS is to use soft ionization techniques, such as electrospray, that provide molecular mass information, with little fragmentation. These techniques are ideally suited for the on-line coupling of liquid chromatography and MS, in which nebulization and ionization are performed in a region at atmospheric pressure.

In dye removal, mass spectrometry is usually coupled to chromatographic techniques to carry out a qualitative and/or quantitative analysis of the byproducts or aromatic intermediates formed during dye degradation processes and to establish the reaction pathway or mechanism.

### 2.2.3. Flow analysis and sequential injection chromatography (SIC) systems

Flow analysis systems have become excellent tools for automating analytical procedures because they allow a high frequency of analysis, require minimum handling of the sample, can be adapted to most analytical instruments

and minimize the consumption of reagents and samples, which in turn minimizes waste.

Sequential injection chromatography (SIC) was described in 2003 [11,12]. It consists of the coupling of a short monolithic chromatography column to a standard SIA manifold (second generation flow systems) [13,14]. Fig. 4 shows a scheme of SIA (a) and SIC (b) configurations, the only difference between which is the monolithic column in the SIC set-up.

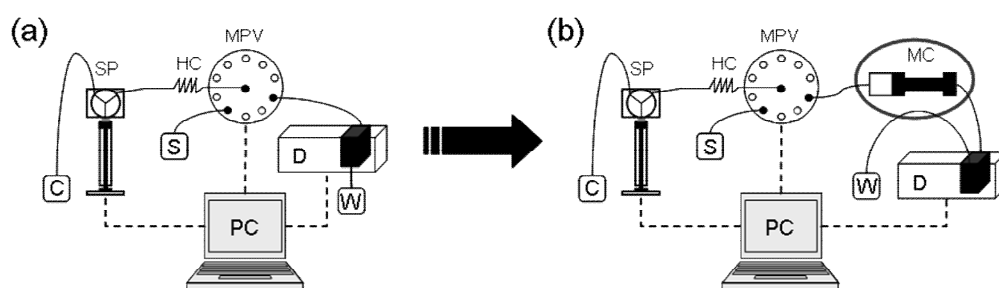


**Fig. 4.** SIA (a) and SIC (b) configurations. C, carrier; S, sample; SP, syringe pump; HC, holding coil; MPV, multi-position valve; MC, monolithic column; D, detector; W, waste.

SIC methodologies involve the following steps. Firstly, the mobile phase, the sample (which consists of a mixture of analytes) and the reagents (if required) are aspirated into the syringe. Secondly the direction of the flow is changed and the syringe pushes the mobile phase and the sample towards the monolithic column, which separates the different components of the sample mixture depending on their affinity with the column. Finally, the analytes reach the detector, which provides a chromatogram.

The use of SIC opens up new horizons in flow analysis because it can solve problems with simple mixture analysis and it has several advantages over high pressure chromatographic techniques (for example, low organic solvent consumption, low operating cost, cheaper instrumentation, little waste and high sample throughput). The main drawbacks are that SIC is limited to short monolithic columns and a maximal amount of mobile phase for one analysis (the

## Chapter 2

---

syringe pump has a reservoir of 5 or 10 mL). This means that SIC is not particularly useful in the analysis of complex mixtures [15].

In 1999, Cerdà introduced multisyringe flow analysis (MSFIA) as a robust alternative to its predecessors [16]. The basic element of MSFIA is a multisyringe burette, which is an adaptation of an automated syringe, and which allows the simultaneous movement of four syringes all connected to the same step motor. The advantages of SIC can be extended by on-line coupling MSFIA to a monolithic column to create multisyringe chromatography (MSC) [17], which enables several mobile phases to be used at once. These phases can be switched without the use of gradient because monolithic columns can be equilibrated rapidly without altering the baseline [18].

Neither SIC nor MSC methodologies have yet been used in the field of dye removal.

## 2.3. CHEMOMETRIC TECHNIQUES

This section describes the theoretical background of the chemometric techniques used in this thesis. In the first part experimental design are presented. In the second part the procedure for the multivariate data treatment is described.

### 2.3.1. Experimental design

Experimental design or design of experiments (DOE) refers to the process of making systematic plans to extract maximum information with minimum experimentation and to draw meaningful conclusions from the data using statistical tools [19,20]. The two main applications of experimental design are: screening, in which the factors that influence the experiment are identified, and optimization, in which the optimal settings or conditions for an experiment are found [21].

#### 2.3.1.1. Screening designs

Screening designs determine the experimental variables that have a significant influence on the response. To this end, this thesis uses full factorial and fractional factorial designs.

Full factorial designs investigate all possible combinations of the levels and the variables (factors). In general, a design in which  $k$  factors (quantitative or qualitative) are studied at  $m$  levels contains a total of  $m^k$  experiments. The advantage that factorial designs have over other experimentation methodologies is that they make it possible to estimate not only the main effect of each factor on the response, but also the interactions between factors when the effect of one factor depends on the level chosen for another factor. The main drawback of full factorial designs is that the number of experiments to be carried out increases rapidly when the number of factors increases.

The most used factorial design has two levels (and therefore  $2^k$  experiments). Since there are only two levels for each factor, we assume that the response is approximately linear over the range of the factor levels chosen; this is a reasonable assumption when the study of a process is about to be initiated.

Fractional factorial designs run for only a fraction of the complete factorial experiment. They are used when the number of factors or the experimentation cost is high. It is assumed that certain high-order interactions are negligible, so information on the main effects and low-order interactions may be obtained.

In two-level fractional factorial designs the number of experiments is  $2^{k-q}$  where  $k$  is the number of factors and  $q$  indicates the reduction (a half, a quarter, etc.). The effect of the main factors in this case is confused with high-order interactions. The principal advantage of this kind of design is that it allows sequential experimentation which means that a subsequent step can include appropriate experimentation to form a full factorial design. The drawback of fractional factorial designs is that it has to be careful assuming that two or three-factor interactions do not have a significant effect on the response.

The way to calculate the influence of the factors on the response is the same in all factorial designs at two levels (Eq. (10)):

$$b_A = \bar{y}_{A^+} - \bar{y}_{A^-} \quad (10)$$

where  $b_A$  is the value of the A effect and  $\bar{y}_{A^+}$  and  $\bar{y}_{A^-}$  are, respectively, the average of the responses of the experimentation where A is at the high level and the average of the responses of the experimentation where A is at the low level.

The significance of the effects is studied by statistical tools. The most important is ANOVA, which compares the variability of the effects with an estimation of the experimental error. If these values are not comparable, then the effect of the factor studied is important in the response [22].

Another way to determine if the effect of the factors is important is by visual interpretation using Pareto charts, which are frequency bar graphs where each bar is proportional to the absolute value of its associated estimated effect or the standardized effect.

### 2.3.1.2. Response surface methodology

Response surface methodologies cover strategies that aim to establish, in a particular experimental domain, a mathematical model that relates the response with the variables that influence this response.

The relationship between the response and the independent variables is often unknown. Initially, a low-order polynomial in some region of the independent variables is used to find an approximation of the true relationship (Eq. (11)):

$$y = \beta_0 + \sum_{i=1}^k \beta_i x_i + \sum_{i < j} \sum \beta_{ij} x_i x_j + \varepsilon \quad (11)$$

where  $y$  is the value of the response,  $\beta_0$ ,  $\beta_i$  and  $\beta_{ij}$  are the coefficients of the model and  $x_i$ ,  $x_j$  are the codified values of the variables.  $\beta_0$  is the constant term which estimates the response when the values of all the factors are in the center points of the model,  $\beta_i$  are the linear coefficients which describe the sensitivity of the response to the variations in the corresponding factors and  $\beta_{ij}$  are the cross-product coefficients which are enable these first-order response surfaces to be obtained.

If the model obtained is not validated more experiments need to be conducted to obtain the coefficients of a higher-degree polynomial model. One common strategy for obtaining second-order response surfaces is to use central composite designs which contain embedded factorial designs, center points and twice as many axial (star) points as there are factors. These points enable curvature to be estimated. Central composite design makes it possible to take advantage of the previous experimentation carried out to obtain the first-order model. This design leads to response surfaces such as (Eq. (12)):

$$y = \beta_0 + \sum_{i=1}^k \beta_i x_i + \sum_{i=1}^k \beta_{ii} x_i^2 + \sum_{i < j} \sum \beta_{ij} x_i x_j + \varepsilon \quad (12)$$



where  $y$ ,  $b_i$ ,  $b_{ij}$ ,  $x_i$  and  $x_j$  have the same meaning as in the previous case (Eq. (11)) and  $\beta_{ii}$  is the new coefficient that corresponds to quadratic terms that describe the curvature.

If the independent variable domain is adjusted appropriately, one or both of these models are a reasonable approximation of the true functional relationship between the response and the variables.

Fig. 5 shows a schematic representation of the usual approach to an analytical problem. It starts with screening methodologies such as fractional factorial design, which shows the main effects of the factors, and full factorial design, which shows the interactions between the selected variables and establishes a rough first-order response surface that can be validated in linear processes. Finally, the modeling step involves a central composite design that includes the axial points and establishes a second-order response surface that accurately fits the experimental domain studied.

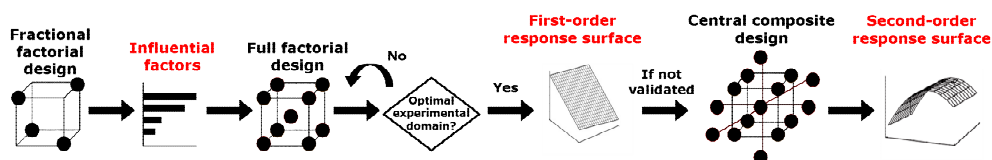


Fig. 5. Experimental design methodology for three variables.

### 2.3.2. Multivariate data treatment

The appropriate treatment of second-order data (one data matrix per sample) enables the sources of variability to be isolated, resolved and quantified. One chemometric technique that is useful for this purpose is based on the application of multivariate curve resolution (MCR) methods.

### 2.3.2.1. Multivariate curve resolution with alternating least squares (MCR-ALS)

MCR-ALS decomposes a data matrix into the product of two matrices (Eq. (13)) assuming that the experimental data follow a linear model similar to that of the Lambert Beer law in absorption spectroscopy [23].

$$\mathbf{D} = \mathbf{C}\mathbf{S}^T + \mathbf{E} \quad (13)$$

where, in spectroscopic measures,  $\mathbf{D}$  is the experimental data matrix acquired at different values of a particular variable (e.g. time) during a chemical reaction or process,  $\mathbf{C}$  is the matrix related to the concentration profiles and  $\mathbf{S}^T$  contains the spectral profiles of the spectroscopically active chemical species involved in the reaction or process.  $\mathbf{E}$  is the residual data matrix that contains the unexplained data by  $\mathbf{C}\cdot\mathbf{S}^T$  and ideally is close to the experimental error. The dimensions of these matrices are  $\mathbf{D}$  ( $m \times n$ ),  $\mathbf{C}$  ( $m \times a$ ),  $\mathbf{S}^T$  ( $a \times n$ ) and  $\mathbf{E}$  ( $m \times n$ ), where  $m$  is the number of spectra analyzed,  $n$  is the number of spectroscopic channels or wavelengths recorded for each spectrum and  $a$  is the number of chemical species actives to the detector involved in the chemical reaction or process.

To perform a MCR-ALS, the scheme shown in Fig. 6 is usually followed. In the first step the number of components, which is related to the number of chemical species present in the process, is determined. Then, the concentration or the spectral profiles for the number of significant components found is initially estimated. Finally, the alternating least squares (ALS) algorithm is applied to obtain the spectral and the concentration profiles of the species involved in the process. At this step some constraints can be applied in order to give chemical significance to the results.

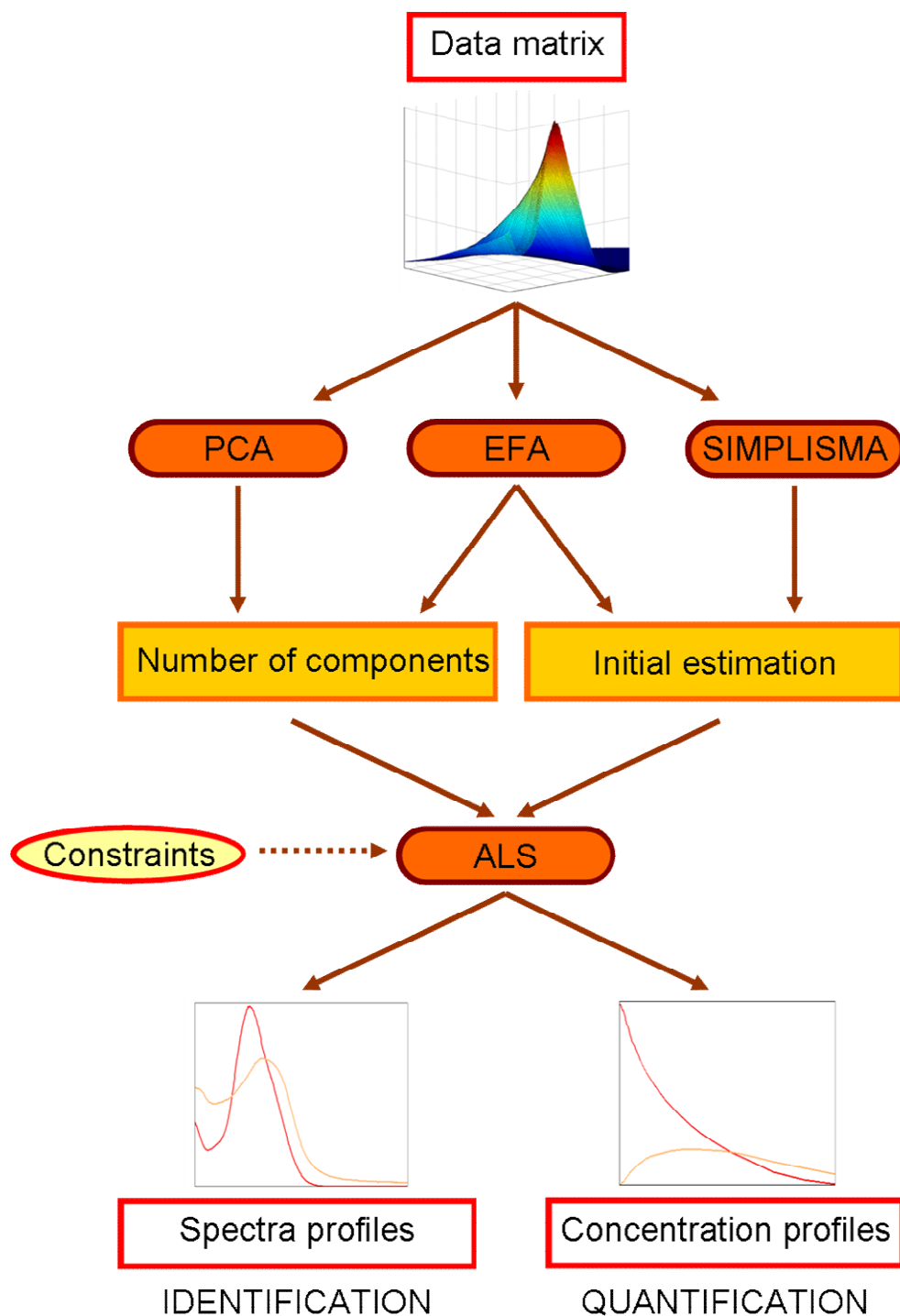


**Fig. 6.** Scheme of the resolution process of the MCR-ALS method.

---

### *Evaluation of the number of components*

Principal Components Analysis (PCA) is one of the most basic and widely used tools for evaluating how many components or chemical species are involved in the reaction or the process studied. The relevant information contained in the experimental data matrix is expressed with a reduced number of hierarchized variables known as principal components. The factors that have low singular values are associated with noise.

### *Search for initial estimations*

Once the number of chemical species involved in the reaction is known, **C** (concentration profiles) or **S<sup>T</sup>** (spectral profiles) can be initially estimated using techniques such as evolving factor analysis (EFA) [24-26] or the Simple-to-use Interactive Self-Modeling Mixture (SIMPLISMA) [27,28]. In this thesis, pure spectra and EFA profiles were used as initial estimates. EFA enables the profile of all the species to be obtained in each stage of the reaction or process. The EFA plot, which represents the logarithm of the eigenvalues versus the row number (time), is useful for investigating the emergence and decay of the process contributions.

### *Iterative resolution process by Alternating Least Squares (ALS)*

The initial estimates for **C** and **S<sup>T</sup>** are optimized using Eq. (13) iteratively by means of the alternating least squares (ALS) algorithm. At each iteration, new estimates of **C** and **S<sup>T</sup>** matrices are obtained (Eq. (14,15)).

$$\mathbf{C}^+ \mathbf{D}^* = \mathbf{C}^+ \mathbf{C} \mathbf{S}^T = \mathbf{S}^T \quad (14)$$

$$\mathbf{D}^* (\mathbf{S}^T)^+ = \mathbf{C} (\mathbf{S}^T) (\mathbf{S}^T)^+ = \mathbf{C} \quad (15)$$

where matrix **D<sup>\*</sup>** is the experimental data matrix reconstructed by PCA for the selected number of components, **C<sup>+</sup>** is the pseudoinverse of matrix **C** and **(S<sup>T</sup>)<sup>+</sup>** is the pseudoinverse of matrix **S<sup>T</sup>**. The use of **D<sup>\*</sup>** instead of the experimental matrix **D** improves the calculation stability because when PCA is used a considerable amount of noise is removed from the experimental data. These calculations are

## Chapter 2

---

repeated until the difference between the residual of one iteration and the next is less than a preset value.

This iterative process can be improved if more information is given to the system by applying soft or hard restrictions [29-34] or using augmented matrices [30,35].

### *Constraints*

Additional information can be given to the system during the optimization process of MCR-ALS in order to give the results more physical and chemical meaning. This information is given in the form of constraints that can be applied to all the species or only to some of them and in one matrix or several matrices, if they are applied to augmented matrices. In most cases constraints are soft. For example:

- Non-negativity, which forces the concentration and/or spectral profiles to have positive or zero values.
- Unimodality, which is used when it is known that the profiles have a single maximum (quite common in concentration profiles).
- Closure, which is a mass balance constraint that can be applied when the sum of the concentrations of all or some of the species involved in the reaction is forced to be constant at each stage of the reaction.
- Selectivity, which can be applied in zones that are totally selective for one of the species. The concentrations or signals of the other components are forced to be zero in these zones.
- Correspondence between species, which is used when augmented matrices are analyzed. This constraint specifies the species present in each matrix.
- Trilinearity (three-way structure), which imposes that the profiles of one analyte in the various matrices used must be equal.

Hard constraints, which include kinetic and thermodynamic models, [32-34] can also be applied to drastically reduce the rotational ambiguity. These

constraints force one or more species to follow an initially postulated physicochemical law.

Both types of constraint are applied in the HS-MCR-ALS algorithm.

### *Matrix augmentation*

If more than one experiment (matrix) is available and the data matrices have the same number of rows and/or columns, we can create a three-way data structure and analyze them together by MCR-ALS. These matrices can be arranged by creating a column-wise augmented data matrix, row-wise augmented data matrix or a column- and row-wise augmented data matrix. In this thesis, the experimental data were augmented using the pure spectra of some components because this strategy improves the resolution by reducing the rotational ambiguity of the MCR-ALS algorithm.

### *Parameters of quality*

Since there is a certain level of ambiguity in the results of the MCR-ALS optimization, several parameters evaluate the goodness of the resolution. In particular the parameters that are most used for this purpose are the lack of fit (*lof*) of the model (Eq. (16)), the variance explained (Eq. (17)) and, if the spectra of the pure analyte is available, the correlation between the spectra retrieved by MCR-ALS and the pure spectra (Eq. (18))

$$lof = \sqrt{\frac{\sum_{i,j} (d_{ij} - \hat{d}_{ij})^2}{\sum_{i,j} d_{ij}^2}} \quad (16)$$

where  $d_{ij}$  is each of the elements of the raw data matrix or each of the elements of the matrix reconstructed from the principal components selected in the principal component analysis (PCA). Depending on the matrix used,  $lof_{exp}$  or  $lof_{pca}$  is obtained.  $\hat{d}_{ij}$  are the corresponding values calculated after the MCR-ALS optimization process.

Chapter 2

---

$$R^2 = \frac{\sum_i \sum_j \hat{d}_{ij}^2}{\sum_i \sum_j d_{ij}^2} \quad (17)$$

$$r = \cos \gamma = \frac{S_i^T \hat{S}_i}{\|S_i\| \|\hat{S}_i\|} \quad (18)$$

where  $\gamma$  is the angle defined by the vectors associated with the profile recovered by MCR-ALS ( $\hat{S}_i$ ) and the real profile ( $S_i$ ), for a particular species  $i$ .

## 2.4. REFERENCES

- [1] M.A. Rauf, S.S. Ashraf, *J. Hazard. Mater.* 166 (2009) 6-16.
- [2] L. Wojnárovits, E. Takács, *Radiat. Phys. Chem.* 77 (2008) 225-244.
- [3] E. Forgacs, T. Cserháti, G. Oros, *Environ. Int.* 30 (2004) 953-971.
- [4] P.K. Malik, S.K. Sanyal, *Sep. and Purif. Technol.* 36 (2004) 167-175.
- [5] G.M. Colonna, T. Caronna, B. Marcandalli, *Dyes Pigm.* 41 (1999) 211-220.
- [6] M.A. Rauf, M.A. Meetani, S. Hisaindee, *Desalination* 276 (2011) 13-27.
- [7] I.K. Konstantinou, T.A. Albanis, *Appl. Catal., B* 49 (2004) 1-14.
- [8] U.G. Akpan, B.H. Hameed, *J. Hazard. Mater.* 170 (2009) 520-529.
- [9] C. Chen, W. Ma, J. Zhao, *Chem. Soc. Rev.* 39 (2010) 4206-4219.
- [10] R. Kellner, J.M. Mermet, M. Otto, H.M. Widmer, *Analytical Chemistry*, Wiley, Weinheim, 1998.
- [11] D. Satínský, P. Solich, P. Chocholous, R. Karlíček, *Anal. Chim. Acta* 499 (2003) 205-214.
- [12] J. Huclová, D. Satínský, R. Karlíček, *Anal. Chim. Acta* 494 (2003) 133-140.
- [13] J. Ruzicka, G.D. Marshall, *Anal. Chim. Acta* 237 (1990) 329-343.
- [14] A. Cladera, C. Tomas, E. Gómez, J.M. Estela, V. Cerdà, *Anal. Chim. Acta* 302 (1995) 297-308.
- [15] P. Chocholous, P. Solich, D. Satínský, *Anal. Chim. Acta* 600 (2007) 129-135.
- [16] V. Cerdà, J.M. Estela, R. Forteza, A. Cladera, E. Becerra, P. Altimira, P. Sitjar, *Talanta* 50 (1999) 695-705.
- [17] H.M. González-San Miguel, J.M. Alpízar-Lorenzo, V. Cerdà, *Talanta* 72 (2007) 296-300.
- [18] M. Fernández, H.M. González-San Miguel, J.M. Estela, V. Cerdà, *Trends Anal. Chem.* 28 (2009) 336-346.
- [19] D.C. Montgomery, *Design and Analysis of Experiments*, Wiley, USA, 2001.
- [20] T. Lundstedt, E. Seifert, L. Abramo, B. Thelin, A. Nyström, J. Pettersen, R. Bergman, *Chemom. Intell. Lab. Syst.* 42 (1998) 3-40.
- [21] G. Hanrahan, K. Lu, *Crit. Rev. Anal. Chem.* 36 (2006) 141-151.
- [22] D.L. Massart, B.G.M. Vandeginste, L.M.C. Buydens, S. de Jong, P.J. Lewi, J. Smeyers-Verbeke, *Handbook of Chemometrics and Qualimetrics Part A*, Elsevier, Amsterdam, 1997.
- [23] R. Tauler, *Chemom. Intell. Lab. Syst.* 30 (1995) 133-146.
- [24] H.R. Keller, D.L. Massart, *Chemom. Intell. Lab. Syst.* 12 (1992) 209-224.
- [25] M. Maeder, *Anal. Chem.* 59 (1987) 527-530.
- [26] H. Gampp, M. Maeder, Ch. Meyer, A.D. Zuberbühler, *Talanta* 32 (1985) 1133-1139.
- [27] W. Windig, J. Guilment, *Anal. Chem.* 63 (1991) 1425-1432.
- [28] W. Windig, *Chemom. Intell. Lab. Syst.* 36 (1997) 3-16.
- [29] R. Tauler, E. Cassasas, A. Izquierdo-Ridosas, *Anal. Chim. Acta* 248 (1991) 447-458.



## Chapter 2

---

- [30] R. Tauler, A. Izquierdo-Ridosá, E. Cassasas, *Chemom. Intell. Lab. Syst.* 18 (1993) 293-300.
- [31] A. de Juan, R. Tauler, *Crit. Rev. Anal. Chem.* 36 (2006) 163-176.
- [32] A. de Juan, M. Maeder, M. Martínez, R. Tauler, *Chemom. Intell. Lab. Syst.* 54 (2000) 123-141.
- [33] J. Diewok, A. de Juan, M. Maeder, R. Tauler, B. Lendl, *Anal. Chem.* 75 (2003) 641-647.
- [34] A. de Juan, M. Maeder, M. Martínez, R. Tauler, *Anal. Chim. Acta* 442 (2001) 337-350.
- [35] R. Tauler, D. Barceló, *Trends Anal. Chem.* 12 (1993) 319-327.



### **3. EXPERIMENTAL PART AND RESULTS**

UNIVERSITAT ROVIRA I VIRGILI

ANALYTICAL METHODOLOGIES BASED ON CHEMOMETRICS TO OPTIMIZE THE PHOTODEGRADATION OF DYES

Cristina Fernández Barrat

DL:T. 160-2012

### 3.1. Removing dyes

Over the years, many different methodologies have been proposed to remove organic dyes from wastewater and to monitor the removal process. This section presents a paper that provides a general vision of the state of the art in dye removal. It is entitled ***An analytical overview of processes for removing organic dyes from wastewater effluents***, which responds to objective (a) announced in chapter 1. The overview reviews and discusses:

- The different strategies for dye removal and the advantages and drawbacks of each one.
- The analytical methodologies most commonly used to monitor dye removal processes and to identify intermediates in degradation reactions.
- The strategies used to evaluate the influence of the process variables, with special regard to the use of experimental designs, and the criteria followed to choose the responses and the factors in the different type of processes.
- Some suggestions for future research into dye removal systems.

UNIVERSITAT ROVIRA I VIRGILI

ANALYTICAL METHODOLOGIES BASED ON CHEMOMETRICS TO OPTIMIZE THE PHOTODEGRADATION OF DYES

Cristina Fernández Barrat

DL:T. 160-2012

### **3.1.1. Paper**

*An analytical overview of processes for removing organic dyes from wastewater effluents*

Cristina Fernández, M. Soledad Larrechi, M. Pilar Callao

**Trends in Analytical Chemistry 29 (2010) 1202-1211**



UNIVERSITAT ROVIRA I VIRGILI

ANALYTICAL METHODOLOGIES BASED ON CHEMOMETRICS TO OPTIMIZE THE PHOTODEGRADATION OF DYES

Cristina Fernández Barrat

DL:T. 160-2012

---

## An analytical overview of processes for removing organic dyes from wastewater effluents

Cristina Fernández, M. Soledad Larrechi, M. Pilar Callao

*Department of Analytical and Organic Chemistry, Rovira i Virgili University,  
Marcel·lí Domingo s/n Campus Sescelades, E-43007 Tarragona, Spain*

### Abstract

Organic dyes are used in a wide range of industrial applications (e.g., textiles, food products, cosmetics and pharmaceuticals), so they are frequently found in wastewaters and are increasingly becoming an environmental problem. This critical overview covers the most frequently used strategies for dye removal and the most common analytical techniques for monitoring these processes and identifying any intermediates generated. We also analyze experimental design strategies for optimizing removal processes. Finally, our concluding remarks include a future outlook for dye-removal processes and the analytical techniques employed.

**Keywords:** Advanced oxidation processes (AOP); Biodegradation; Dye degradation; Dye determination; Dye removal; Effluent; Environmental problem; Experimental design; Intermediate; Wastewater.

### 1. Introduction

Organic dyes are used in a wide range of industrial applications [e.g., textiles (the most significant), food products, cosmetics, pharmaceuticals or paper printing], which means that they are frequently found in industrial wastewater. Several groups of dyes can be distinguished on the basis of their compound structure (e.g., phtalocyanins, anthraquinones, quinone-imines and xanthenes) [1]. However, the most commonly used dyes are azo dyes, because they are easier and more cost effective to synthesize than natural dyes. To get an idea of the annual market in dyes, in 2003, the production of dyes was more than  $7 \times 10^5$



tonnes [2]. Dyes are considered hazardous to the environment because many are toxic to living organisms, directly or through their absorption and reflection of sunlight entering the water, which interferes with the growth of aquatic organisms. Furthermore, they impart color to wastewater, giving rise to aesthetic issues [3-4].

Efforts are being made to study dye-removal or dye-degradation processes and to develop analytical methodologies for evaluating these processes. As evidence of the growing interest in this field, we made a bibliographic search for articles appearing in the Scopus database since the year 2007. Keywords "dye determination" yielded more than 2500 references, and "dye degradation" 7810 references.

The objectives of this overview are the following:

- (1) critical review of the most frequently employed strategies for dye removal from wastewater; and,
- (2) review of the analytical techniques most commonly used to evaluate these strategies.

We have structured the review in three main parts, as follows.

- (1) The first part presents the various dye-removal methodologies along with their respective uses since 2007. We also describe the drawbacks and the advantages of each technique.
- (2) The second and most extensive part concerns the various analytical approaches in the field of dye removal. We discuss how experimental design is used to optimize removal processes and how separation or spectroscopic techniques are used to monitor degradation processes and to identify reaction intermediates.
- (3) The last section contains our concluding remarks and suggests what the future has in store for dye-removal processes and the analytical techniques employed.

The studies cited result from a representative selection of research dealing with some of the strategies considered. The vast scope of these scientific fields prevents our study from being exhaustive. Furthermore, many very interesting

papers focusing on the theoretical bases of degradation processes or on specific technological aspects are beyond the scope of this overview and are not discussed here.

## 2. Dye-removal methodologies

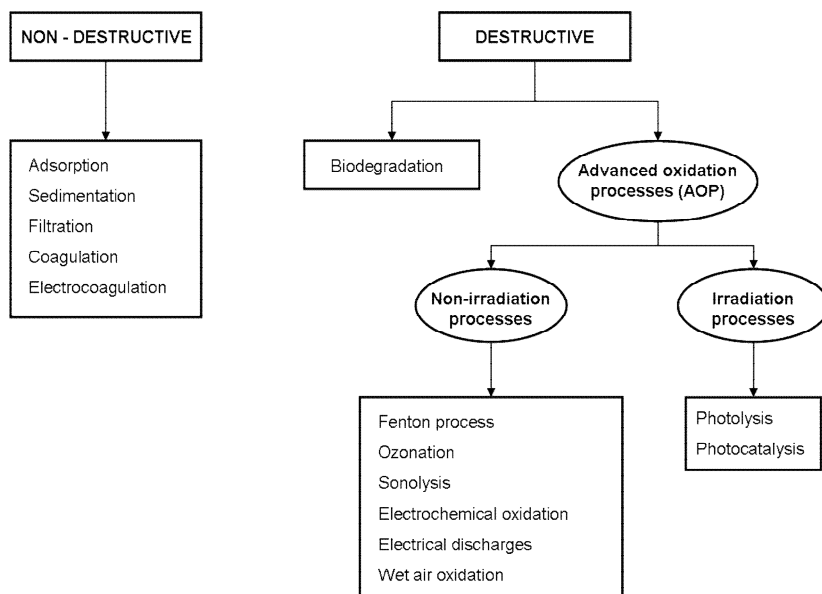
Fig. 1 shows the most common techniques used to remove dyes from wastewater. Fig. 2 shows the percentage of all available scientific papers (since 2007) that use the different techniques, and was created from the information obtained through a search using the keywords "organic dyes" and the name of each technique.

Table 1 lists the studies published in the bibliographic sources that we focused on most closely in preparing our review. The referenced papers were selected to cover the whole range of dye-removal strategies, analytical techniques and experimental designs. The most recent papers were selected. The first three columns in Table 1 indicate the name of the dye, the type of chemical and the process employed to remove the dye.

Non-destructive techniques were the focus of 19% of the papers published. In 75% of these papers, the dyes were removed using different kinds of adsorbent [5-9]. The primary advantage of these techniques was that they were very effective in most cases with all dye types [7,8,10]. However, when they were used to treat colored wastewater they generated new secondary waste, transferring dyes to other phases that required potentially expensive post-treatment to be removed or regenerated [2,3].

In biodegradation, as the name indicates, removal occurs by means of living microorganisms (e.g., bacteria or fungi) [11-21]. These treatments are based on a first step comprising anaerobic treatment that cleaves the dyes' azo linkages and removes the coloration of the wastewater. Hazardous aromatic amines are formed during this step, and that means that a second step is needed for aerobic treatment to mineralize these byproducts completely [4]. It has been demonstrated that immobilized microbial systems improve bioreactor efficiency,

increase process stability and decrease the generation of biological sludge [5]. It is important to note that these techniques involve living organisms, so drastic conditions (e.g., pH and temperature) cannot be present during them. Another drawback is that these techniques cannot be applied to most textile wastewaters due to the toxicity of most commercial dyes to the organisms used in the processes [22]. The main advantage of these techniques is that they are capable of removing dyes from large volumes of wastewater at a low cost [2].



**Fig. 1.** Dye-removal techniques.

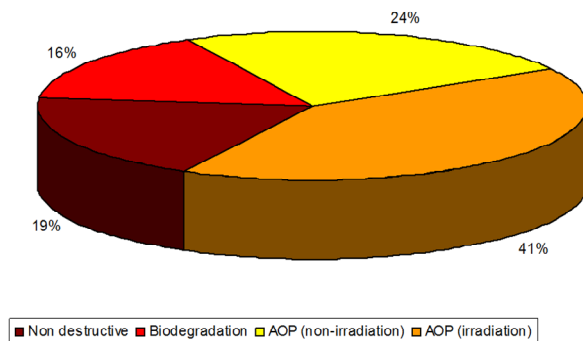


**Fig. 2.** Papers published on dye removal according to the process employed.

**Table 1.** Overview of applications of dye-removal processes.

Dyes	Dye Class	Elimination Technique	Analytical techniques to monitor the process	Analytical techniques to determine intermediates	Ref
Acid Orange 7	Azo	Adsorption/Biodegradation	UV-Vis/COD	-	[5]
Remazol Brilliant Violet 5R	Azo	Biodegradation	UV-Vis/COD	HPLC-UV	[11]
Reactive Red 180	Azo	Biodegradation	UV-Vis	-	[12]
Orange G azo dye	Azo	Biodegradation	UV-Vis	RMN	[13]
Reactive Red 239	Azo	Biodegradation	UV-Vis	-	[14]
Reactive Yellow 15					
Reactive Blue 114					
Reactive Black 5	Azo	Biodegradation	UV-Vis	-	[15]
Reactive Blue 114					
Reactive Yellow 15					
Reactive Red 239					
Reactive Yellow 176					
Reactive Red 180					
Direct Violet 51	Azo	Biodegradation	UV-Vis	FTIR	[16]
Direct blue 6, Green HE4B	Azo	Biodegradation	UV-Vis	FTIR	[17]
Red HE7B					
Methyl Orange	Azo	Biodegradation	HPLC	GC and GC-MS	[18]
Reactive Red 272	Azo	Biodegradation	UV-Vis/COD	GC-MS	[19]
Acid Orange 5, Acid Orange 52	Azo	Biodegradation/Ultrasonics	UV-vis, HPLC	HPLC-MS	[35]
Direct Blue 71, Reactive Black 5					
Reactive Orange 16					
Reactive Orange 107					
Direct Red 23	Azo	Ozonation/Ultrasonics	UV-Vis	GC-MS and IC	[36]
Reactive Black 5	Azo	Sonochemical	UV-Vis/TOC	IC	[37]
Acid Red B	Azo	Sonocatalytic	UV-Vis	-	[38]
Textil effluent	Non specified	Coagulation-Flocculation Membrane processes Adsorption	UV-Vis/COD/turbidity	-	[6]
Reactive Black 5	Azo	Electrocoagulation	UV-Vis	-	[60]
Reactive Red 141	Azo	Electrocoagulation	UV-Vis	-	[71]
Acid Red 97, Acid Orange 6	Azo	Adsorption (activated carbon)	SIA UV-Vis	MCR ALS	[7-8]
Acid Brown 425					
Methyl Violet	Triarylmethane	Adsorption (cationic membrane)	UV-Vis	-	[9]
Reactive Black 5	Azo	Ozonation	-	IC, HPLC-MS and RMN	[32]
Reactive Blue 49					
Reactive Red 35					
Reactive Orange 96					
Reactive Red 2	Azo	Ozone based systems	UV-Vis	-	[33]
Reactive Red 120	Azo	Ozonation	UV-Vis/TOC	HPLC-MS or MS/MS and IC	[34]
Methylene Blue	Thioquinone	Electrical discharges	UV-Vis	GC-MS and IR	[39]
Methyl yellow, Methyl red	Azo	Electrical discharges	UV-Vis	GC-MS	[40]
Methyl orange, Phenol red					
Methylene blue					
Methyl Orange	Azo	Electrical Discharges/ Activated Carbon	UV-Vis/COD	FTIR	[41]
Acid Orange 7	Azo	Electrochemical	UV-Vis/COD/TOC	HPLC	[23]
Procion Blue	Azo	Photocatalytic and Electrochemical	UV-Vis/COD	-	[24]
Acid Brown 14	Azo	Electrochemical	COD	HPLC-UV	[25]
Cationic Red X-GRL	Azo	Wet Air Oxidation	UV-Vis	GC-MS and IC	[42]
Cationic Red X-GRL	Azo	WO, WEO*, EO	UV-Vis/COD	GC-MS	[43]
Safranin-T	Quinone-imine	CWAO**	UV-Vis/COD/TOC	IR	[44]
Safranin-O	Quinone-imine	Photolysis	UV-Vis	-	[46]
Safranin-O	Quinone-imine	Photolysis	UV-Vis	-	[47]

**Table 1.** (continued)

Dyes	Dye Class	Elimination Technique	Analytical techniques to monitor the process	Analytical techniques to determine intermediates	Ref
Acid Red 94	Xanthene	Photolysis	UV-Vis	-	[48]
Disperse Blue 56	Anthraquinone	UV/NaClO	UV-Vis/COD/conductivity	HPCE and IC	[67]
Reactive Black 5	Azo	Fenton/Biodegradation	UV-Vis	-	[26]
Direct Orange 61	Azo	Electro-Fenton	UV-Vis/TOC	HPLC and IC	[27]
Malachite Green	Triarylmethane	Electro-Fenton	COD	HPLC, IC and exclusion chromatography	[28]
Alizarin Red	Anthraquinone	Electro-Fenton	UV-Vis/COD	-	[29]
Acid Red 14	Azo	Heterogeneous Photo-Fenton	TOC	-	[58]
Acid blue 193, Reactive Black 39	Azo	Photo-Fenton	UV-Vis/COD/TOC	-	[63]
Acid Orange 7, Acid Orange 8 Acid Red 14, Acid Red 73	Azo	Oxidation by $KMnO_4$	UV-Vis/TOC	-	[61]
Reactive Red 45	Azo	UV/ $TiO_2$ , UV/ZnO Photo-Fenton	UV-Vis/TOC	-	[62]
Acid Black 1, Acid Orange 7 Basic Orange 66	Azo	Photocatalysis	UV-Vis	HPLC	[49]
Rohdamine B	Xanthene	Adsorption/Photocatalysis	UV-Vis/COD	-	[50]
Metanil Yellow	Azo	Photocatalysis	UV-Vis/TOC	HPLC-DAD, GC-MS and IC	[51]
Acid Red 97 Acid Orange 61 Acid Brown 425	Azo	Photocatalysis	UV-Vis	MCR ALS	[52-53]
Methyl Orange, Rhodamine 6G	Azo, Xanthene	Photocatalysis	UV-Vis/COD	-	[54]
Textil effluent	Azo	Electrochemical	COD	FTIR and HPLC	[22]
Rhodamine 6G	Xanthene	silver-coated $ZnO$ , $NaBH_4$	UV-Vis	SERS	[70]
Acid Orange 10, Acid Orange 12 Acid Orange 8	Azo	Photocatalysis	UV-Vis/TOC $NH_4^+$ formation	-	[55]
Reactive Blue 4	Anthraquinone	WAO WPO*** Photocatalysis Electro-Fenton	UV-Vis/TOC	IC and GC-MS	[30]
Procion Red H-EXL	Azo	Fenton	UV-Vis/TOC	-	[59]
Alizarin Red	Anthraquinone	Fenton	UV-Vis/TOC	-	[31]
Orange I, Orange II, Ethylorange	Azo	Photocatalysis	TOC	HPLC-DAD-ESI-MS and IC	[56]
Orange II, Acid Orange 8 Food Yellow 3 4-[4-hydroxyphenyl]azo]- benzenesulfonic acid	Azo	Biodegradation	-	CE-MS	[21]
Acid Orange 7, Acid Orange 8 Mordan Violet 5	Azo	Biodegradation	-	HPLC and CE-MS	[20]
Sunset Yellow, Chromotrope	Azo	Photocatalysis	-	HPLC and IC	[57]

\* WO, WEO: wet oxidation, wet electrochemical oxidation. \*\*CWAO: catalytic wet air oxidation. \*\*\* WPO: wet peroxide oxidation

As shown in Fig. 2, 65% of the dye-removal processes that we studied were advanced oxidation processes (AOPs) in which strong oxygen-based oxidizers (e.g.,  $OH^\bullet$ ,  $HO_2^\bullet$ ,  $O_2^{\bullet-}$ ) were formed from the water and  $O_2$  present in the reaction medium with the aid of an oxidant source. These radicals were used to degrade dye molecules completely.

In processes without irradiation, the most common ways of obtaining oxidant radicals were through:

- electrochemical oxidation [23-25] (40% of papers studied);
- Fenton's reagent [26-31] (35%); and,
- ozone [32-34] (13%).

Less studied mechanisms included:

- ultrasound [35-38];
- electrical discharges (pulsed corona discharges) [39-41]; and,
- use of an oxidant gas in hydrothermal conditions (wet air oxidation) [42-44].

Another type of AOP uses radiation treatment with ultraviolet (UV) light [45]. In this case, radicals are formed by irradiating an oxidant {e.g.,  $\text{H}_2\text{O}_2$  (photolysis) [46-48]} or using a heterogeneous catalyst {usually  $\text{TiO}_2$  or  $\text{ZnO}$  (photocatalysis) [49-57]}. Papers on the use of photocatalysis are quite numerous (80% of the papers studied that use irradiation treatments).

AOPs are cleaner because dyes totally decompose to  $\text{CO}_2$ ,  $\text{H}_2\text{O}$ , low-molecular-weight compounds (e.g., small aldehydes, carboxylic acids or small inorganic compounds) and no significant or solid secondary pollution is generated. These are the fastest, cleanest removal processes and are very effective at degrading organic dyes. The drawback is that they can be energy-intensive and costly. However, considerable effort is being made to improve them with the following possibilities:

- constructing reactors that can use sunlight as a source of irradiation [54];
- incorporating new materials or catalysts (e.g., composites of  $\text{TiO}_2/\text{ZnO}$ ) [38];
- using a heterogeneous Fenton catalyst with a Fe zeolite, which has a better microporous structure and ion-exchange capacity (among other advantages) [58]; or,
- immobilizing the photocatalyst on inert surfaces, which favors recovery of the catalyst [55].

Other tendencies in dye degradation treatments are the combination of:

- oxidants (e.g.,  $\text{O}_3/\text{H}_2\text{O}_2$ ,  $\text{O}_3/\text{Fe}^{3+}$ ,  $\text{O}_3/\text{H}_2\text{O}_2/\text{Fe}^{3+}$ , UV light / $\text{O}_3/\text{Fe}^{3+}$ , UV light / $\text{O}_2/\text{H}_2\text{O}_2/\text{Fe}^{3+}$ ) [33]; or,

- degradation processes.

Some examples of this last approach are:

- (a) the combination of wet air oxidation and electrochemical oxidation to make wet electrochemical oxidation [43];
- (b) the use of photocatalysis or an anaerobic biotreatment in a first stage and subsequent degradation of byproducts by electrochemical oxidation [23-24];
- (c) the combination of ozonation, photocatalysis or biodegradation with sonolysis [35-36, 38];
- (d) coagulation-flocculation coupled with membrane processes or adsorption [6]; and,
- (e) activated organic carbon in combination with high-voltage pulse discharge [41].

### **3. Analytical focus**

#### **3.1. Experimental design to optimize removal processes**

The main criteria when choosing a dye-removal process is that the removal rate is high. However, other criteria (e.g., removal time and cost) should also be considered. For example, in AOPs, the  $E_{EO}$  parameter (energy per order) [33, 55] could be used.  $E_{EO}$  is the number of kWh of electrical energy required to reduce the concentration of a pollutant by one order of magnitude (90%) in  $1\text{m}^3$  of contaminated water.

A great deal of research focuses on whether one new condition (e.g., use of a new reagent or adsorbent) has a positive effect on the selected criteria (or response). The optimization of the entire process taking all the possible factors into account is not contemplated, even though, in dye-removal processes, numerous parameters might affect their results. Table 2 shows the relationship between removal techniques and the most important factors considered in the papers reviewed.

Generally, the way that a factor affects in the response is known (e.g., in adsorption processes and, considering the % of dye removal as response, the

amount of adsorbate and the time of contact have a positive effect [8]). Nevertheless, the real effect of each factor is difficult to predict because it depends on the range of factor values studied (domain) and on the values of the other factors that could have synergistic effects with the factor considered. As examples of the influence of the factor domain, the temperature in degradation processes does not significantly affect over 20°C [59], and the oxidant concentration can have a quadratic or a linear effect on the response, depending on the domain considered [53]. With regard to synergies (e.g., in photocatalytic degradations), the effect of the pH depends on the kind of catalyst used [54].

**Table 2.** Most important factors studied in the different dye-removal processes.

Dye-elimination process	Studied Factors
Adsorption or coagulation	Dye concentration Amount of adsorbate Concentration of coagulant Kind of adsorbate or coagulant Time contact
Biodegradation	Temperature pH Microorganism concentration Presence of: sugars, organic acids or metals ions Dye concentration
Advanced oxidation processes (AOP)	pH Dye concentration Kind of catalyst (TiO <sub>2</sub> , ZnO...) Concentration of catalyst Irradiation (if sample is irradiate) Treated Volume Presence and kind of gas introduced (if necessary) Temperature Stirring speed Concentration and kind of oxidant (e.g. H <sub>2</sub> O <sub>2</sub> ) Applied current (electro processes)

Many studies tackle optimization through the one-factor-at-a-time method [15,17,18,23,24,26,29,36-39,41,44,46,54,60-62]. This method can provide a general idea of the behavior of the process, but costs more because several experiments have to be conducted for each factor. Furthermore, synergistic or



antagonistic effects between different factors are not considered, and such actions can affect the effectiveness of systematically removing dyes.

The use of experimental designs to optimize processes for removing dyes is on the rise. These methodologies provide maximum information about the process in relation to the number of experiments. The drawback is that the conclusions drawn cannot be validated if the process guidelines are erroneous (e.g., linear or quadratic behavior in the domain studied, and the kind and the number of factors). In most cases in which an experimental design is used, a response surface is established [8,12,14,27,42,47,48,51,53,58,59,63] with factors chosen from previous knowledge. The aim of the response surface is to develop an empirical model in which the response to be optimized is the dependent variable and the factors that influence this response are the independent variables. With this information, the optimum operating conditions can be estimated. Central composite designs are the most common experimental designs used to establish a response surface [51,58,59,63], although other designs are also suitable for this purpose [8] (e.g., D-optimal designs [47-48], the Dohelert design [27], the hybrid design [42] and the Box Behnken design [12-14]).

Few papers use a screening experimental design. This type of design is very useful for experimentally determining which factors are important in a particular process and how they affect it. The most common design for this purpose is the fractional factorial design [6, 52].

Another less developed aspect in the field of dye removal is the application of one experimental design to more than one response [e.g., the percentage of dye degradation (or color removal) and the degradation time or energy per order]. This requires optimal compromises to be found between all the responses. In these cases, desirability functions could be of great interest. The general approach is to convert each response  $y_i$  into an individual desirability function  $d_i$  that varies over the range (0-1). Through these functions an overall desirability function  $D$  is evaluated [64-66].

### **3.2. Analytical techniques**

In dye removal studies two interesting focuses can be distinguished:

- (1) dye removal rate; and,
- (2) the chemical or physical processes involved.

If degradation processes are studied, information about the intermediate products formed is of interest, because they may be as dangerous for the environment as the initial dye. The information required in these two types of study is different, as are the analytical techniques used to obtain it.

#### **3.2.1. Global monitoring of the removal processes**

Removal processes can be monitored by determining:

- (1) analytical indices; and,
- (2) dye or subproduct concentrations.

*3.2.1.1. Determination of analytical indices.* As shown in the fourth column of Table 1, the most common analytical indices used to monitor removal processes are total organic carbon (TOC), chemical oxygen demand (COD), and absorbance in UV-visible at the wavelength of maximum absorption ( $A_{\max}$ ). The value of these three indices is directly related to the dye concentration, so a decrease in any one of them in the process indicates a decrease in the dye concentration. Nevertheless, it should be pointed out that none of them is selective.

TOC is usually determined by catalytic oxidation followed by quantification of the  $\text{CO}_2$  formed through infrared spectrometry [59, 61]. The decay of this parameter in all degradation processes involves ultimate mineralization of both parent dye and its intermediates [30, 37].

COD evaluates the oxygen required for the oxidation of organic and inorganic matter in the sample and is determined by oxidizing the sample with potassium dichromate and then titrating its excess with a standard solution of ferrous ammonium sulfate [11, 23].

TOC and COD can provide complementary information. An important observation is that COD removal is always greater than that of TOC, suggesting

that conversion rather than combustion plays an important role in the degradation process [23].

Evaluation of  $A_{\max}$  is experimentally simple but does not consider possible changes in color or formation of intermediates. For this reason, some studies monitor not only maximum wavelength but also the total integrated area of the spectrum in order to take into account the conversion of dye molecules to other compounds absorbing at different wavelengths [12,14,15,35]. Dye spectra can also be used to characterize the dye solution with regard to the two main absorption bands – one in the visible region and the other in the UV region. The disappearance of peaks and the appearance of new peaks in the UV and visible region indicate that dyes degrade into low-molecular-weight aromatic compounds [17,22,25,29,33,34,40,43,55,67].

Other indices are less generalized than those mentioned above: turbidity, which can be important in coagulation processes [6]; or, conductivity, which may be related to ions such as proton, nitrate or bromine [67].

Although some parameters are measured, others can be calculated using TOC, COD and  $A_{\max}$  measurements. One commonly calculated parameter is color removal, in which the initial and final  $A_{\max}$  are compared [12,14-15,22,24,26,44-48,54,62]. Another very similar parameter, if degradation processes are used [23,30,43,60], is removal efficiency or degradation efficiency, which compares the concentration of initial and final remaining dye. This parameter can be the same as color removal if the concentration is calculated using the wavelength of maximum absorbance. If TOC values are used instead of  $A_{\max}$  or concentration values, the parameter is called percentage of mineralization [61]. COD-removal efficiency can be calculated in the same way using COD values [43]. Parameters based on COD and TOC give some idea of the quality of the treated wastewater.

*3.2.1.2. Determination of sub-product or dye concentrations.* The ammonium ion is determined by the Nessler method. This ion is formed when the nitrogen-to-nitrogen double bond is attacked by a hydroxyl radical and two amino

groups are formed, which can lead to  $\text{NH}_4^+$  ions by means of successive radical attacks [55]. Other byproducts that can be determined are carbon monoxide and carbon dioxide, resulting from the gas phase of the reaction. These species can be determined using an IR-absorption detector – a large amount of  $\text{CO}_2$  detected is a sign of the complete mineralization of the dye. Ozone can also be detected using a UV-absorption detector and the presence of nitrogen oxides can be determined with a  $\text{NO}_x$  detector [39].

UV-Vis spectrophotometry with second order multivariate techniques has been used to determine the concentration of several dyes during the degradation process [7-8,52,53]. The use of these chemometric techniques enables the concentrations of the three dyes to be determined even if their spectra overlap or interferences are present. In spite of their advantages, these kinds of methods are not usually used in routine laboratory analyses.

Chromatographic and related techniques have considerable potential for determining different dyes in mixtures [68,69], but only one of the papers we reviewed uses chromatographic techniques in removal processes [49].

### **3.2.2 Monitoring and identifying reaction intermediates**

When destructive techniques are used, it is interesting to determine the degradation mechanism, the intermediates and the final degradation products. The fifth column in Table 1 shows the identification techniques employed in the papers we reviewed.

*3.2.2.1. Chromatographic techniques.* These are most frequently used for this purpose, but the sample must usually be submitted to some pretreatment. The sample to be analyzed is normally extracted with an organic solvent and evaporated to dryness or extracted using SPE cartridges, depending on the dye characteristics [22,24,32].

HPLC is the most frequently used technique, usually with a UV-visible spectrophotometer [diode-array detection (DAD)], using an interval or one fixed wavelength [22,51]. Reverse-phase chromatography with a C18 column is the

most common of these approaches. The mobile phase usually involves a mixture of water that includes buffers (e.g., ammonium acetate or sodium phosphate) and methanol [22,49,51,57] or acetonitrile [18-20,27,28,32,35,56]. Ion chromatography can be used to determine organic and inorganic ions formed during the degradation process. Carboxylic acids (e.g., methanoate or oxalate), nitrate, nitrite and ammonium are the ions most commonly identified with this technique. Other inorganic anions (e.g., sulfate or chlorine) can appear if the dye molecule contains chlorine and/or sulfur atoms [28,34,36,37]. Ion chromatography combined with other techniques (e.g., TOC) can reveal the complete mineralization of dye [51]. Ion-exclusion chromatography can be used to identify the short-chain carboxylic acids generated (e.g., formic or oxalic acids) [27,28].

High-performance liquid chromatography with mass spectrometry (HPLC-MS) is the best way to identify dye and intermediates. With this technique, byproducts and aromatic intermediates can be monitored and the reaction mechanism established [32,51]. A tandem-MS ( $MS^2$ ) detector can be used with selected-ion monitoring (SIM) mode to identify accurately and to confirm degradation intermediates. For example, in the Reactive Red 120 ozonation process, intermediates (e.g., phenol and hydroxysulfobenzenes) were detected [34], and, in the Brilliant Blue and Sunset Yellow photodegradation process, substituted naphthalenes were found [57].

High-performance capillary electrophoresis (HPCE) with a UV detector is useful for determining some dyes and their byproducts (mainly aromatic amines), which have an ionic character. During the degradation period the dye peak decreases, then new peaks appear and finally the peaks disappear, indicating that the dye has degraded into smaller, undetectable molecular compounds [67]. If an MS detector is used, byproducts can be identified more accurately. To identify abundant intermediates better, an electrospray ionization (ESI) source can be used as it causes minimal fragmentation in sulfonated azo dyes. This technique has been used to study the biodegradation of Orange II, Acid Orange 8, Food Yellow 3, Acid Orange 7 and Mordant Violet 5, the most common identification being benzenesulfonic and hydroxybenzenesulfonic acids [20,21].

Gas chromatography (GC) is not the best choice for these analytes because of the poor thermal stability and low volatility of dyes (e.g., sulfonated azo dyes). Despite these disadvantages, GC-MS can easily be used to identify most intermediates (including aromatic amines) and analyze reaction pathways [34]. If necessary, intermediates can be derivatized to verify their structure (e.g., in the biodegradation of methyl orange the samples were esterified and trimethylsilylated) [18]. However, due to the complexity of the reaction system and the formation of inorganic salts in the reaction, it is not possible to carry out a quantitative analysis of organic moieties using GC-MS [36,42,43,51].

*3.2.2.2. Spectroscopic techniques.* These techniques are used less often than separation techniques for the identification of intermediates because they have low selectivity. The most common technique is Fourier-transform infrared (FTIR) spectroscopy [16,22,44], which shows structural changes in the dye molecules and the metabolites of the dye degradation. Due to the aromaticity of most organic dyes, peaks attributed to =C-H bending and C-O-H stretching are frequently found. Other commonly found peaks are those corresponding to aromaticity. After degradation, two peaks can usually be found in the aliphatic-amine zone, while peaks corresponding to the azo group and primary and secondary amines are completely absent. With this technique the appearance of some ions can also be monitored with peaks that indicate the formation of  $\text{ClO}_3^-$  and  $\text{OCl}^-$ ,  $\text{HCO}_3^-$  or  $\text{NO}_3^-$ , depending on the initial dye. The presence of C-N symmetric stretching indicates the asymmetric cleavage of these dyes, which can be useful in predicting degradation mechanisms.

Despite its potential to determine reaction intermediates and to evaluate the degradation process, nuclear magnetic resonance (NMR) is less used as a technique. It can show whether the initial dye signals of the aromatic protons (6-9 ppm) decrease continuously and whether significant amounts of any intermediate are generated. The lack of predominant reaction products indicates that the degradation process involves reactive radicals, which can oxidize most of the intermediate-reaction products [13].

Surface-enhanced Raman spectroscopy (SERS) can be used in conjunction with a heterogeneous catalyst. With this powerful technique, lower detection limits can be obtained, because it is capable of recording the behavior of the reaction molecules on the catalyst surface to single-molecule sensitivity without interference from water molecules. Raman can be combined with UV-visible to compare the behavior of degradation processes in aqueous solution and on the surface of the catalyst. In SERS spectra for dye molecules, several Raman bands can be assigned to C-C-C bending and C-C stretching vibrations of dye molecules. It has been observed that the major Raman bands gradually lose intensity over time and no new bands emerge, indicating dye degradation [70].

Table 3 presents some general characteristics of the separation and spectroscopic techniques, which are important in the determination of reaction intermediates.

**Table 3.** Some characteristics of analytical techniques used in dye-removal processes.

Analytical techniques	Advantages	Limitations
Separation techniques (HPLC, HPCE, GC, ...)	<ul style="list-style-type: none"> <li>- High selectivity</li> <li>- Degradation byproducts can be accurately identified with an MS detector</li> </ul>	<ul style="list-style-type: none"> <li>- Analysis time can be high</li> <li>- Samples normally need to be pretreated</li> <li>- Organic solvents need to be used</li> </ul>
Spectroscopic techniques (UV-vis, FTIR, NMR, SERS, ...)	<ul style="list-style-type: none"> <li>- Low analysis time</li> <li>- Sample pretreatment is simple or not necessary</li> <li>- Dyes can be determined on the catalyst surface (SERS)</li> <li>- Chemometrics can be used to simultaneously identify and quantify several dyes and intermediates</li> </ul>	<ul style="list-style-type: none"> <li>- Low selectivity</li> <li>- The presence of interferents (degradation byproducts) can lead to erroneous results</li> <li>- Expensive deuterated solvents need to be used (NMR)</li> </ul>

#### 4. Concluding remarks and future outlook

The papers that we have reviewed prove that there is a huge body of work on degradation processes and the analytical techniques for monitoring them. In our opinion, research into dye degradation can develop in three main areas:

- (1) study of developments in removal processes;

- 
- (2) improvement of experimental designs to optimize removal processes;  
and,
  - (3) improvement of multi-component analyses.

#### **4.1. Study of developments in elimination processes**

One way of improving processes would be develop new materials (e.g., adsorbents, catalysts or microorganisms). Immobilizing photocatalysts or microbial systems on inert surfaces can improve bioreactor efficiency and favor the recovery of the catalyst. Also, the combination of various dye-removal techniques gives rise to synergistic effects that can markedly reduce reaction time and economic cost.

#### **4.2. Improvement of experimental designs**

We believe that, in this area, two aspects will be developed in the future:

- (1) experimental results will be used to choose the most influential factors, perhaps by first conducting a screening experimental design (e.g., a Plackett-Burman or saturated fractional factorial)
- (2) attempts will be made to analyze more than one response in the optimization stage, which requires finding optimal compromises between all the responses considered; in these cases, the use of desirability functions could be of great interest.

#### **4.3. Improvement of multicomponent analyses**

Separation techniques, specifically HPLC, could extend the application of multi-component analyses and establish new methodologies (e.g., kinds of technique, phases and detectors). Related techniques [e.g., multi-syringe chromatography (MSC) or ultra-fast liquid chromatography (UFLC)], which may reduce analysis time, might also be developed. Also to be expected is the development of spectrophotometric techniques (UV-visible, FTIR, NMR or SERS) linked to chemometric tools, particularly multi-way analysis.



## Acknowledgements

The authors would like to thank the Spanish Ministry of Science and Innovation (Project CTQ2007-61474/BQU) for economic support and for providing Cristina Fernández with a doctoral fellowship (AP2007-03788).

## References

- [1] M.A. Rauf, S.S. Ashraf, *J. Hazard. Mater.* 166 (2009) 6-16.
- [2] C.I. Pearce, J.R. Lloyd, J.T. Guthrie, *Dyes Pigm.* 58 (2003) 179-196.
- [3] U.G. Akpan, B.H. Hameed, *J. Hazard. Mater.* 170 (2009) 520-529.
- [4] F.P. van der Zee, S. Villaverde, *Water Res.* 39 (2005) 1425-1440.
- [5] O. Soonan, T. Eiichi, H. Makoto, H. Tadashi, *J. Environ. Sci.* 20 (2008) 952-956.
- [6] F. Harrelkas, A. Azizi, A. Yaacoubi, A. Benhammou, M.N. Pons, *Desalination* 235 (2009) 330-339.
- [7] V. Gómez, M.S. Larrechi, M.P. Callao, *Chemosphere* 69 (2007) 1151-1158.
- [8] V. Gómez, M.P. Callao, *Talanta* 77 (2008) 84-89.
- [9] R. Lin, B. Chen, G. Chen, J. Wu, H. Chiu, S. Suen, *J. Membr. Sci.* 326 (2009) 117-129.
- [10] T. Robinson, G. McMullan, R. Marchant, P. Nigam, *Bioresour. Technol.* 77 (2001) 247-255.
- [11] O. Çinar, S. Yasar, M. Kertmen, K. Demiröz, N.O. Yigit, M. Kitis, *Process Saf. Environ. Prot.* 86 (2008) 455-460.
- [12] R.O. Cristovao, A.P.M. Tavares, J.M. Loureiro, R.A.R. Boaventura, E.A. Macedo, *Environ. Technol.* 29 (2008) 1357-1364.
- [13] N. Casas, P. Blánquez, X. Gabarrell, T. Vicent, G. Caminal, M. Sarrà, *Environ. Technol.* 28 (2007) 1103-1110.
- [14] A.P.M. Tavares, R.O. Cristovao, J.M. Loureiro, R.A.R. Boaventura, E.A. Macedo, *J. Hazard. Mater.* 162 (2009) 1255-1260.
- [15] A.P.M. Tavares, R.O. Cristovao, J.M. Loureiro, R.A.R. Boaventura, E.A. Macedo, *J. Chem. Technol. Biotechnol.* 83 (2008) 1609-1615.
- [16] V. Vitor, C.R. Corso, *J. Ind. Microbiol. Biotechnol.* 35 (2008) 1353-1357.
- [17] S. Kalme, S. Jadhav, M. Jadhav, S. Govindwar, *Enzyme Microb. Technol.* 44 (2009) 65-71.
- [18] P. Seesuriyachan, S. Takenaka, A. Kuntiya, S. Klayraung, S. Murakami, K. Aoki, *Water Res.* 41 (2007) 985-992.
- [19] L.V. González-Gutiérrez, G. González-Alatorre, E.M. Escamilla-Silva, *World J. Microbiol. Biotechnol.* 25 (2009) 415-426.
- [20] Y. Lu, D.R. Phillips, L. Lu, I.R. Hardin, *J. Chromatogr., A* 1208 (2008) 223-231.

- [21] X. Zhao, Y. Lu, D.R. Phillips, H. Hwang, I.R. Hardin, *J. Chromatogr., A* 1159 (2007) 217-224.
- [22] S. Raghu, C.W. Lee, S. Chellammal, S. Palanichamy, C.A. Basha, *J. Hazard. Mater.* 171 (2009) 748-754.
- [23] C. Carvalho, A. Fernandes, A. Lopes, H. Pinheiro, I. Gonçalves, *Chemosphere* 67 (2007) 1316-1324.
- [24] M.G. Neelavannan, M. Revathi, C.A. Basha, *J. Hazard. Mater.* 149 (2007) 371-378.
- [25] N. Mohan, N. Balasubramanian, C.A. Basha, *J. Hazard. Mater.* 147 (2007) 644-651.
- [26] M.S. Lucas, A.A. Dias, A. Sampaio, C. Amaral, J.A. Peres, *Water Res.* 41 (2007) 1103-1109.
- [27] S. Hammami, N. Oturan, N. Bellakhal, M. Dachraoui, M.A. Oturan, *J. Electroanal. Chem.* 610 (2007) 75-84.
- [28] M.A. Oturan, E. Guivarch, N. Oturan, I. Sirés, *Appl. Catal., B* 82 (2008) 244-254.
- [29] M. Panizza, G. Cerisola, *Water Res.* 43 (2009) 339-344.
- [30] B. Gözmen, B. Kayan, A.M. Gizir, A. Hesenov, *J. Hazard. Mater.* 168 (2009) 129-136.
- [31] A.C.V. dos Santos, J.C. Masini, *Talanta* 77 (2009) 1081-1086.
- [32] M. Constapel, M. Schellenträger, J.M. Marzinkowski, S. Gäb, *Water Res.* 43 (2009) 733-743.
- [33] C. Wu, H. Ng, *J. Hazard. Mater.* 152 (2008) 120-127.
- [34] F. Zhang, A. Yediler, X. Liang, *Chemosphere* 67 (2007) 712-717.
- [35] M.M. Tauber, G.M. Gübitz, A. Rehorek, *Bioresour. Technol.* 99 (2008) 4213-4220.
- [36] S. Song, H. Ying, Z. He, J. Chen, *Chemosphere* 66 (2007) 1782-1788.
- [37] S. Vajnhandl, A.M. Le Marechal, *J. Hazard. Mater.* 141 (2007) 329-335.
- [38] J. Wang, Z. Jiang, L. Zhang, P. Kang, Y. Xie, Y. Lv, R. Xu, X. Zhang, *Ultrason. Sonochem.* 16 (2009) 225-231.
- [39] M. Magureanu, D. Piroi, F. Gherendi, N.B. Mandache, V. Parvulescu, *Plasma Chem. Plasma Process* 28 (2008) 677-688.
- [40] M. Magureanu, N.B. Mandache, V.I. Parvulescu, *Plasma Chem. Plasma Process* 27 (2007) 589-598.
- [41] Y. Zhang, J. Zheng, X. Qu, H. Chen, *J. Colloid Interface Sci.* 316 (2007) 523-530.
- [42] L. Lei, Q. Dai, M. Zhou, X. Zhang, *Chemosphere* 68 (2007) 1135-1142.
- [43] M. Zhou, J. He, *Electrochim. Acta.* 53 (2007) 1902-1910.
- [44] Y. Zhang, D. Li, Y. Chen, X. Wang, S. Wang, *Appl. Catal., B* 86 (2009) 182-189.
- [45] L. Wojnarovits, E. Takacs, *Radiat. Phys. Chem.* 77 (2008) 225-244.
- [46] F.H. Abdullah, M.A. Rauf, S.S. Ashraf, *Dyes Pigm.* 72 (2007) 349-352.
- [47] B.K. Körbahti, M.A. Rauf, *Chem. Eng. J.* 138 (2008) 166-171.
- [48] M.A. Rauf, N. Marzouki, B.K. Körbahti, *J. Hazard. Mater.* 159 (2008) 602-609.
- [49] W. Baran, E. Adamek, A. Makowski, *Chem. Eng. J.* 145 (2008) 242-248.
- [50] R. Jain, M. Mathur, S. Sikarwar, A. Mittal, *J. Environ. Manage.* 85 (2007) 956-960.

- [51] M. Sleiman, D. Vildoza, C. Ferronato, J.M. Chovelon, *Appl. Catal., B* 77 (2007) 1-11.
- [52] C. Fernández, M.S. Larrechi, M.P. Callao, *Talanta* 79 (2009) 1292-1297.
- [53] C. Fernández, M.S. Larrechi, M.P. Callao, *J. Hazard. Mater.* 180 (2010) 474-480.
- [54] S.K. Kansal, M. Singh, D. Sud, *J. Hazard. Mater.* 141 (2007) 581-590.
- [55] A.R. Khataee, M.N. Pons, O. Zahraa, *J. Hazard. Mater.* 168 (2009) 451-457.
- [56] A.B. Prevot, D. Fabbri, E. Pramauro, C. Baiocchi, C. Medana, *J. Chromatogr., A* 1202 (2008) 145-154.
- [57] F. Gosetti, P. Frascarolo, E. Mazzucco, V. Gianotti, M. Bottaro, M.C. Gennaro, *J. Chromatogr., A* 1202 (2008) 58-63.
- [58] M.B. Kasiri, H. Aleboyeh, A. Aleboyeh, *Environ. Sci. Technol.* 42 (2008) 7970-7975.
- [59] C.S.D. Rodrigues, L.M. Madeira, R.A.R. Boaventura, *J. Hazard. Mater.* 164 (2009) 987-994.
- [60] I.A. Sengil, M. Ozacar, *J. Hazard. Mater.* 161 (2009) 1369-1376.
- [61] A. Aleboyeh, M.E. Olya, H. Aleboyeh, *J. Hazard. Mater.* 162 (2009) 1530-1535.
- [62] I.T. Peternel, N. Koprivanac, A.M.L. Bozic, H.M. Kusic, *J. Hazard. Mater.* 148 (2007) 477-484.
- [63] I. Arslan-Alaton, G. Tureli, T. Olmez-Hanci, *J. Photochem. Photobiol., A* 202 (2009) 142-153.
- [64] D.C. Montgomery, *Design and Analysis of Experiments*, John Wiley&Sons, New York, 1997.
- [65] A. Pasamontes, M.P. Callao, *Talanta* 68 (2006) 1617-1622.
- [66] C. Reguera, M.C. Ortiz, A. Herrero, L.A. Sarabia, *Talanta* 75 (2008) 274-283.
- [67] Q. Zeng, J. Fu, Y. Shi, H. Zhu, *Ozone: Sci. Eng.* 31 (2009) 37-44.
- [68] D. Vanerková, P. Jandera, J. Hrabica, *J. Chromatogr., A* 1143 (2007) 112-120.
- [69] C. Fernández, M.S. Larrechi, R. Forteza, V. Cerdà, M.P. Callao, *Talanta* 82 (2010) 137-142.
- [70] X. Zhao, B. Zhang, K. Ai, G. Zhang, L. Cao, X. Liu, H. Sun, H. Wang, L. Lu, *J. Mater. Chem.* 19 (2009) 5547-5553.
- [71] F. Zidane, P. Drogui, B. Lekhlif, J. Bensaid, J.F. Blais, S. Belcadi, K. El kacemi, *J. Hazard. Mater.* 155 (2008) 153-163.

---

### 3.2. Optimization of photodegradation processes

This section focuses on the simultaneous photodegradation of three organic azo dyes—Acid Red 97, Acid Orange 61 and Acid Brown 425—which were obtained from the tanning industry. The experimentation proposed and discussed is in agreement with objectives (b) and (c) specified in chapter 1.

The methodologies developed record UV-visible spectra throughout the photodegradation processes and use MCR-ALS to treat the data. The influence of the operational variables is studied and the process optimized using:

- Full and fractional factorial designs to determine the most influential variables.
- Central composite designs to establish response surfaces that make it possible to model the photodegradation behavior.

As a result of this work two papers have been published: ***Study of the influential factors in the simultaneous photocatalytic degradation process of three textile dyes*** and ***Modelling of the simultaneous photodegradation of Acid Red 97, Acid Orange 61 and Acid Brown 425 using factor screening and response surface strategies***. As the titles indicate, the main aim of the first paper is to study the influence of several factors taking into account that in a simultaneous photodegradation this influence could not be the same for each of the three studied dyes. In the second paper, the methodology developed is used to extend the scope and study more variables and to obtain a response surface that relates the selected response with the studied factors.

UNIVERSITAT ROVIRA I VIRGILI

ANALYTICAL METHODOLOGIES BASED ON CHEMOMETRICS TO OPTIMIZE THE PHOTODEGRADATION OF DYES

Cristina Fernández Barrat

DL:T. 160-2012

### **3.2.1. Paper**

*Study of the influential factors in the simultaneous photocatalytic degradation process of three textile dyes*

Cristina Fernández, M. Soledad Larrechi, M. Pilar Callao

**Talanta 79 (2009) 1292-1297**



UNIVERSITAT ROVIRA I VIRGILI

ANALYTICAL METHODOLOGIES BASED ON CHEMOMETRICS TO OPTIMIZE THE PHOTODEGRADATION OF DYES

Cristina Fernández Barrat

DL:T. 160-2012

## **Study of the influential factors in the simultaneous photocatalytic degradation process of three textile dyes**

Cristina Fernández, M. Soledad Larrechi, M. Pilar Callao

*Department of Analytical and Organic Chemistry, Rovira i Virgili University,  
Marcel·lí Domingo s/n Campus Sescelades, E-43007 Tarragona, Spain*

### **Abstract**

The influence of several factors in the simultaneous photocatalytic degradation of three textile dyes - Acid Red 97, Acid Orange 61 and Acid Brown 425 - has been studied using a fractional factorial design  $2^{5-1}$ . The considered factors were: the initial concentration of each dye, the catalyst concentration ( $\text{TiO}_2$ ) and pH.

First, we developed a rapid analytical methodology based on recording UV-visible spectra during the degradation process and a data treatment using multivariate curve resolution with alternating least squares (MCR-ALS), which enabled the three dyes to be quantified simultaneously despite the overlap of their spectra.

The kinetic constant of degradation for each dye in all the experiments was evaluated. In all cases the degradation followed a first order kinetics. For a significance level of 5%, the most important factor in the photodegradation of each dye is the concentration of Acid Red 97, the degradation is more effective at higher pHs and, in the studied range, the concentration of the catalyst is not important.

**Keywords:** Photodegradation;  $\text{TiO}_2$ ; Experimental design; MCR-ALS; Textile dyes.



## 1. Introduction

Dyes are organic compounds that can be dangerous to the environment. The tanning industry uses a wide spectrum of dyes to impart colour to the leather matrix. About 10-15% of these dyes are released in effluents during the dyeing processes [1]. The discharge of coloured waste is highly problematic, firstly due to the toxic nature of some dyes or of their biodegradation products and secondly due to their visual impact because dyes are visible even at low concentrations.

Dyes in wastewater can be treated by many different processes: coagulation [2], foam flotation [3], electrochemical oxidation [4], Fenton or photo-Fenton oxidation [5,6], adsorption in waste materials [7], membranes [8], adsorption using activated carbon [9], combined coagulation/carbon adsorption [10], etc. Most of these methods are non-destructive but they generate secondary pollution, because the dyes are transferred to another phase and this phase has to be regenerated. One way to eliminate dyes without generating secondary toxic waste is photodegradation [11-15]. In this process the dyes decompose mainly to  $\text{CO}_2$ ,  $\text{H}_2\text{O}$ , and some intermediates, commonly low molecular weight acids.

In this paper we study the photocatalytic degradation process of three dyes, widely used in textile industries: Acid Red 97, Acid Orange 61 and Acid Brown 425.

In dye photodegradation studies, the dyes are usually quantified with univariate calibration, which records absorbance at one wavelength of the UV-visible spectra [11-13], or with the total carbon content determination (TOC) [14-15] during the degradation. This information only gives information about the behaviour of one species and if there is more than one dye or an interferent in the reaction medium, or if a byproduct is generated during the photodegradation, there is a risk of obtaining erroneous results.

We propose here to make a simultaneous catalytic degradation study of these dyes and evaluate the kinetic order and the corresponding degradation constants for each dye.

We first established a rapid analytical methodology, which recorded UV-visible spectra during the photodegradation process, and a data treatment using multivariate curve resolution – alternating least squares method (MCR-ALS) which allows quantification of analytes in the presence of interfering [16]. These methodologies have been applied successfully by our research group to the resolution of mixtures from data obtained using other instrumental configurations [17-18].

Subsequently, because the optimization of experimental conditions is a subject of interest in photocatalytic processes, we aimed to determine the effect of several factors on the degradation rate so that we could propose the most convenient experimental conditions for carrying out the degradation.

The effect of each variable on the reaction kinetics may not be independent, but research articles that have been published in the field of catalysis usually analyse the influent factors by varying one factor at time [13,14]. This methodology often gives limited information about the process. In the last years, can be found some papers [19-21] where the effect of some factor in the photocatalytic degradation of some dye using the response surface methodology is analyzed, but in all situations only one dye is considered.

In our case, in order to understand how several factors affected the response we used a fractional factorial design  $2^{5-1}$ . The factors considered are: the initial concentration of each dye, the amount of catalyst ( $\text{TiO}_2$ ) and the pH. A simultaneous and exhaustive analysis of all factors (as the background matrix, temperature, etc.) that could affect the feasibility of a photodegradation process of several dyes would be an excessively extensive work. The consideration of initial concentrations of each dye as a factor makes it possible to determine whether there is any competition between dyes during the photodegradation process and if the priority of degradation is conserved in any of the conditions studied. Different dyes do not have the same visual impact, which should be taken into account when fixing the optimal conditions for their degradation from a practical point of view. The present work is focussed in show a useful strategy to analyze quickly the effect

of several influential factors in a complex problem as the photodegradation of several dyes.

The responses studied are the half-life time of each dye. The significance of the effects was corroborated using an ANOVA test.

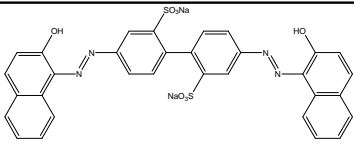
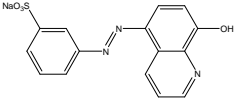
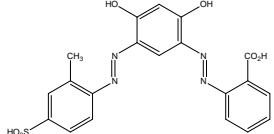
## 2. Experimental

### 2.1. Chemicals

In all analyses, we used analytical grade chemicals. These were NaOH and H<sub>2</sub>SO<sub>4</sub> from PROLABO and purified water from a Milli-Q water system from MILLIPORE, USA. The anatase form of TiO<sub>2</sub> (99.8%) (Sigma-Aldrich) was used as the photocatalyst without further treatment.

Acid Red 97, Acid Brown 425 and Acid Orange 61 dyes were obtained from Trumpler Española, S.A. (Barberà del Vallès, Barcelona, España). These compounds have acid-base characteristics, acid species and basic species have different UV-visible spectra. The acidic and basic spectra are strongly overlapped [17]. Table 1 shows some physicochemical proprieties of these dyes.

**Table 1.** Structure, name, chemical index, colour, p*K*<sub>a</sub>, λ<sub>max</sub> and molecular weight of the dyes.

Structure	Name	Colour	p <i>K</i> <sub>a</sub>	λ <sub>max</sub>	MW
	Acid Red 97	Bright yellowish red	11-12	498	698
	Acid Orange 61	Orange	2-3	446	351
	Acid Brown 425	Dull reddish brown	10-11	445	456

---

Standard buffer solutions of pH 4 and 7 (Hamilton) were used to calibrate the pH meter.

## **2.2. Instrumental and software**

The photodegradation studies were carried out in a cylindrical annular batch reactor. The reactor consists of an immersion quartz tube (2.5 cm i.d., and 38 cm long) which holds a low pressure mercury vapour lamp (LPML) of 15 W (Heraeus Noblelight, Germany). The light source emitted by the LPML is predominantly at 254 nm and the incident photon flux of the UV reactor is  $0.1 \text{ W cm}^{-1}$ . The quartz tube was placed in a Pyrex glass outer reactor (0.7 L capacity) in dark conditions.

The data were acquired and monitored by a Hewlett-Packard 8452A spectrophotometer using the HP89531A software. The spectra were recorded from 244 to 720 nm in 2 nm steps. A Crison pH meter was used to measure the pH of the samples.

Calculations for multivariate curve resolution with alternating least squares (MCR-ALS) were performed with laboratory-written software under a MATLAB 7.0 computer environment [22]. This software is available in Ref. [23]. Calculations for experimental design were performed with STATGRAPHICS Plus 5.0 [24].

## **2.3. Standards**

Individual standards of  $100 \text{ mg}\cdot\text{L}^{-1}$  for Acid Orange 61 and Acid Brown 425 and of  $50 \text{ mg}\cdot\text{L}^{-1}$  for Acid Red 97 at pH 6 in ultrapure Milli-Q water were prepared. The reference spectrum for each dye was recorded with their standard.

Using the referenced standards a total of 13 samples (see Table 2), were prepared in aqueous solution, in order to evaluate the ability of the model MCR-ALS to resolve and quantify these analytes.

## **2.4. Photocatalytic experiments**

A total of 16 photodegradation experiments were carried out. The experimental conditions of each experiment were designed according to a  $2^{5-1}$  fractional factorial experimental design. The first six columns in Table 3 show the

experimental plan. The chosen factors and their high and low levels were: 20-60 mg·L<sup>-1</sup> for the initial concentration of Acid Red 97, Acid Orange 61 and Acid Brown 425 (code-named A, B, C, respectively), 8-24 mg/500mL for the amount of catalyst (TiO<sub>2</sub>) (code-name, D) and 2-6 for the pH (code-named E). In addition, in order to evaluate the experimental error, there was prepared a triplicate sample in the experimental conditions corresponding to the central point of the experimental domain of each factor (the three last rows in the Table 3). The responses evaluated were the degradation constants of each dye and the experimental half-life time of each dye.

The degradations were carried out in a cylindrical reactor, such as the one described in section 2.2. The total volume of the solution was 500 mL. The pH was adjusted using H<sub>2</sub>SO<sub>4</sub> and NaOH solutions. The reactions were carried out at room temperature with continuous stirring, until the solution lost its colour. Six-millilitre samples were taken through the reactor using a syringe. In the first 10 min samples were taken every minute, then every 2 min (to 20 min), every 5 min (to 60 min), every 10 min (to 220 min), and every 20 min (to the end of degradation). The total volume of extracted sample varies between 180 and 240 mL, depending on the photodegradation rate in each experience. The samples were stored in dark conditions until they were centrifuged in order to separate the catalyst and record the spectra.

**Table 2.** Concentration of the calibration standards (mg·L<sup>-1</sup>).

Standard number	Dye		
	A. Red 97	A. Orange 61	A. Brown 425
1	5	5	10
2	10	10	5
3	15	20	15
4	30	15	20
5	20	25	25
6	25	30	30
7	5	5	20
8	15	5	5
9	5	20	5
10	30	30	30
11	25	35	25
12	25	40	25
13	20	45	20

**Table 3.** Experimental plan and kinetic constants of the dyes in each experiment.

Experimental Plan						Responses					
Exp	A	B	C	D	E	A. Red 97		A. Orange 61		A. Brown 425	
						$k \cdot 10^{-2}$	r	$k \cdot 10^{-2}$	r	$k \cdot 10^{-2}$	r
1	20	20	20	8	6	4.44	0.9976	3.04	0.9934	0.85	0.9426
2	60	20	20	8	2	2.41	0.9918	1.17	0.9549	1.15	0.9661
3	20	60	20	8	2	4.47	0.9938	1.83	0.9629	3.44	0.9790
4	60	60	20	8	6	1.39	0.9921	0.83	0.9804	0.44	0.9723
5	20	20	60	8	2	3.19	0.9989	3.38	0.9643	1.37	0.9817
6	60	20	60	8	6	1.49	0.9954	0.83	0.9529	0.50	0.9979
7	20	60	60	8	6	2.27	0.9950	1.57	0.9855	0.76	0.9811
8	60	60	60	8	2	1.89	0.9994	0.53	0.9277	0.99	0.9910
9	20	20	20	24	2	4.23	0.9964	1.55	0.9551	2.44	0.9811
10	60	20	20	24	6	2.06	0.9932	2.92	0.9461	0.57	0.8970
11	20	60	20	24	6	3.48	0.9984	1.95	0.9872	0.72	0.9545
12	60	60	20	24	2	1.50	0.9983	0.95	0.9356	0.08	0.9709
13	20	20	60	24	6	2.72	0.9966	2.96	0.9429	1.24	0.9493
14	60	20	60	24	2	1.70	0.9979	1.25	0.9367	0.68	0.9280
15	20	60	60	24	2	3.26	0.9982	2.11	0.9887	0.91	0.9776
16	60	60	60	24	6	0.98	0.9952	0.59	0.9901	0.33	0.9637
CP <sup>a</sup> 1	40	40	40	16	4	1.18	0.9951	0.89	0.9898	0.32	0.9459
CP <sup>a</sup> 2	40	40	40	16	4	1.33	0.9972	0.77	0.9441	0.39	0.9362
CP <sup>a</sup> 3	40	40	40	16	4	1.34	0.9977	0.78	0.9855	0.41	0.9761

<sup>a</sup> CP: central point

### 2.5. Establishment of the calibration model

The aim of the multivariate curve resolution method with alternating least squares is to transform the theoretical solution obtained by factor analysis of the experimental data matrix **D** and obtain matrices **C** and **S<sup>T</sup>** which have real chemical significance [16,25].

With this resolution method, the data matrices are modelled using Eq. (1):

$$\mathbf{D} = \mathbf{C} \cdot \mathbf{S}^T + \mathbf{E} \quad (1)$$

where **D** is the data matrix of the spectra acquired during the photodegradation process at different times, matrix **C** ( $m \times p$ ) has column vectors corresponding to the concentration profiles of the  $p$  pure components that are present in matrix **D**.

The row vectors of matrix  $\mathbf{S}^T$  ( $p \times n$ ) correspond to the spectra of the  $p$  pure components, and  $\mathbf{E}$  is the matrix of the residuals. The times and the wavelengths at which the absorbance is recorded are  $m$  and  $n$  respectively.

The resolution was performed using the strategy of augmented matrices [16]. An augmented matrix  $\mathbf{D}_{\text{aug}}$  was constructed appending in the direction of column wise, a matrix  $\mathbf{D}_1$  that contains the spectra of the 13 standards, a matrix  $\mathbf{D}_2$  that contains the spectra recorded during the photodegradation process considered and the vectors  $\mathbf{v}_i$  corresponding to the spectra of each present species in the solution.

The chemical rank of the  $\mathbf{D}_{\text{aug}}$  was estimated analyzing the value of eigenvalues obtained by singular value decomposition (SVD) [26].

The optimization step of MCR-ALS was initiated using the spectra of the individual components  $\mathbf{S}^T$ . We applied non-negativity constraints to the data matrices. To determine the efficiency of the model we used the lack of fit (lof) and correlation coefficients ( $r$ ) between the spectra used as references and those retrieved by MCR-ALS.

After the application of the curve resolution methodology, with the concentration profiles of the standards, a calibration curve of pseudo-zero order was built, as in the univariate calibration approach [27].

$$r_i = b_1 \cdot c_i + b_0 \quad (2)$$

where  $r_i$  is the relative value obtained by estimating the concentration in the resolution process (the quotient between the value of each standard relative to the most concentrated analyte) and  $c_i$  is the correspondent relative concentration. The calibration line was validated by comparing the line obtained with the line of identity (regression slope = 1, regression intercept = 0) [26].

With the concentration values obtained during each experiment a first order kinetic model was proposed using the following equation:

$$\ln \frac{C_0}{C_i} = kt \quad (3)$$

where  $C_0$  and  $C_i$  are the concentrations at time zero and time  $t$ , respectively.

### 3. Results

In order to prove the resolution possibilities of the proposed methodology, MCR-ALS was first applied to the augmented matrix  $[\mathbf{D}_1; \mathbf{v}_1; \mathbf{v}_2; \mathbf{v}_3]$ , where  $\mathbf{v}_1$ ,  $\mathbf{v}_2$  and  $\mathbf{v}_3$  are the spectra for Acid Orange 61, Acid Red 97 and Acid Brown 425, respectively. After the resolution, two matrices were obtained: a matrix  $\mathbf{C}$ , with the calculated values of the 13 calibration standards, and a matrix  $\mathbf{S}$ , containing the spectra of each standard. The spectral correlation was higher than 0.9990 for the three dyes. Using the values of matrix  $\mathbf{C}$ , a calibration line was established by applying Eq. (2). Table 4 shows the values obtained for the slopes and regression intercepts of the regression lines, the correlation coefficient and the F value calculated in the joint test of slope 1 and regression intercept 0. All the regression lines passed the test, so the methodology was considered valid for quantifying these three dyes simultaneously.

**Table 4.** Figures of merit for the calibrations of the three dyes Acid Red 97, Acid Orange 61 and Acid Brown 425.

	Dye		
	A. Red 97	A. Orange 61	A. Brown 425
$b_1$	10.126	10.112	0.9910
$b_0$	0.0098	-0.0071	0.0067
$r$	0.9987	0.9982	0.9969
$n$	13	13	13
$F_{cal}$	1.98	0.58	0.91
$F_{critic} (0.05, 2, 11)$	5.26		

As an example, Fig. 1 shows the graphic to data matrix ( $\mathbf{D}_2$ ) for the first experiment of the design. When SVD was applied to the data matrices augmented for each of the 16 degradation experiments, 4 significant components were obtained in all cases. This may be because of the presence of a degradation compound of these dyes.



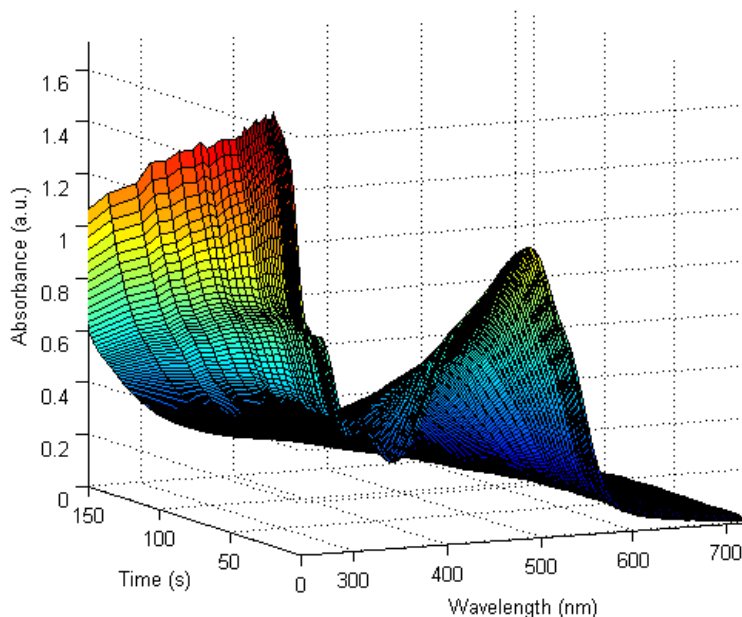


**Fig. 1.** Spectra recorded during the photodegradation process ( $D_2$ ) for the first experiment in Table 3.

Fig. 2 shows for the first experiment, the spectral and concentration profiles for the three dyes and the fourth component obtained by MCR-ALS. To improve the resolution, we have added a vector corresponding to the last degradation time at which this fourth component was predominant over the dyes studied. The figures of merit of this method for the 16 experiments were satisfactory: lof had a mean value of 1.2656, and the similarities between the spectra profiles obtained for each component and the pure spectra of each dye were evaluated by the correlation coefficient and shown to be higher than 0.9990 in all cases. Fig. 3 shows the degradation curves for each dye for the 16th experiment of the experimental design, which was the slowest one.

Assuming that in the experimental conditions the photodegradation reactions fitted to a kinetic of pseudo-first-order, the concentrations values obtained by MCR-ALS were used to calculate, using Eq. (3), a constant  $k$  representative of kinetic of each dye in each experiment. These values and the correlation coefficient of the model adjustment for each dye and experiment are

shown in the last six columns in Table 3. The correlation coefficients are close to 1 so we can conclude that the photodegradations in all the conditions studied follow a pseudo-first-order kinetic. The values obtained for the degradation constants are of the same order of magnitude as the degradation constants obtained for Methyl Orange and Rhodamine 6G [13] and for a six-dye mixture from a textile effluent [11].

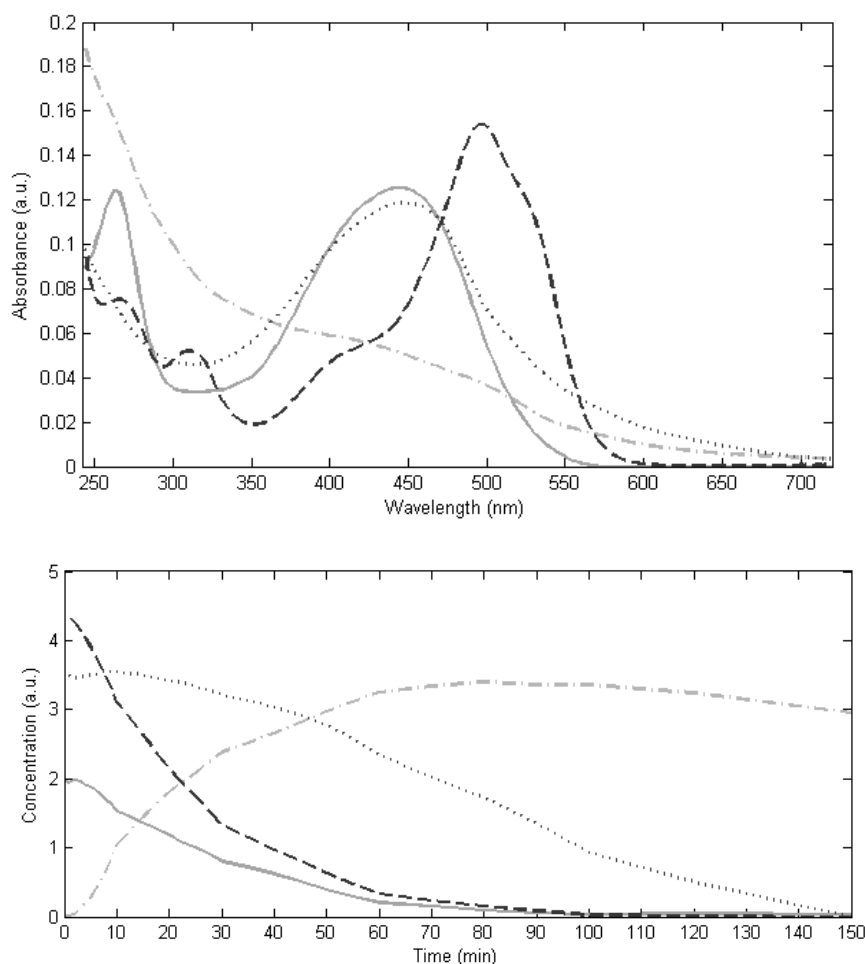


**Fig. 2.** Pure spectra and normalized concentration profiles obtained by multivariate curve resolution of the data matrix arising from the first experiment in Table 3. (--) corresponds to Acid Red 97, (-) to Acid Orange 61, (·) to Acid Brown 425 and (-·) to the new compound formed during the photodegradation.

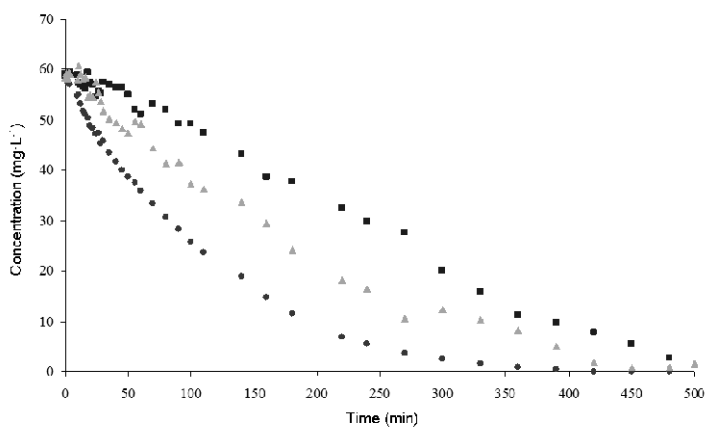


**Fig. 3.** Kinetic profiles for the 16th experiment in Table 3. (●) is Acid Red 97, (▲) is Acid Orange 61 and (■) is Acid Brown 425.

It was observed that the red dye always degraded faster than the others, and that the orange dye tended to degrade faster than the brown dye, although this was not the case in all the experiments. Some possible explanations for this behaviour are: (a) the degree and the rate of the photocatalytic degradation of each dye would be higher for the dye with higher molar absorption coefficient that is the Acid Red 97. (b) The catalyst at the working pH is charged positively (pH 2) or neutral (pH 6), so the dye with the greatest tendency to be charged negatively (red dye), has the greatest affinity in the adsorption process. Studies carried out with dyes of similar characteristics [28-30] reinforce this hypothesis. (c) Another aspect to consider in the ease of degradation is the number of azo groups present in the molecule. Azo bonds are the most active bonds in azo-dye molecules and can be oxidized by positive hole or hydroxyl radicals or reduced by electrons in the conduction band [31]. These tendencies have been reported in several studies on azo-dyes [32,33]. The orange dye, then, would be the most favourably degraded, although the results obtained showed that some mechanisms have a competitive influence on the degradation.

In order to evaluate the effect of the factors considered on the degradation kinetics, we decided to study the half-life time obtained experimentally because this response takes into account the induction period of the catalyst (that is, the

time during which the catalyst adsorbs the dyes before the degradation process starts.

Fig. 4. shows the Pareto chart obtained for each dye. It can be observed that most of the effects of the factors considered are positive. To evaluate the importance of these effects, we used an ANOVA test [27]. Table 5 shows the values of the relevant factors for the significance level considered.

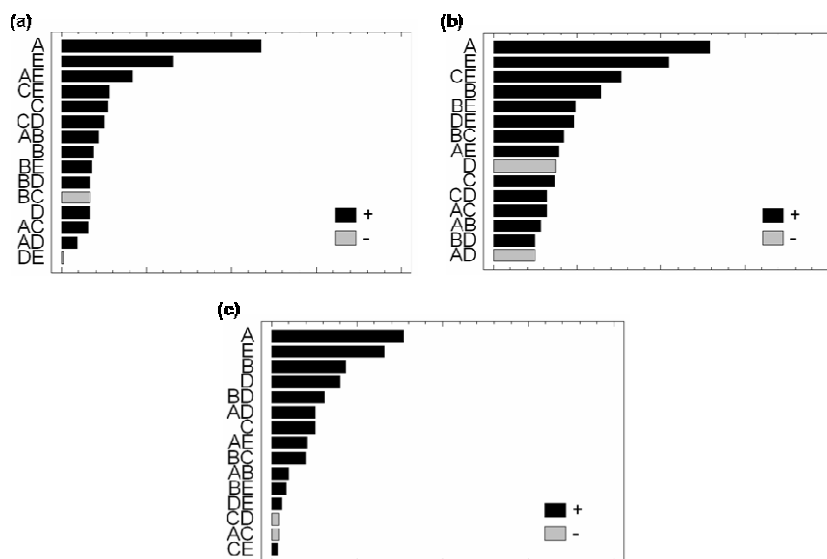


**Fig. 4.** Pareto charts from the fractional factorial design considering the  $t_{1/2}$  of each dye as response. **(a)** corresponds to Acid Red 97, **(b)** to Acid Orange 61 and **(c)** to Acid Brown 425.

**Table 5.** Results of ANOVA test for the relevant factors

Dye	Effect	d.f.	SS x 10 <sup>+3</sup>	MS x 10 <sup>+3</sup>	F <sub>cal</sub>
A. Red 97	A	1	3.192	3.192	48.861
A. Orange 61	A	1	6.765	6.765	241.609
	B	1	1.660	1.660	59.306
	E	1	4.455	4.455	159.127
	CE	1	2.376	2.376	84.877
A. Brown 425	A	1	13.225	13.225	106.653
	E	1	9.801	9.801	79.040
F <sub>critic</sub> (1,2,0,05)		38.5			

The commented results can indicate that: (a) the concentration of red dye has an important effect on the behaviour of the three dyes. As has been mentioned

above, this dye has a great tendency to be adsorbed on the catalyst, which blocks the surface of the catalyst to a greater or lesser extent (depending on the concentration) thus affecting the behaviour of other species. (b) The concentration of catalyst is not a relevant factor in the degradation of any dye. Since is known that when the catalyst loading increases the adsorption and degradation also increase, one possible interpretation of the obtained results is that our range of catalyst concentrations was too small to detect its influence and as a consequence small changes in its concentration do not affect the degradation process.

The other factors influence the degradation of each dye in a different way. The red dye degradation was not affected by the concentration of the other two dyes. This may be because this dye degrades very easily and because the other two dyes do not compete in the degradation process. Although the ANOVA test shows that pH is not an influential factor for the level of significance considered, the Pareto chart for this dye (Fig. 4a) shows that the pH and its interaction with the red dye concentration are the following influential factors in the degradation. This result can indicate that a higher pHs higher degradation periods have been obtained, probably because the catalyst reduces their positive charge and this fact difficult the adsorption process of the dye.

As well as the red dye concentration mentioned above, the factors that affect orange dye degradation are the pH, the concentration of orange dye and the interaction between the pH and the brown dye concentration. The reasons why pH has an influence may be the same as those for the red dye. The influence of the initial concentration is as expected. The interaction between the pH and the brown dye concentration is important because the concentration is indirectly influenced by the pH of the solution. This influence is strong at high pH because the two dyes start to compete in the adsorption process on the catalyst.

The brown dye is affected by the red dye concentration and the pH, which have the same effect as the cases above. The Pareto chart (Fig. 4c) shows that the next most influential factors are the catalyst concentration and the orange dye concentration. It should be pointed out that its own concentration does not affect its degradation. To explain this result, which at first sight is surprising, we must

take into account that the considered response is the half-life time and that the three dyes compete in a degradation process in which the brown dye is the least favoured. Probably if longer times of degradation are considered, in which the other dyes have had time to disappear from the medium, the concentration of brown dye may be important for its own degradation.

#### **4. Conclusions**

Using spectrophotometric measurements in the UV-visible region during the degradation process and the curve resolution method MCR-ALS, a rapid methodology can be established for simultaneously quantifying three dyes - Acid Red 97, Acid Orange 61 and Acid Brown 425 - despite the presence of unknown interferences.

Photodegradation using  $\text{TiO}_2$  as catalyst is efficient at removing the three acid dyes from wastewater. The kinetics of these degradations follows a first-order model and a new compound, probably of low molecular weight, appears.

Experimental design methodology allows to determine the influence of the factors considered on the half-life time of the dyes and shows that the most important factor in photodegradation is the initial concentration of Acid Red 97, that the amount of catalyst does not affect the response in the studied region for a significance level of 5%, that photocatalysis is more effective at pH 6 and that the photodegradation process is competitive because the adsorption of the dyes in the catalyst depends on their concentration in the solution.

#### **Acknowledgements**

The authors would like to thank Trumpler Española, S.A., for supplying the synthetic dyes and the Spanish Ministry of Science and Innovation (Project CTQ2007-61474/BQU) for economic support and for providing Cristina Fernández with a doctoral fellowship (AP2007-03788).

## References

- [1] A.A. Vaida, K.V. Datye, *Colourage* 14 (1982) 3-10.
- [2] S. Papic, N Koprivanac and Loncaric Bozic, *J. Soc. Dyers Color* 116 (2000) 352-358.
- [3] S.H. Lin, C.C. Lo, *Environ. Technol.* 17 (1996) 841-849.
- [4] V. López-Grimau, M.C. Gutiérrez, *Chemosphere* 62 (2006) 106-112.
- [5] J.M. Monteagudo, A. Durán, C. López-Almodóvar, *Appl. Catal., B* 83 (2008) 46-55.
- [6] L. Núñez, J.A. García-Hortal, F. Torrades, *Dyes Pigm.* 73 (2007) 1-6.
- [7] A. Bousher, X. Shen, R.G.J. Edyvean, *Water Res.* 31 (1997) 2084-2092.
- [8] M. Arami, N.Y. Limaee, N.M. Mahmoodi, *Chemosphere* 65 (2006) 1999-2008.
- [9] V. Gómez, M.S. Larrechi, M.P. Callao, *Chemosphere* 69 (2007) 1151-1158.
- [10] S. Papic, N. Koprivanac, A.L. Bozic, A. Metes, *Dyes Pigm.* 62 (2004) 291-298.
- [11] O. Prieto, J. Feroso, Y. Nuñez, J.L. del Valle, R. Irusta, *Sol. Energy* 79 (2005) 376-383.
- [12] M. Sameiro, T. Gonçalves, E.M.S. Pinto, P. Nkeonye, A.M.F. Oliveira-Campos, *Dyes Pigm.* 64 (2005) 135-139.
- [13] S. K. Kansal, M. Singh, D. Sud, *J. Hazard. Mater.* 141 (2007) 581-590.
- [14] I.T. Peternel, N. Koprivanac, A.M.L. Bozic, H.M. Kusic, *J. Hazard. Mater.* 148 (2007) 477-484.
- [15] M. Qamar, M. Saquib, M. Muneer, *Desalination* 186 (2006) 255-271.
- [16] R. Tauler, *Chemom. Intell. Lab. Syst.* 30 (1995) 133-146.
- [17] V. Gómez, J. Font, M.P. Callao, *Talanta* 71 (2007) 1393-1398.
- [18] M. Bosco, M. S. Larrechi, *Anal. Bioanal. Chem.* 390 (2008) 1203-1207.
- [19] J. Nieto, J. Freer, D. Contreras, R.J. Candal, E.E. Sileo, H.D. Mansilla, *J. Hazard. Mater.* 155 (2008) 45-50.
- [20] A.F. Caliman, C. Cojocar, A. Antoniadis, I. Poullos, *J. Hazard. Mater.* 144 (2007) 265-273.
- [21] B.K. Körbahti, M.A. Rauf, *Chem. Eng. J.* 136 (2008) 25-30.
- [22] Matlab, The Mathworks, South Natick, MA, USA.
- [23] <http://www.ub.es/gesq/mcr/mcr.htm>.
- [24] <http://www.statgraphics.com>.
- [25] J. Jaumot, R. Gargallo, A. de Juan, R.Tauler, *Chemom. Intell. Lab. Syst.* 76 (2005) 101-110.
- [26] D.L. Massart, B.G.M. Vandeginste, et al., *Handbook of Chemometrics and Qualimetrics Part A*, Elsevier, Amsterdam, 1997.
- [27] N.M. Faber, *Chemom. Intell. Lab. Syst.* 50 (2000) 107-114.
- [28] M. Luo, D. Bowden, P. Brimblecombe, *Water Air Soil Pollut* 198 (2009) 233-241.
- [29] W.Y. Wang, Y. Ku, *Colloids Surf. A* 302 (2007) 261-268.
- [30] W. Baran, A. Makowski, W. Wardas, *Dyes Pigm.* 76 (2008) 226-230.

- [31] S. Mozia, M. Tomaszewska, A.W. Morawski, *Desalination* 185 (2005) 449-456.
- [32] Z. Zainal, L.K. Hui, M.A. Hussein, Y.H. Taufiq-Yap, A.H. Abdullah, I. Rambla, *J. Hazard. Mater.* 125 (2005) 113-120.
- [33] E. Forgacs, T. Cserhádi, G. Oros, *Environ. Int.* 30 (2004) 953-971.



UNIVERSITAT ROVIRA I VIRGILI

ANALYTICAL METHODOLOGIES BASED ON CHEMOMETRICS TO OPTIMIZE THE PHOTODEGRADATION OF DYES

Cristina Fernández Barrat

DL:T. 160-2012

### **3.2.2. Paper**

*Modelling of the simultaneous photodegradation of Acid Red 97, Acid Orange 61 and Acid Brown 425 using factor screening and response surface strategies*

Cristina Fernández, M. Soledad Larrechi, M. Pilar Callao

**Journal of Hazardous Materials 180 (2010) 474-480**



UNIVERSITAT ROVIRA I VIRGILI

ANALYTICAL METHODOLOGIES BASED ON CHEMOMETRICS TO OPTIMIZE THE PHOTODEGRADATION OF DYES

Cristina Fernández Barrat

DL:T. 160-2012

---

## **Modelling of the simultaneous photodegradation of Acid Red 97, Acid Orange 61 and Acid Brown 425 using factor screening and response surface strategies**

Cristina Fernández, M. Soledad Larrechi, M. Pilar Callao

*Department of Analytical and Organic Chemistry, Rovira i Virgili University,  
Marcel·lí Domingo s/n Campus Sescelades, E-43007 Tarragona, Spain*

### **Abstract**

In this paper the influence of seven variables that could be relevant in the photodegradation of three textile dyes – Acid Red 97, Acid Orange 61 and Acid Brown 425 – has been studied with the aim of determining the most efficient conditions for this process. The type and concentration of catalyst, the presence and concentration of  $H_2O_2$ , the stirring, the pH and the dye concentration have been studied as variables. In the first stage the more basic variables were analyzed using a screening methodology (saturated fractional factorial design) and it was concluded that the most influential variable was the presence of  $H_2O_2$ . In the second stage, a central composite design was used to establish a response surface for the behaviour of the photodegradation. In this stage the concentration of Acid Brown 425 was fixed and the degradation was carried out without catalyst. The most remarkable aspects of the experiment are that brown dye is always the most persistent in the solution and that a catalyst is not needed to degrade the dyes quickly. A second-order equation is needed to model this process. The response surface obtained could be useful for reducing the time and money needed to treat effluent wastewater.

**Keywords:** Photolysis; Textile dyes degradation; Sulphonated azo dyes; Experimental design.

## 1. Introduction

The presence of dyes in wastewater is an important environmental problem and many processes have been proposed for eliminating them such as physicochemical treatments involving adsorption onto activated carbon [1], adsorption onto waste materials that are used as low cost adsorbents [2], electrochemical oxidation [3] and biodegradation [4]. In recent years technologies based on advanced oxidation processes have been shown to be efficient procedures. In these processes, highly reactive species (mainly hydroxyl radicals) are used as primary oxidants and no secondary pollution is generated [5]. Some examples of these processes are the photo-Fenton process, in which hydroxyl radicals are generated using iron catalysers and oxygen peroxide [6,7], photolysis, in which the radicals are formed when an oxidant, normally  $H_2O_2$ , is irradiated with UV radiation [8-12] photocatalysis, in which a semiconductor adsorbs UV radiation and generates redox reactions that eliminate the contaminants [13,14], ozonation processes, in which ozone is used as an oxidant [15] and even a combination of electrochemical and photocatalytic processes [16].

There has been much research into determining the most efficient conditions for these processes and in recent years experimental designs have been used because it is known that the ability to systematically remove dyes will vary depending on the synergistic or antagonistic action between different variables. Most studies apply this methodology to the degradation of one dye [5,11,13,15,17-19]. Experimental designs have been used also to study the degradation of dye mixtures using the maximum absorbance of the dyes at different wavelengths [20-22] or the concentration values of the different dyes over time using multivariate methodologies [14,23].

In a previous study [14], our research group developed a rapid methodology that applied the multivariate curve resolution with alternating least squares method (MCR-ALS) to the set of spectra obtained in the UV-Vis during the catalytic photodegradation process of three dyes (Acid Red 97, Acid Orange 61 and Acid Brown 425) using  $TiO_2$  as catalyst. The aim of MCR-ALS method is to decompose a data matrix composed by  $m$  rows (spectra recorded at different

---

times) and  $n$  columns (absorbance at different wavelengths) in a product of two matrices, one corresponding to the concentration profiles of each compound along the time and another that contains information about the spectral profiles of these compounds [14,24]. This allows the concentrations of the three dyes to be determined over the time of degradation despite their spectra overlapping. In this study we also concluded that the initial concentration of Acid Red 97 has a critical effect on the simultaneous photodegradation of the three dyes.

The primary aim of the actual study is to extend the scope of the previously developed methodology so as to (a) increase the number of variables in order to determine the effect of multiple variables on the photodegradation process and (b) to apply different experimental methodologies to obtain the maximum information with the minimum experimental cost.

The studied variables and their domain were selected according to a previous knowledge and bibliographic revision. The chosen variables were the type of catalyst, the catalyst concentration, the pH, the oxidant concentration and the presence of stirring. We used ZnO and TiO<sub>2</sub> as catalysts because their efficiency in photodegradation processes has been demonstrated [25]. The oxidant H<sub>2</sub>O<sub>2</sub> was employed to determine its influence on the process [18,26]. The pH range was chosen on the basis of Kansas et al.'s findings [25]. The catalyst concentration was selected from a previous study [14]. The presence of stirring was evaluated because could be relevant in the simplicity of the process.

To achieve this, first, we employed a screening factor methodology (a saturated fractional factorial, 2<sup>5-2</sup>) because this kind of design allows to obtain the main effects of the variables and new experiences could be added, using the experimentation carried out, if more information is required. Secondly, we used the information obtained in the screening process to reduce the number of variables and to find a suitable approximating function in order to predict the behavior of the degradation. For this, we have used a central composite design, that allows to obtain the main effects of the variables, the quadratic effects and the interactions. With this design a second-order response surface could be established.

To our knowledge, no study has investigated screening as an initial step for creating a response surface for dye degradation processes. We are also unaware of any paper that has modelled the effect of various experimental variables on the behavior of various dyes, despite the fact that many residual waters contain several dyes simultaneously.

## **2. Experimental**

### **2.1. Chemicals**

We used analytical grade chemicals in all the analyses. These were NaOH and H<sub>2</sub>SO<sub>4</sub> from PROLABO and purified water from a Milli-Q water system from MILLIPORE, USA. We used H<sub>2</sub>O<sub>2</sub> (30%) from Scharlau as an oxidant. In the screening process, we used TiO<sub>2</sub> in the anatase form (99.8%) and ZnO powder <1µm (99,9%) as photocatalysts without further treatment and these were obtained from Sigma-Aldrich.

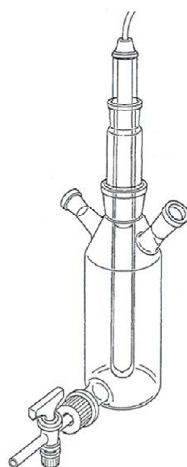
Dyes were obtained from Trumpler Española, S.A. (Barberà del Vallès, Barcelona, Spain). Solutions of dyes were prepared in Ultrapure Milli-Q water.

### **2.2. Instrumental and software**

Photodegradation studies were carried out in the cylindrical annular batch reactor illustrated in Fig. 1. The data were acquired and monitored with a Hewlett-Packard 8452A spectrophotometer using HP89531A software. The spectra were recorded from 244 to 720 nm in 2 nm steps.

A Crison pH meter was used to measure the pH of the samples. The pH meter was calibrated each day.

Multivariate curve resolution with alternating least squares (MCR-ALS) was performed using software written in the laboratory with a MATLAB 6.5 computer environment [27]. This software can be found in Ref. [28]. Calculations for the experimental design were made using STATGRAPHICS Plus 5.0 [29] and The Unscrambler 9.0 [30].



Immersion quartz tube (2.5 cm  
i.d. and 38 cm in length)

Light source: Low pressure  
mercury vapor lamp (LPML)

15 W

$\lambda = 254$  nm

Heraeus Noblelight, Germany

Capacity of 0.7 L

**Fig. 1.** Photoreactor scheme.

### **2.3. Photodegradation procedure**

Degradation samples were prepared diluting different amounts of each dye according to the values indicated by the experimental designs in the corresponding experience. The pH was adjusted using  $\text{H}_2\text{SO}_4$  and NaOH solutions and the final sample volume was 500 mL. Degradations were carried out in a cylindrical reactor and different samples of 6 mL of the degradation solution were taken from the reactor during the degradation time. After photodegradation, all the samples were stored in dark conditions and samples containing catalyst were centrifuged in order to separate the catalyst and register the spectra. More details of the experiment can be found in Ref. [14].

### **2.4. Experimental design**

In this paper the photodegradation of the dyes is studied using experimental designs. The different experiments are designed, firstly, according a saturated factorial fractional design and, secondly, according a response surface design. The variables are codified with low and high levels. Each experiment was evaluated by analyzing the response that was related to the reaction rate. Each experience provides a matrix with the spectra obtained throughout the degradation time. In order to improve the results we constructed a new matrix that is the experimental matrix augmented with the pure dye spectra. The spectrum of  $\text{H}_2\text{O}_2$  was added to the augmented matrix in the resolutions of the experiments in which



this oxidant was used. The augmented matrices were treated with MCR-ALS. This methodology allowed us to quantify each dye at each moment of the degradation, despite the overlap of their spectra, to construct the degradation curves and to determine either the half-life time of each dye or the remaining concentration at a particular time. As an example in Fig. 2 is represented the degradation spectra and the concentration profiles recovered by MCR-ALS of one experience carried out.

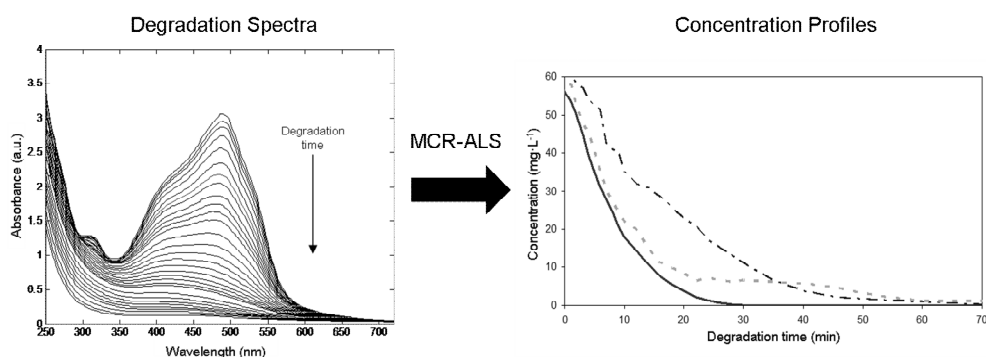


**Fig. 2.** Degradation spectra and concentration profiles of each dye recovered by MCR-ALS. (-) Corresponds to Acid Red 97, (. . .) to Acid Orange 61 and (-.-.-) to Acid Brown 425. Experimental conditions: concentration of each dye =  $60 \text{ mg}\cdot\text{L}^{-1}$ ,  $\text{H}_2\text{O}_2$  concentration =  $0.005 \text{ M}$ ,  $\text{pH} = 2$ , without catalyst and with stirring.

### 2.4.1. Screening step

In the screening designs, the relation between the information obtained about the influence of the variables and the number of experiments is high. For this reason, these designs are employed when there are many controllable variables that may influence the experiment [31]. These designs allow us to determine the main effects of the variables without taking into account the possible effect of interactions between variables that could influence in the response. In this paper we used a saturated fractional factorial experimental design, which had the advantage that, if necessary, more experiments could be added to build a full factorial and thus determine the effects of the interactions [32,33].

### 2.4.2. Surface response establishment

With the selected variables in the previous stage, we constructed a  $2^3$  full factorial design in order to determine the effect of the main variables, all the

interactions between variables and the suitability of the experimental domain pre-established for the different variables.

When the full factorial design is studied in the suitable domain we can obtain the coefficients to establish the following first-order response surface:

$$y = b_0 + b_1x_1 + b_2x_2 + b_3x_3 + b_{12}x_1x_2 + b_{13}x_1x_3 + b_{23}x_2x_3 + b_{123}x_1x_2x_3 \quad (1)$$

where  $b_i$  are the estimation of the effects and  $x_i$  are the codified values from -1 to +1 (-1 corresponds to the value of the low level of the variable and +1 corresponds to the value of the high level).

In order to validate this model design, we evaluated the pure quadratic curvature sum of squares ( $SS_{\text{pure quadratic}}$ ) using Eq. 2 [32]:

$$SS_{\text{pure quadratic}} = \frac{n_F n_C (\bar{y}_F - \bar{y}_C)^2}{n_F + n_C} \quad (2)$$

where  $\bar{y}_F$  is the average of the results obtained in the runs at the factorial points of the design,  $\bar{y}_C$  is the average of the response at the central point, and  $n_F$  and  $n_C$  are the number of runs, in our case  $n_F$  is 8 because we employed a  $2^3$  factorial design and  $n_C$  is 3 that are the replications in the central point.

An F-test is used to compare the  $SS_{\text{pure quadratic}}$  and  $SS_{\text{residual}}$  obtained with the three replications of the central point. If both values are comparable, there is no quadratic curvature. On the other hand if they are not comparable, this means that a quadratic curvature is present and the model has to be represented by a second-order equation [32].

The central composite design (CCD) is the most popular class of design for fitting second-order models; CCD is often practically deployed through sequential experimentation; that is, a  $2^k$  full factorial design is used to fit a first-order model and then axial runs are added to allow the curvature to be estimated [32].

In all of the experimental designs employed, an ANOVA test was carried out by making an additional triplicate central point in order to evaluate the significance of the effects [34].

### 3. Results and discussion

#### 3.1. Screening process

Three of the five variables studied were qualitative. These were the type of catalyst (high level  $\text{TiO}_2$  (+) or low level  $\text{ZnO}$  (-)); the presence (+) or not (-) of oxidant  $\text{H}_2\text{O}_2$ ; and the presence (+) or not (-) of stirring. The other two variables were quantitative. These were pH 9 (+) or 2 (-) and catalyst concentration  $1 \text{ g}\cdot\text{L}^{-1}$  (+) or  $0.05 \text{ g}\cdot\text{L}^{-1}$  (-). We used  $\text{ZnO}$  and  $\text{TiO}_2$  as catalysts because their efficiency in photodegradation processes has been demonstrated [25]. The oxidant  $\text{H}_2\text{O}_2$  was used to determine its influence on the process [18,26]. The pH range was chosen on the basis of Kansas et al.'s findings [25] regarding the effects of the catalysts on pH. The catalyst concentration of the previous study [14] was increased in order to determine its possible influence on the present study. Dye concentration was fixed at 180 ppm (60 ppm of each dye) because the concentration effect of the different dyes has already been evaluated in previous studies [14]. The responses studied were the half-life time of each dye.

Table 1 describes the experimental conditions of the 8 experiments performed. The results are represented in Fig. 3a. In this figure in the center of each square, the half-life time for each dye at each pH level has been represented to analyze the effect of the variables. The figure does not include the levels of stirring or the catalyst concentration for dimensionality reasons and because these are the least influential variables.

Fig. 3a clearly shows two remarkable results: the first is that brown dye is always the most persistent in the solution and the second is that the presence of hydroxide peroxide (experiments 3, 4, 7 and 8) notably reduces the half-life time of the degradation of the three dyes. Other less marked tendencies are that the pH effect in the domain does not significantly alter the degradation rate of the three dyes and that better results are obtained when  $\text{ZnO}$  is employed instead of  $\text{TiO}_2$

(experiments 3 and 4 vs. 7 and 8). However, it should be pointed out here that other variability variables are involved in this comparison (pH and stirring).

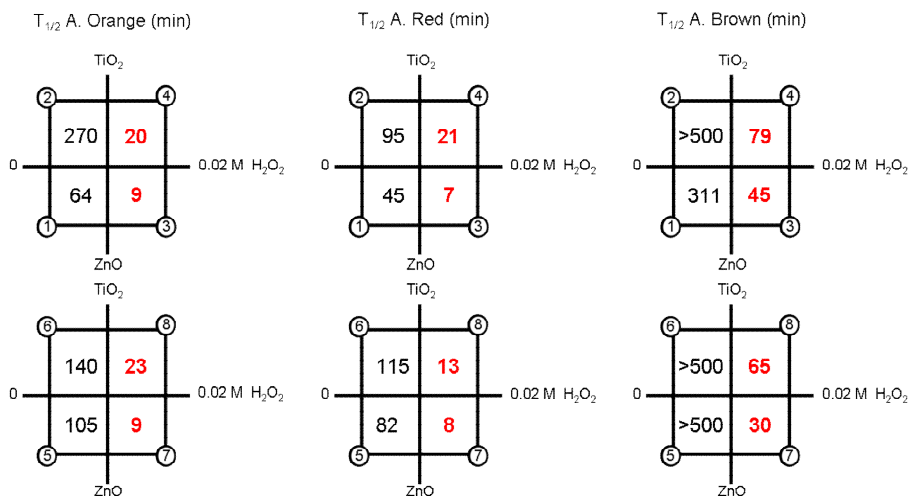
**Table 1.** Screening experimental plan.

Exp	Catalyst	H <sub>2</sub> O <sub>2</sub> (mol·L <sup>-1</sup> )	pH	[catalyst] (g·L <sup>-1</sup> )	Stirring
1	ZnO	0	4	1	Yes
2	TiO <sub>2</sub>	0	4	0.05	No
3	ZnO	0.02	4	0.05	Yes
4	TiO <sub>2</sub>	0.02	4	1	No
5	ZnO	0	9	1	No
6	TiO <sub>2</sub>	0	9	0.05	Yes
7	ZnO	0.02	9	0.05	No
8	TiO <sub>2</sub>	0.02	9	1	Yes

It is known that the presence of an oxidant in a heterogeneous catalyst increases the rate of the degradation by enhancing the quantum yield of hydroxyl radicals. However, because of the great magnitude of H<sub>2</sub>O<sub>2</sub> effect, we evaluated the degradation rate in a homogeneous medium without a catalyst because this notably simplified the process. We thus carried out three experiments using H<sub>2</sub>O<sub>2</sub> but without catalyst. Fig. 3b shows the experimental conditions and the responses obtained.

From the results we deduced that red and orange dyes degrade at the same rate independently of the pH. If the results obtained at pH 9 are compared with the results of the screening experiments 7 and 8 (Fig. 3a), it could be concluded that the degradation is faster without the catalyst TiO<sub>2</sub> than when this catalyst is used, and that when ZnO is employed as catalyst with red and orange dyes the results are similar to those obtained when it is not used. Degradation only improves when ZnO is used for brown dye, although the best values for this dye (which is the most persistent) were obtained at pH 2 and without a catalyst. It is at first sight surprising that the photodegradation results are better without catalyst when an oxidant such H<sub>2</sub>O<sub>2</sub> is employed in the reaction. One possible explanation of this fact is that at high dosage, H<sub>2</sub>O<sub>2</sub> is a powerful OH<sup>\*</sup> scavenger [35] and furthermore that high concentrations of this oxidant could cause the dye and the H<sub>2</sub>O<sub>2</sub> to compete when adsorbing onto the catalyst, depending on the adsorption behavior of the dyes [36].

a)



b)

	T <sub>1/2</sub> A. Orange	T <sub>1/2</sub> A. Red	T <sub>1/2</sub> A. Brown
pH = 2	10	9	28
pH = 6	10	8	40
pH = 9	11	8	50

Presence of stirring and [H<sub>2</sub>O<sub>2</sub>] = 0.02 g/l

**Fig. 3.** Screening results.

### 3.2. Response surface establishment

#### 3.2.1. Preliminary studies

In this first stage, prior to establishing the response surface, three variables were selected and a full factorial 2<sup>3</sup> was designed in order to analyze whether the experimental domain was suitable for the parameters that could influence the photodegradation process. Given the results of the previous experiments, we decided to work without a catalyst because this way the degradation was just as effective, more economic and left no catalyst residues. The degradation took place with stirring and at a constant pH of 2.

The variables studied were the concentration of H<sub>2</sub>O<sub>2</sub> (A): 0.02 - 0.1 mol·L<sup>-1</sup>; the initial concentration of Acid Red 97 (B): 0 - 60 mg·L<sup>-1</sup>; and the initial concentration of Acid Orange 61 (C): 0 - 60 mg·L<sup>-1</sup>. As can be seen, the H<sub>2</sub>O<sub>2</sub> concentration was increased with respect to the screening step in order to more

accurately study the effect of the most influential variable. The chosen response was the concentration of brown dye at 20 min of degradation because this dye is the most persistent in the solution (see Fig. 3a) and low concentrations of this dye at this time mean that the other two dyes are almost eliminated. The concentration of brown dye was fixed at  $60 \text{ mg}\cdot\text{L}^{-1}$ . The first 8 rows of Table 2 detail the experimental plan and the results expressed as a percentage of Acid Brown 425 in the medium at 20 min of photodegradation.

**Table 2.** Full factorial and central composite experimental plan.

Exp	Factors			Response
	H <sub>2</sub> O <sub>2</sub>	A. Red	A. Orange	% A. Brown
1	0.02	0	0	4.26
2 <sup>a</sup>	0.1	0	0	14.34
3	0.02	60	0	25.73
4 <sup>a</sup>	0.1	60	0	34.93
5	0.02	0	60	15.68
6 <sup>a</sup>	0.1	0	60	26.04
7	0.02	60	60	32.92
8 <sup>a</sup>	0.1	60	60	34.22
CP <sup>b</sup> 1	0.06	30	30	10
CP <sup>b</sup> 2	0.06	30	30	11.5
CP <sup>b</sup> 3	0.06	30	30	12
9	0.005	0	0	3.06
10	0.005	60	0	23.45
11	0.005	0	60	24.96
12	0.005	60	60	50.25
CP <sup>b</sup> 4	0.0525	30	30	19.5
CP <sup>b</sup> 5	0.0525	30	30	18.24
CP <sup>b</sup> 6	0.0525	30	30	17.67
13 <sup>c</sup>	0.005	30	30	29.68
14 <sup>c</sup>	0.1	30	30	23.37
15 <sup>c</sup>	0.0525	0	30	12.89
16 <sup>c</sup>	0.0525	60	30	27.78
17 <sup>c</sup>	0.0525	30	0	13.86
18 <sup>c</sup>	0.0525	30	60	29.37

<sup>a</sup> Experiences employed in the second experimental design

<sup>b</sup> CP means central point

<sup>c</sup> Axial points to complete the central composite design

The coefficients of the principal effects and interactions were calculated and are shown in the Pareto chart in Fig. 4a. The significance of the effects was

evaluated by analysis of variance (ANOVA) and the vertical line in Fig. 4a corresponds to the value above which the effects are significant for a level of significance  $\alpha = 0.05$ . The analysis of the effects shows that all of the variables are influential and their effects are positive, which means that the concentration of brown dye at 20 min of degradation is higher if the variable values are higher. The effects of the interactions are not relevant. The positive effect of the initial concentration of red dye and orange dye was expected. On the other hand, the positive effect of  $\text{H}_2\text{O}_2$  means that at high values of oxidant the degradation is less efficient. This fact does not agree with the results obtained in the previous step which demonstrate that hydrogen peroxide favored the degradation process. An initially surprising explanation of this result is that excess  $\text{H}_2\text{O}_2$  can generate secondary reactions which interfere in the degradation process [8-10]. This indicates that there is an optimum concentration that maximizes the photooxidation rate of this oxidant when it is used to remove the dyes and that we have been working in a domain outside this optimum zone.

At this point of the study, we decided to extend the experimental domain toward lower values of  $\text{H}_2\text{O}_2$ , where the  $\text{H}_2\text{O}_2$  concentration is A:  $0.005 - 0.1 \text{ mol}\cdot\text{L}^{-1}$ . For this purpose a full factorial design  $2^3$  was completed for the experiments marked with (<sup>a</sup>) in Table 2 and for the new experiments represented in the rows 9-12 of the same table.

Fig. 4b shows a Pareto chart containing the values of the variable effects for this second  $2^3$  design. As in the previous figure, the vertical line shows the value above which the effects are relevant for a significance level of  $\alpha = 0.05$ . In this case the influential variables were the concentrations of red dye and orange dye, and these were as positive as could be expected. The effect of the  $\text{H}_2\text{O}_2$  concentration was not significant but the interaction of this variable with the other two variables is relevant and negative. This indicates that the concentration of hydrogen peroxide affects the response in different ways depending on the level of the other variables.

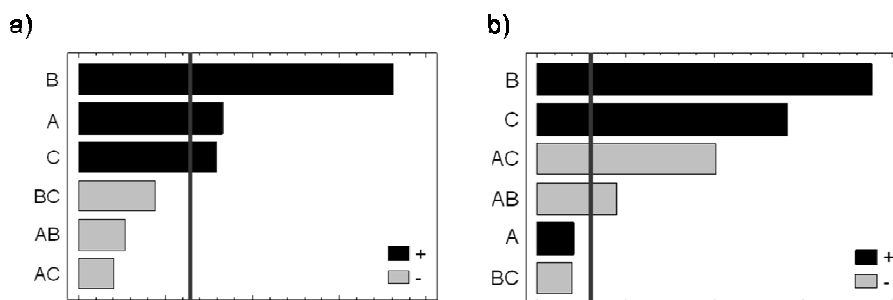


**Fig. 4.** Pareto charts from the  $2^3$  experimental designs using the % of Acid Brown 425 at 20 min of degradation as the response. a) corresponds to the first design and b) to the second design. The variables are: A (H<sub>2</sub>O<sub>2</sub> concentration), B (Acid Red 97 concentration) and C (Acid Orange 61 concentration).

### 3.2.2. Establishment and validation of response surface

The results obtained in the last stage were used to establish a first-order response surface. Once the coefficients of this model had been determined, the curvature test explained in the section 2.4.2 was calculated. The  $F_{cal}$  value was 137.42 and the value of  $F_{tab(1,2,0.05,2 \text{ tails})}$  was 38.5, therefore  $SS_{pure \text{ quadratic}}$  calculated with Eq. (2) and  $SS_{residual}$  were not comparable and this means that the response surface was not validated because a quadratic curvature is present and the model had to be represented by a second-order equation.

In order to fit a second-order model we used a face-centered central composite design in which  $\alpha = 1$ . This design locates the axial points on the centers of the faces of the cube formed in the full factorial design. Table 2 (experiments 13 – 18) shows the experimental conditions of the axial points added to the full factorial design to complete the central composite.

The response surface obtained is described in the following equation:

$$y = 19.6 + 0.2A + 8.9B + 7.5C + 6.0A^2 - 2.1AB - 4.7AC - 0.2B^2 - 0.9BC + 1.1C^2$$

in which  $y$  is the concentration of brown dye at 20 min of degradation and A, B, C correspond to, in codified variables (from -1 to +1), the concentration values of



H<sub>2</sub>O<sub>2</sub>, red dye and orange dye respectively. This equation shows that H<sub>2</sub>O<sub>2</sub> presents important coefficients in the quadratic term and in the interactions.

Finally, the model was validated with the experimental points that were used to create the model along with 8 other selected points within the experimental domain in order to cover the whole range of responses. Fig. 5 compares the experimental results with the predicted results for the second-order response surface; (●) corresponds to the points used to elaborate the model and (▲) corresponds to the selected external points. We then applied a joint test of slope 1 and a regression intercept of 0 to the regression between the experimental and predicted responses. The curve obtained ( $y = 1.004x - 0.1599$ ) was statistically comparable with the ideal curve ( $y = x$ ) and had significance of 5%. This fact proved that the second-order model fits the process studied.

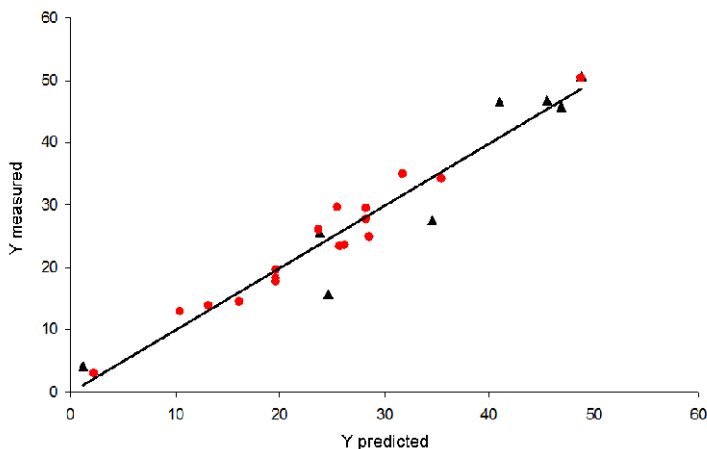


**Fig. 5.** Comparison of measured results vs predicted results calculated using the second order response surface.

Fig. 6a and b shows the concentration of H<sub>2</sub>O<sub>2</sub>, red dye and orange dye on the response surface (i.e. the concentration of brown dye at 20 min of degradation). In Fig. 6a, the concentration of the orange dye is fixed at 30 mg·L<sup>-1</sup> whereas in Fig. 6b, the concentration of the red dye is fixed at 30 mg·L<sup>-1</sup>. The model shows that at low values of red or orange dye concentration, it is better to work with low concentrations of H<sub>2</sub>O<sub>2</sub> because the concentration of the brown dye

increases when there is an excess of this oxidant. It can be also seen that red dye needs a lower concentration of oxidant for degradation than orange dye. These models could be useful for the tanning industry because it is possible to determine the optimum concentration of  $H_2O_2$  for the degradation of a fixed concentration of dyes. This methodology could reduce the time and money needed for the water treatment.

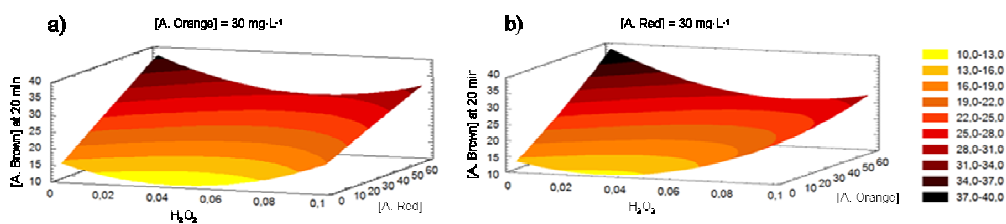


Fig. 6. Second order response surfaces.

#### 4. Conclusions

Acid Brown 425 is the most persistent dye in all the photodegradation processes. For this reason, its concentration could be related to the degradation time of the other dyes given that the remaining dyes are completely eliminated at low values of brown dye concentration.

Screening showed that the presence of an oxidant, specifically  $H_2O_2$ , has the most important effect on photodegradation. It has been demonstrated that if this compound is added then no catalyst is needed and that the pH does not affect degradation. Using photolysis instead of photocatalysis could be interesting from a practical, economical and environmental point of view because dyes could be degraded without the use of a catalyst.

In the domain studied the concentration of brown dye at 20 min of degradation follows a second order equation because  $H_2O_2$  has a quadratic influence in the process.

The quadratic function obtained has been validated by experimenting with different points of the domain. Furthermore, this methodology could be used in the textile industry to reduce the cost and time of degradation because, if the concentrations of dyes in textile effluent are known, the optimum amount of H<sub>2</sub>O<sub>2</sub> could be calculated in order to eliminate the dyes in little more than 20 min.

### Acknowledgements

The authors would like to thank Trumpler Española, S.A. for supplying the synthetic dyes and the Spanish Ministry of Science and Innovation (Project CTQ2007-61474/BQU) for economic support and for providing Cristina Fernández with a doctoral fellowship (AP2007-03788).

### References

- [1] V. Gómez, M.S. Larrechi, M.P. Callao, *Chemosphere* 69 (2007) 1151-1158.
- [2] I.D. Mall, V.C. Srivastava, N.K. Agarwal, I.M. Mishra, *Chemosphere* 61 (2005) 492-501.
- [3] V. López-Grimau, M.C. Gutiérrez, *Chemosphere* 62 (2006) 106-112.
- [4] R.O. Cristovao, A.P.M. Tavares, J.M. Loureiro, R.A.R. Boaventura, E.A. Macedo, *Environ. Technol.* 29 (2008) 1357-1364.
- [5] L. Wojnárovits, E. Takács, *Radiat. Phys. Chem.* 77 (2008) 225-244.
- [6] J. Chen, L. Zhu, *Chemosphere* 65 (2006) 1249-1255.
- [7] I. Arslan-Alaton, G. Tureli, T. Olmez-Hanci, *J. Photochem. Photobiol., A* 202 (2009) 142-153.
- [8] N. Daneshvar, M. Rabbani, N. Mordirshahla, M.A. Behnajady, *Chemosphere* 56 (2004) 895-900.
- [9] M.A. Rauf, S. Ashraf, S.N. Alhadrami, *Dyes Pigm.* 66 (2005) 197-200.
- [10] F.H. Abdullah, M.A. Rauf, S.S. Ashraf, *Dyes Pigm.* 72 (2007) 349-352.
- [11] L.A. Pérez-Estrada, A. Agüera, M.D. Hernando, S. Malato, A.R. Fernández-Alba, *Chemosphere* 70 (2008) 2068-2075.
- [12] M.A. Rauf, N. Marzouki, B.K. Körbahti, *J. Hazard. Mater.* 159 (2008) 602-609.
- [13] K. Dai, H. Chen, T. Peng, D. Ke, H. Yi, *Chemosphere* 69 (2007) 1361-1367.
- [14] C. Fernández, M.S. Larrechi, M.P. Callao, *Talanta* 79 (2009) 1292-1297.
- [15] S. Gomes de Moraes, R.S. Freire, N. Durán, *Chemosphere* 40 (2000) 369-373.
- [16] K. Wang, H. Chen, L. Huang, Y. Su, S. Chang, *Chemosphere* 72 (2008) 299-305.
- [17] C. Lizama, J. Freer, J. Baeza, H.D. Mansilla, *Catal. Today.* 76 (2002) 235-246.

- 
- [18] A.F. Caliman, C. Cojocar, A. Antoniadis, I. Poullos, *J. Hazard. Mater.* 144 (2007) 265-273.
- [19] B.K. Körbahti, M.A. Rauf, *Chem. Eng. J.* 138 (2008) 166-171.
- [20] B.K. Körbahti, *J. Hazard. Mater.* 145 (2007) 277-286.
- [21] A.P.M. Tavares, R.O. Cristóvão, J.M. Loureiro, R.A.R. Boaventura, E.A. Macedo, *J. Chem. Technol. Biotechnol.* 83 (2008) 1609-1615.
- [22] A.P.M. Tavares, R.O. Cristóvão, J.M. Loureiro, R.A.R. Boaventura, E.A. Macedo, *J. Hazard. Mater.* 162 (2009) 1255-1260.
- [23] V. Gómez, M.P. Callao, *Talanta* 77 (2008) 84-89.
- [24] V. Gómez, M.P. Callao, *Anal. Bioanal. Chem.* 382 (2005) 328-334.
- [25] S.K. Kansas, M. Singh, D. Sud, *J. Hazard. Mater.* 141 (2007) 581-590.
- [26] O. Prieto, J. Hermoso, Y. Nuñez, J.L. del Valle, R. Hirsuta, *Solar Energy* 79 (2005) 376-383.
- [27] Matlab, The Mathworks, South Natick, MA, USA.
- [28] Tauler, R., de Juan, A., 2006. Multivariate Curve Resolution homepage <<http://www.ub.es/gesq/mcr/mcr.htm>>.
- [29] Statgraphics <<http://www.statgraphics.com/>>.
- [30] Unscrambler <<http://www.camo.com/rt/Products/Unscrambler/unscrambler.html>>.
- [31] G. Hanrahan, K. Lu, *Crit. Rev. Anal. Chem.* 36 (2006) 141-151.
- [32] D.C. Montgomery, Design and Analysis of Experiments. John Wiley&Sons, New York, 1997.
- [33] T. Lundstedt, E. Seifert, L. Abramo, B. Thelin, A. Nyström, J. Pettersen, R. Bergman, *Chemom. Intell. Lab. Syst.* 42 (1998) 3-40.
- [34] D.L. Massart, B.G.M. Vandeginste, L.M.C. Buydens, S. de Jong, P.J. Lewi, J. Smeyers-Verbeke, Handbook of Chemometrics and Qualimetrics Part A. Elsevier, Amsterdam, 1997.
- [35] T. Sauer, G.C. Neto, H.J. José, R.F.P.M. Moreira, *J. Photochem. Photobiol., A* 149 (2002) 147-154.
- [36] C. Hachem, F. Bocquillon, O. Zahraa, M. Bouchy, *Dyes Pigm.* 49 (2001) 117-125.

UNIVERSITAT ROVIRA I VIRGILI

ANALYTICAL METHODOLOGIES BASED ON CHEMOMETRICS TO OPTIMIZE THE PHOTODEGRADATION OF DYES

Cristina Fernández Barrat

DL:T. 160-2012

### 3.3. Kinetic studies

The experimentation proposed and discussed in this section corresponds to objective (d) of chapter 1 and is related to the determination of the rate constants, which are important values for evaluating the efficiency of photodegradation processes.

The evaluation of the rate constants involved in photodegradation processes takes into account the possible formation of intermediates, which can be as hazardous as the initial dye or even more so. The presence of these intermediates must be taken into account when evaluating the optimal experimental conditions.

The results have given rise to two papers: ***Kinetic analysis of C.I. Acid Yellow 9 photooxidative decolorization by UV-visible and chemometrics*** and ***The evaluation of the adsorption and rate constants of the photocatalytic degradation of C.I. Acid Yellow 9 by means of HS-MCR-ALS: a study of process variables***. In both cases only one dye, C.I. Acid Yellow 9, is studied. The data obtained, as in the previous section, are UV-visible spectra recorded throughout the photodegradation processes and the data are treated using MCR-ALS. In this case, however, hard constraints are applied to force the reaction profiles to follow specific kinetic models.

In the first paper, a photolytic degradation is studied. Its pathway is established by EFA and MCR-ALS. The intermediates are identified and the degradation pathway is confirmed by means of MS analysis. The rate constants are evaluated by using, as a hard constraint in the MCR-ALS optimization, the kinetic model based on the proposed pathway.

In the second paper, photocatalytic degradation using two heterogeneous catalysts is studied. The adsorption and rate constants are obtained using the Langmuir-Hinshelwood model as hard constraint. The effect of several variables is evaluated for the two catalysts used.

UNIVERSITAT ROVIRA I VIRGILI

ANALYTICAL METHODOLOGIES BASED ON CHEMOMETRICS TO OPTIMIZE THE PHOTODEGRADATION OF DYES

Cristina Fernández Barrat

DL:T. 160-2012

### **3.3.1. Paper**

*Kinetic analysis of C.I. Acid Yellow 9 photooxidative decolorization by UV-visible and chemometrics*

Cristina Fernández, M. Pilar Callao, M. Soledad Larrechi

**Journal of Hazardous Materials 190 (2011) 986-992**





UNIVERSITAT ROVIRA I VIRGILI

ANALYTICAL METHODOLOGIES BASED ON CHEMOMETRICS TO OPTIMIZE THE PHOTODEGRADATION OF DYES

Cristina Fernández Barrat

DL:T. 160-2012

---

## Kinetic analysis of C.I. Acid Yellow 9 photooxidative decolorization by UV-visible and chemometrics

Cristina Fernández, M. Pilar Callao, M. Soledad Larrechi

*Department of Analytical and Organic Chemistry, Rovira i Virgili University,  
Marcel·lí Domingo s/n Campus Sescelades, E-43007 Tarragona, Spain*

### Abstract

A kinetic study of the C.I. Acid Yellow 9 photooxidative decolorization process, using H<sub>2</sub>O<sub>2</sub> as oxidant, was carried out by chemometric analysis of the UV-visible data recorded during the process. The number of chemical species involved in the photooxidative decolorization process was established by singular value decomposition (SVD) and evolving factor analysis (EFA). Information about the different chemical species along the process was obtained from the spectral and concentration profiles recovered by soft multivariate curve resolution with alternating least squares (MCR-ALS). This information was complemented by mass spectrometry (MS) to postulate a reaction pathway. The dye photooxidative decolorization process involved consecutive and parallel reactions. The consecutive pathway consists of a first stage of dye oxidation followed by the rupture of the azo linkage to form smaller molecules that are degraded in a subsequent stage. The parallel reactions form products that are undetectable in the UV-visible spectra. Kinetic constants of the reactions postulated in the photooxidative process were retrieved by applying a hybrid hard and soft MCR-ALS resolution. All constants were similar for the consecutive stages and higher than those obtained for the parallel reactions.

**Keywords:** Azo dye degradation; C.I. Acid Yellow 9; Kinetic studying; Mass spectroscopy; MCR-ALS.

## 1. Introduction

Organic azo dyes are involved in many industrial processes, so they are frequently found in industrial wastewater [1]. Concretely, C.I. Acid Yellow 9, is used in the textile industry [2-4]. Moreover, it was recently reported that this dye has properties that make it suitable as a dispersing agent for carbon nanotubes [5-6] which means that their industrial use could increase in the future. Organic azo dyes are contaminants and must be eliminated.

Degradation processes of C.I. Acid Yellow 9 using Mn oxide [2], biodegradation [3] and electrochemical oxidation [4,7] have been reported. Nowadays, however, homogeneous and heterogeneous catalytic dye removal techniques that allow fast degradations are the methods most commonly used for the degradation of organic dyes [1,8-14]. Regardless of which technique is used, the challenge of determining the optimal conditions for rapid dye removal is usually solved by determining the kinetic rate and using it as a reference parameter. This study focuses on the kinetic analysis of the photooxidative decolorization process of C.I. Acid Yellow 9 using H<sub>2</sub>O<sub>2</sub> as oxidant.

Usually, dye removal reactions are monitored by UV-visible spectroscopy [1,8,10,15] and the degradation rate constant is established fitting the absorbance values obtained at one wavelength to a pseudo first-order reaction. During the degradation processes, however, as a consequence of the radical reaction, intermediates—some sensitive to UV-visible spectra and others not—can be formed [3-4,7,16-18]. This univariate approach can lead to erroneous results if intermediates absorbing in the same wavelength range that the studied dye are formed during the process.

The use of selective techniques such separation techniques coupled with mass spectrometry (MS) [19-22] are useful to avoid the problem of the intermediates interference. With techniques of this sort, however, the samples usually need to be submitted to some sort of pre-treatment and the analysis time may be long. Another possibility to overcome this problem is using UV-visible

spectroscopy coupled to multivariate curve resolution methods. This approach was used in the present study.

In this study, the number of variability sources related to the number of chemical species present in the reaction was analysed using singular value decomposition (SVD) and evolving factor analysis (EFA) of the UV-visible spectra recorded during dye photooxidative decolorization. Subsequently, a soft multivariate curve resolution with alternating least squares (MCR-ALS) was carried out to obtain information about the spectral profiles of each compound. This information was complemented by MS analysis of some representative samples taken during the degradation process to propose a reaction pathway. In a second step a hybrid hard and soft modelling technique [23] was used to evaluate the kinetic constants of different reactions involved in the photooxidative process. To our knowledge, no strategies of this type have previously been used in kinetic studies of dye photooxidative decolorization, so this study represents an advance in the field.

## **2. Experimental**

### **2.1. Chemicals**

The reagents used in this study were analytical-grade chemicals. C.I. Acid Yellow 9 (2-Amino-5-([4-sulphophenyl]azo)benzenesulfonic acid)) (95%) was purchased from Sigma-Aldrich and H<sub>2</sub>O<sub>2</sub> (30%) was purchased from Scharlau. Degradation solutions were prepared in ultrapure Milli-Q water from a system supplied by Millipore (USA).

### **2.2. Instruments, measuring conditions and software**

#### **2.2.1. Reactor**

The cylindrical annular batch reactor consisted of a Pyrex glass outer reactor with 0.7 L of capacity and a quartz immersion tube (2.5 cm i.d. and 38 cm long). The tube contained a 15 W low-pressure mercury-vapour lamp (LPML) (TNN 15/32 56001721), from Heraeus Noblelight, Germany. This UVC light source emitted at 254 nm and the incident photon flux of the UV reactor was 0.1 W cm<sup>-1</sup>.

### **2.2.2. UV-visible spectrophotometer**

Spectral data were acquired using a diode-array spectrophotometer (Shimadzu MultiSpec-1501) and Hyper-UV 1.51 software. The UV-visible spectra of the dye-degradation samples and the blank, in which only H<sub>2</sub>O<sub>2</sub> is present, were recorded at each nm from 270 to 720 nm.

### **2.2.3. Mass spectrometer**

The MS spectra were acquired in negative centroid acquisition mode by direct injection using a 6210 LC/TOF mass spectrometer (Agilent Technologies, Palo Alto, USA), equipped with an electrospray ionization source. MS spectra of six samples obtained at 0, 8, 18, 25, 30 and 60 min of degradation process were recorded in the 70-400 *m/z* range.

### **2.2.4. Software**

The UV-visible spectra were exported and converted in MATLAB binary files. The data matrix was analysed by MCR-ALS [24]. Nonlinear fitting was performed using home-made software with a MATLAB 6.5 computer environment [25].

## **2.3. Photooxidative decolorization procedure**

A 0.5 L solution of 60 mg·L<sup>-1</sup> of C.I. Acid Yellow 9 and H<sub>2</sub>O<sub>2</sub> 0.05 M in Milli-Q water was introduced into the cylindrical reactor. This solution was irradiated at 254 nm during the process. The concentrations were selected from preliminary studies [8, 26, 27]. Samples of 3 mL of the degradation solution were taken at the beginning of the experiment (t=0 min) and after each minute throughout the degradation time (t=60 min). Two repetitions of the experiment were carried out in order to calculate the standard deviation (SD) of the results.

In order to determine the noise in this process, degradation of H<sub>2</sub>O<sub>2</sub> was carried out as the degradation blank under the same reaction conditions.

## **2.4. Methodology and chemometric analysis**

The methodology followed to obtain the spectral and concentration profiles of the chemical species and to calculate the rate constants of the reactions

involved in the photooxidative process was: (a) evaluation of the number of chemical species along the photooxidative decolorization process by SVD and EFA, (b) analysis of the spectral and concentration profiles retrieved by soft MCR-ALS and analysis of MS spectra to propose a reaction pathway, (c) calculation of the rate constants by hybrid hard and soft MCR-ALS.

The procedure begins with the arrangement of the UV-visible spectra recorded during the blank and the photooxidation of C.I. Acid Yellow 9 in two data matrices, ( $\mathbf{D}_b$  ( $m \times n$ )) for the blank and ( $\mathbf{D}_1$  ( $m \times n$ )) for the dye degradation, where  $m$  is the number of spectra recorded ( $m=61$ ) and  $n$  is the number of wavelengths ( $n=451$ ).

In the two data matrices,  $\mathbf{D}_b$  and  $\mathbf{D}_1$ , the number of variability sources related to species active in the studied UV-visible range was analysed by SVD [28]. Taking into account that in  $\mathbf{D}_b$  only one chemical species is present ( $\text{H}_2\text{O}_2$ ), the value of the second singular value from the analysis of  $\mathbf{D}_b$ , related to the variability representative of the noise in the experimental process, was considered the threshold for determining the number of significant factors in  $\mathbf{D}_1$ .

Information about the evolution of the different factors during the photooxidative decolorization process was obtained by EFA [29] of the data matrix  $\mathbf{D}_1$ . In this method, based on factor analysis, windows of linearly increasing size were subjected to SVD. In the forward analysis, we started by evaluating the SVD of the first two spectra of matrix  $\mathbf{D}_1$  and then repeated this process by adding one spectrum at a time until we reached the total matrix. In the backward analysis, the process was the same but started with the last two spectra of matrix  $\mathbf{D}_1$ .

After the determination of the number of chemical species a soft-modelling MCR-ALS [30] was applied to obtain information about the chemical species involved in the process. With this algorithm, the experimental matrix  $\mathbf{D}_1$  was decomposed into two new matrices according the following equation:

$$\mathbf{D}_1 = \mathbf{C}_1\mathbf{S}_1^T + \mathbf{E}_1$$

where  $\mathbf{C}_1$  and  $\mathbf{S}_1^T$  contain, respectively, information about the concentration and spectral profiles of the species involved in the photooxidative decolorization process and  $\mathbf{E}_1$  is a matrix of the residuals that contains the variance unexplained by  $\mathbf{C}_1\mathbf{S}_1^T$ . MCR-ALS solved this equation iteratively in order to minimize the residual matrix  $\mathbf{E}_1$ . This optimization requires an initial estimation of the concentration or spectral profiles, and some constraints can be applied. In this step, the initial estimation was the EFA profiles and the constraints employed were non-negativity for the concentration and spectral profiles and unimodality for the concentration profiles.

The information obtained was complemented with the MS spectra of six representative samples taken during the degradation process and was employed to postulate a reaction pathway.

In a subsequent stage, rate constants of the reactions involved in the C.I. Acid Yellow 9 photooxidative decoloration were obtained by hybrid hard soft MCR-ALS. This procedure includes a hard modeling constraint the corresponds to the kinetic model postulated. In accordance with this postulated model, a function consisting of the differential equations of each compound present in the reaction was constructed. This function was integrated numerically using an ordinary differential equation solver (ODE23, a Runge-Kutta MATLAB subroutine).

In this step, the concentration profiles retrieved by soft MCR-ALS and an estimation of the rate constants obtained through these profiles were used as initial estimation. Finally the spectral and kinetic profiles and the rate constants that provided the best fit were retrieved.

### 3. Results and discussion

Fig. 1a and Fig. 1b show the UV-visible spectra obtained during the degradation of C.I. Acid Yellow 9 and the blank, respectively. Fig. 1a shows a decrease in the absorbance values as a consequence of the dye degradation, but it is not clear whether any intermediate is present in the solution.

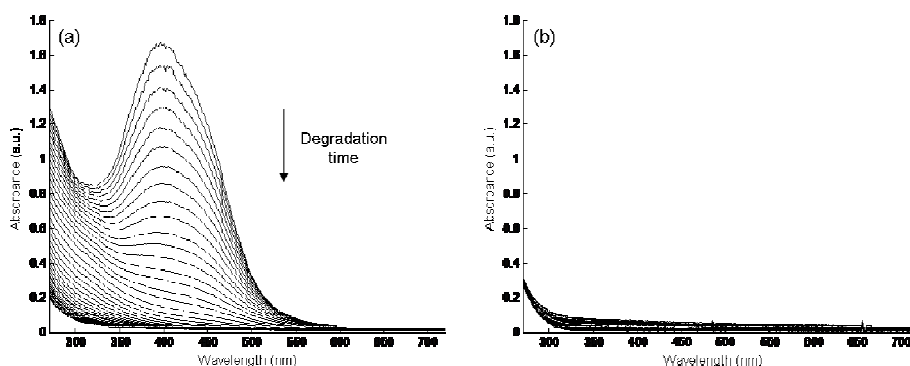


**Fig. 1.** UV-visible spectra recorded during the photooxidative decolorization of C.I. Acid Yellow 9 (a) and the blank (b). For the decolorization of the dye, only the last 45 spectra are plotted.

Table 1 shows the singular values obtained by SVD for both the dye and the blank matrices. Because only one component is present in the degradation blank, the second singular value obtained from the  $\mathbf{D}_b$  matrix is considered representative of the noise, which means that three eigenvalues are significant in the  $\mathbf{D}_1$  matrix. These results lead us to think that intermediates are present in this process.

**Table 1.** Rank analysis of  $\mathbf{D}_1$  and  $\mathbf{D}_b$  matrices. Only the first five singular values are shown.

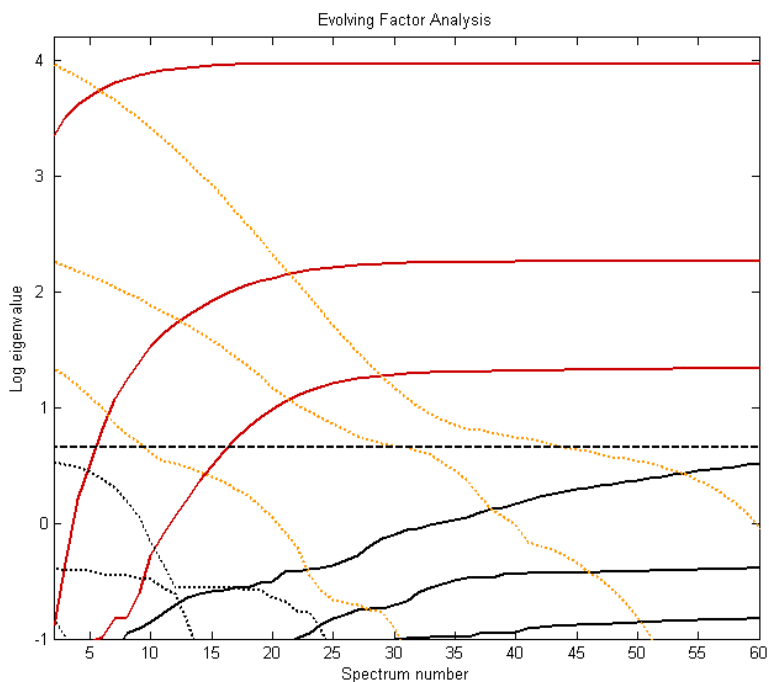
Factors	Blank	C.I. Acid Yellow 9
1	85.488	972.621
2	22.051	135.322
3	0.3117	46.741
4	0.0675	18.442
5	0.0173	0.6436

Fig. 2 shows the EFA plot of the C.I. Acid Yellow 9 degradation. The horizontal line was retrieved by EFA and is associated with noise.

In the forward analysis, from the very first minutes of degradation the variability in the spectral data is explained by two factors. It must be noted that the number of significant factors that contain information on the spectral evolution recorded during degradation is equal to the number of independent reactions +1 or



equal to the number of chemical species that contribute to the spectra analysed [31]. The presence of two factors from the very beginning of the reaction must be related to two chemical species corresponding to a reaction in which the initial dye is degraded. After 15-20 min of reaction time, a new factor becomes relevant, indicating that another variability source has appeared. This could be associated with the presence of another chemical species active in the UV-visible region being studied. After 30 min of degradation, no additional information is obtained.



**Fig. 2.** EFA of the spectral data matrix  $\mathbf{D}_1$ . Forward (continuous lines) and backward (dotted lines) directions.

Similar information is obtained in the backward analysis of the data matrix  $\mathbf{D}_1$ . In this direction, from 60 min since 40-45 min there are no factors of significant value because no changes are present in the reaction, probably because the degradation has finished. At 40-45 min, one factor which can be associated with a chemical species appears. From 28-33 min, the variability is explained by two factors and the third significant factor is observed after 10 min of degradation.

At this point in the discussion, at least three chemical species active in the UV-visible region can be thought to be involved in the process. Information about these species can be obtained by MCR-ALS analysis of matrix  $\mathbf{D}_1$ . This process starts by using the concentration profiles calculated by EFA as an initial estimation. The retrieved spectral profiles were associated with the new chemical species and these profiles jointly with the UV spectra of C.I. Acid Yellow 9 were considered as the initial estimation during the optimization step when a subsequent MCR-ALS was applied to  $\mathbf{D}_1$ . Fig. 3 contains the optimal spectral (Fig. 3a) and concentration (Fig. 3b) profiles, which show the behaviour of each species. The goodness of the resolution can be evaluated by considering the fitting error of the resolution (0.49%), the variance explained (99.92%) and the similarity coefficient (0.9990) between the real C.I. Acid Yellow 9 spectra and the spectra retrieved by MCR-ALS.

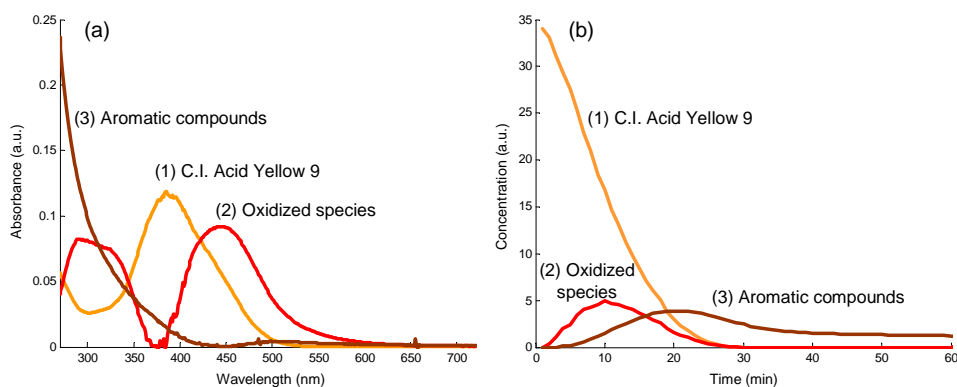


**Fig. 3.** Spectral (a) and concentration (b) profiles of the chemical species involved in the photooxidative decolorization process retrieved by MCR-ALS.

Fig. 3a shows the spectral profiles retrieved by soft MCR-ALS, of the initial dye (1) and the chemicals that appear in the first minutes of the reaction (2). The chemicals (2) have maximum absorbance at higher wavelengths than the initial dye. This profile suggests that the azo dye degrades to form a first intermediate that contains the azo group because absorption at these wavelengths is typical of compounds that contain an azo group. The shape of the third spectrum (3) is related to a second intermediate that appear during the degradation corresponding to the smaller molecules that have high absorbance in the UV region, meaning that

these are probably aromatic molecules that are products of the breakdown of the azo linkage, at the end of the degradation these species are also degraded.

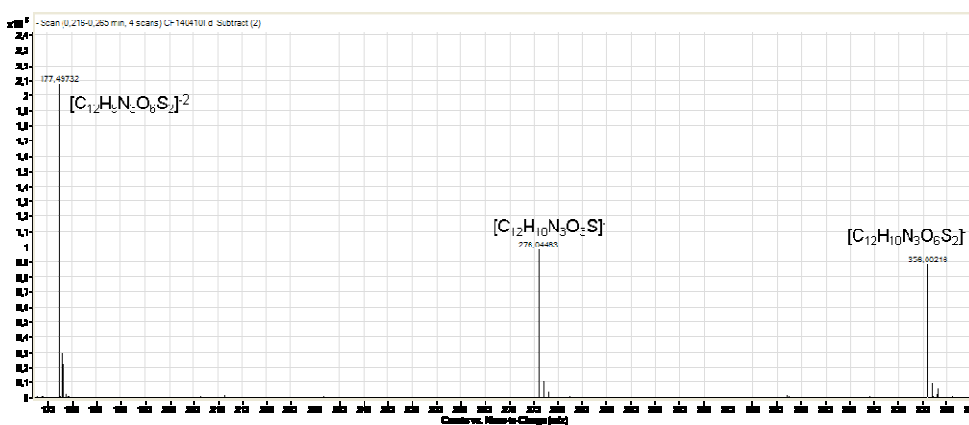
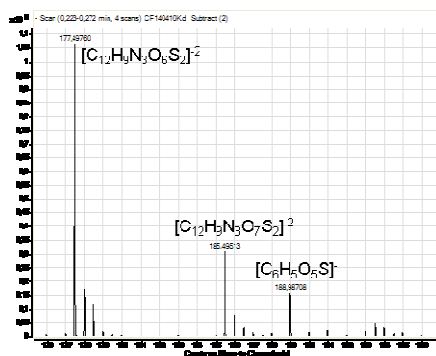
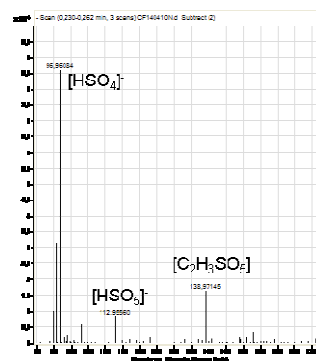
According to Fig. 3b, the rate of dye and intermediates degradation appears to be higher than the rate of intermediates formation. This leads us to think that undetectable UV-visible compounds are perhaps being formed during the degradation stages following a different pathway. These concentration profiles show that degradation could be considered finished at around 30 min and that at this time the compounds corresponding to the third spectrum have been degraded to compounds that are undetectable at the studied wavelength, such CO<sub>2</sub>, H<sub>2</sub>O and small acids that are the main subproducts in reactions of this kind. These results are in agreement with that observed in the EFA profiles where no variability is present after 30 min of degradation.

In order to propose the general degradation pathway, MS spectra were recorded at 0, 8, 18, 25, 30 and 60 min of degradation. These samples were selected according to the appearance of the various factors in the EFA analysis.

Fig. 4 shows the most informative parts of the MS spectra, at the beginning of the reaction (t=0), at an intermediate time (t=18) and at the final time (t=60). These three times are representative of the different stages of the reaction. The MS spectrum of the initial untreated C.I. Acid Yellow 9 (C<sub>12</sub>H<sub>9</sub>N<sub>3</sub>O<sub>6</sub>S<sub>2</sub>Na<sub>2</sub>) (M<sub>r</sub> = 401) was obtained both before and after the addition of H<sub>2</sub>O<sub>2</sub> (time=0). In both cases, two majority peaks were observed, corresponding to [C<sub>12</sub>H<sub>9</sub>N<sub>3</sub>O<sub>6</sub>S<sub>2</sub>]<sup>-2</sup> at m/z 177.50 and [C<sub>12</sub>H<sub>10</sub>N<sub>3</sub>O<sub>3</sub>S]<sup>-</sup> at m/z 276.04. In the sample containing H<sub>2</sub>O<sub>2</sub>, which corresponds to the initial conditions of degradation, a third peak was observed, corresponding to [C<sub>12</sub>H<sub>10</sub>N<sub>3</sub>O<sub>6</sub>S<sub>2</sub>]<sup>-</sup> at m/z 356.00. Fig. 4a shows these peaks.

At 8 min of degradation (not shown), two new peaks appeared, the larger one corresponding to [C<sub>12</sub>H<sub>9</sub>N<sub>3</sub>O<sub>7</sub>S<sub>2</sub>]<sup>-2</sup> at m/z 185.49 and the other corresponding to [C<sub>6</sub>H<sub>5</sub>O<sub>5</sub>S]<sup>-</sup> at m/z 188.99. These peaks were observed at 18 min (Fig. 4b). At subsequent degradation times, these two peaks grew and the peaks corresponding to the initial dye decreased in size. At 25 min of degradation (not shown), these two new peaks started to decrease in size and three new peaks started to appear,

corresponding to  $[\text{C}_2\text{H}_3\text{SO}_5]^-$  at  $m/z$  138.97,  $[\text{HSO}_5]^-$  at  $m/z$  112.96, and  $[\text{HSO}_4]^-$  at  $m/z$  96.96. At 30 min (not shown), the new peaks started to decrease, except for the one corresponding to  $[\text{HSO}_4]^-$ , which increased in size. These three peaks appeared after 60 min of degradation (Fig. 4c), with the one corresponding to  $[\text{HSO}_4]^-$  being the largest of the three.

(a)  $t=0$  min(b)  $t=18$  min(c)  $t=60$  min

**Fig. 4.** MS spectra of the photooxidative decolorization mixture at different reaction times (a) at 0 min, (b) at 18 min and (c) at 60 min.

Taking these results into consideration, we propose the pathway shown in Fig. 5. In this scheme, C.I. Acid Yellow 9 (a) in a first step is oxidized to (b) and then the azo linkage is broken to form (c) and (d). Subsequently, other reactions take place. At the end of the degradation time (60 min),  $\text{C}_2\text{H}_4\text{SO}_3$  (e),  $\text{H}_2\text{SO}_5$  (f) and  $\text{H}_2\text{SO}_4$  (g) can be observed and the other compounds are nearly degraded. As

it is indicated in this figure, in any step of the main reaction undetectable compounds, in the UV-vis range studied, can be formed.

These results are in agreement with those obtained by MCR-ALS (Fig. 3), where the dye (a) corresponds to compound (1), the oxidized species (b) corresponds to (2), and the species (c) and (d), which are aromatic compounds that absorb in the UV region, are considered to be included in the shape of spectra (3). The other compounds observed in MS (g, e and f) are not active in the UV-visible region studied. This is the reason why, in Fig. 3, no compounds are observed at the end of degradation. This degradation pathway agrees with the one obtained for the degradation of C.I. Acid Yellow 9 using biodegradation and electrochemical degradation [3-4]. Other intermediates, of low molecular weight and undetectable in the studied wavelength range, could appear in each stage of degradation.

From a practical point of view, it is important not only to detect the formation of intermediates but also to evaluate their rates of degradation. This information can be obtained if, during the optimization of the MCR-ALS step, a kinetic model is imposed as a restriction.

In accordance with the results discussed above, we propose the following kinetic model:



where A corresponds to the initial dye (a) in Fig. 5, B to the oxidized intermediate (b) in Fig. 5, C to a mixture of the (c) and (d) species of Fig. 5, and D to the small compounds undetectable in the UV-visible range, such (e), (f) and (g)

in Fig. 5 or smaller compounds undetectable by MS analysis in the selected  $m/z$  range.

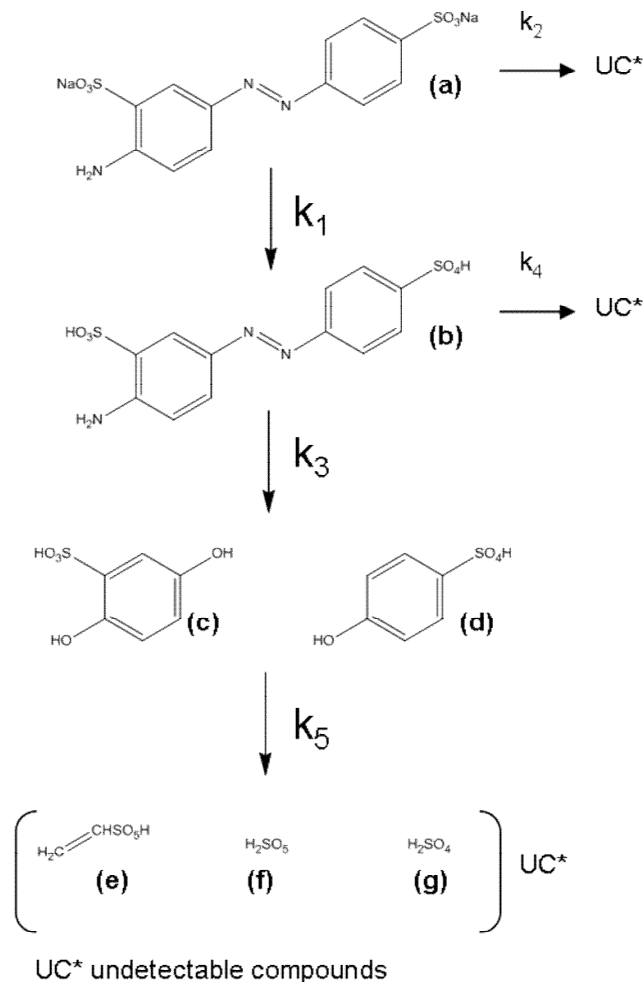


**Fig. 5.** Proposed reaction pathway for C.I. Acid Yellow 9 photooxidative decolorization.

In the selected model, the reactions (1), (3) and (5) are proposed on the basis of the MS spectra results and the pathway shown in Fig. 5. We also included reactions (2) and (4) in which A and B form small undetectable products because this behaviour is common in radicalary reactions and, moreover, in the shape of the degradation profiles obtained by MCR-ALS, the rate of the degradation of the dyes and intermediates is higher than the rate of the formation of intermediates.

The initial estimations of the constants were calculated using the soft MCR-ALS concentration profiles, all of them were adjusted to first-order kinetics which is the common approximation in photooxidation processes [8,10,15]. With this purpose the following equation has been used:

$$\ln \frac{[dye]_0}{[dye]} = k_{ap}t$$

The equations of the reactions used in the hybrid hard and soft MCR-ALS model were as follows:

$$\frac{dA}{dt} = -k_1A - k_2A$$

$$\frac{dB}{dt} = k_1A - k_3B - k_4B$$

$$\frac{dC}{dt} = k_3B - k_5C$$

It has to be remarked that this is a first estimate of the reaction pathway because the mechanism of this reaction is unknown. Therefore, the evaluated rate constants must be considered apparent values, informative of the main reaction stages that can be identified spectrophotometrically. The fitting error of the resolution was 11.90% and the explained variance was 98.50%. The dye spectra retrieved by MCR-ALS was compared with the real dye spectra and a correlation of 0.9983 was obtained.

The values of the kinetic constants were:  $k_1=0.092$  (SD=0.001),  $k_2=0.050$  (SD=0.002),  $k_3=0.099$  (SD=0.003),  $k_4=0.044$  (SD=0.005) and  $k_5=0.122$  (SD=0.006). If the overall process of degradation of A (reactions (1) and (2)), B (reactions (3) and (4)) and C (reaction (5)) is considered, these compounds are found to degrade at the same rate. The values of  $k_2$  and  $k_4$  are lower than the values obtained for  $k_1$ ,  $k_3$  and  $k_5$ , which means that the reactions proposed in Fig. 5 make up the principal pathway of C.I. Acid Yellow 9 photooxidative decolorization.

#### 4. Conclusions

Multivariate tools such EFA and soft MCR-ALS make it possible to obtain information about when intermediates appear in a reaction. This enables to select the most appropriate samples during the photooxidation for MS analysis, identify intermediates and determine reaction pathways. Under our experimental conditions, the photooxidative decolorization of C.I. Acid Yellow 9 was completed in approximately 30 min.

After an initial approach based on MCR-ALS results, the introduction of a hard restriction in MCR-ALS makes it possible to obtain information about all the kinetic constants involved in the photooxidative decolorization process.

C.I. Acid Yellow 9 photooxidative decolorization involves consecutive and parallel reactions. The consecutive pathway—the main one—consists of a first stage of dye oxidation followed by a rupture of the azo linkage to form smaller molecules, which are degraded in a subsequent stage. All of the identified compounds are degraded at similar rates.

#### Acknowledgements

The authors would like to thank the Spanish Ministry of Science and Innovation (Project CTQ2007-61474/BQU) for economic support and for providing Cristina Fernández with a doctoral fellowship (AP2007-03788).

#### References

- [1] C. Fernández, M.S. Larrechi, M.P. Callao, *Trends Anal. Chem.* 29 (2010) 1202-1211.
- [2] C. E. Clarke, F. Kielar, H.M. Talbot, K.L. Johnson, *Environ. Sci. Technol.* 44 (2010) 1116-1122.
- [3] B.V. Pandey, R.S. Upadhyay, *Microbiol. Res.* 161 (2006) 311-315.
- [4] D. Vanerkova, A. Sakalis, M. Holcapek, P. Jandera, A. Voulgaropoulos, *Rapid Commun. Mass Spectrom.* 20 (2006) 2807-2815.
- [5] S.A. Kumar, C. Tang, S. Chen, *Talanta* 74 (2008) 860-866.
- [6] S.A. Kumar, S. Wang, T. Yang, C. Yeh, *Biosens. Bioelectron.* 25 (2010) 2592-2597.



- [7] A. Sakalis, D. Vanerková, M. Holcapek, P. Jandera, A. Voulgaropoulos, *Chemosphere* 67 (2007) 1940-1948.
- [8] C. Fernández, M.S. Larrechi, M.P. Callao, *J. Hazard. Mater.* 180 (2010) 474-480.
- [9] F. H. Abdullah, M.A. Rauf, S.S. Ashraf, *Dyes Pigm.* 72 (2007) 349-352.
- [10] M.A. Behnajady, N. Modirshahla, *Chemosphere* 62 (2006) 1543-1548.
- [11] B. K. Körbahti, M.A. Rauf, *Chem. Eng. J.* 138 (2008) 166-171.
- [12] M.A. Rauf, N. Marzouki, B.K. Körbahti, *J. Hazard. Mater.* 159 (2008) 602-609.
- [13] M.G. Dias, E.B. Azevedo, *Water Air Soil Pollut.* 204 (2009) 79-87.
- [14] A.J. Julson, D.F. Ollis, *Appl. Catal., B* 65 (2006) 315-325.
- [15] N. Daneshvar, A. Aleboyeh, A.R. Khataee, *Chemosphere* 59 (2005) 761-767.
- [16] S. Vajnhandl, A.M Le Marechal, *J. Hazard. Mater.* 141 (2007) 329-335.
- [17] S. Song, H. Ying, Z. He, J. Chen, *Chemosphere* 66 (2007) 1782-1788.
- [18] L. Lei, Q. Dai, M. Zhou, X. Zhang, *Chemosphere* 68 (2007) 1135-1142.
- [19] M. Constapel, M. Schellenträger, J.M. Marzinkowski, S. Gäb, *Water Res.* 43 (2009) 733-743.
- [20] F. Zhang, A. Yediler, X. Liang, *Chemosphere* 67 (2007) 712-717.
- [21] M. Zhou, J. He, *Electrochim. Acta* 53 (2007) 1902-1910.
- [22] W. Feng, D. Nansheng, H. Helin, *Chemosphere* 41 (2000) 1233-1238.
- [23] A. de Juan, M. Maeder, M. Martínez, R. Tauler, *Chemom. Intell. Lab. Syst.* 54 (2000) 123-141.
- [24] A. de Juan, R. Tauler, J. Jaumot, <http://www.mcrals.info/>. Last accessed 24 february 2011.
- [25] Matlab 6.5, The Mathworks, South Natick, MA, USA.
- [26] C. Fernández, M.S. Larrechi, M.P. Callao, *Talanta* 79 (2009) 1292-1297.
- [27] V. Gómez, J. Font, M.P. Callao, *Talanta* 71 (2007) 1393-1398.
- [28] D.L. Massart, B.G.M. Vandeginste, et al., *Handbook of Chemometrics and Qualimetrics Part A*, Elsevier, Amsterdam, 1997.
- [29] H.R. Keller, D.L. Massart, *Chemom. Intell. Lab. Syst.* 12 (1992) 209-224.
- [30] R. Tauler, *Chemom. Intell. Lab. Syst.* 30 (1995) 133-146.
- [31] M. Amrhein, B. Srinivasan, D. Bonvin, M.M. Schumacher, *Chemom. Intell. Lab. Syst.* 33 (1996) 17-33.

### **3.3.2. Paper**

*The evaluation of the adsorption and rate constants of the photocatalytic degradation of C.I. Acid Yellow 9 by means of HS-MCR-ALS: a study of process variables*

Cristina Fernández, Anna de Juan, M. Soledad Larrechi, M. Pilar Callao

**Submitted**

UNIVERSITAT ROVIRA I VIRGILI

ANALYTICAL METHODOLOGIES BASED ON CHEMOMETRICS TO OPTIMIZE THE PHOTODEGRADATION OF DYES

Cristina Fernández Barrat

DL:T. 160-2012

---

## The evaluation of the adsorption and rate constants of the photocatalytic degradation of C.I. Acid Yellow 9 by means of HS-MCR-ALS: a study of process variables

Cristina Fernández<sup>a</sup>, Anna de Juan<sup>b</sup>, M. Soledad Larrechi<sup>a</sup>, M. Pilar Callao<sup>a</sup>

<sup>a</sup> *Department of Analytical and Organic Chemistry, Rovira i Virgili University, Marcel·lí Domingo s/n Campus Sescelades, E-43007 Tarragona, Spain*

<sup>b</sup> *Department of Analytical Chemistry, University of Barcelona Diagonal 645, E-08028 Barcelona, Spain*

### Abstract

This study focuses on the kinetic analysis of the photocatalytic degradation of C.I. Acid Yellow 9. Adsorption and rate constants related to the physical adsorption on the catalyst surface and the degradation of the dye upon illumination were calculated by applying hybrid hard- and soft-multivariate curve resolution alternating least squares (HS-MCR-ALS) to the UV-visible spectra recorded during the photocatalytic degradation process. The influence of the catalyst type, the catalyst concentration and the pH on the degradation rate was assessed using the experimental results obtained from a full factorial 2<sup>3</sup> experimental design. Physical adsorption was more relevant when TiO<sub>2</sub> was employed as a catalyst. The global rate of the photocatalytic degradation of the dye was found to be closely related to the catalyst type, its concentration level and the interaction between both factors. pH was only found to be relevant when TiO<sub>2</sub> was used. The photodegradation of C.I. Acid Yellow 9 was optimal when using high concentrations of ZnO as catalyst.

**Keywords:** C.I. Acid Yellow 9; Langmuir-Hinshelwood; Photocatalytic degradation; Adsorption constants; Experimental design; Hybrid hard- and soft-modeling.

## 1. Introduction

Organic azo dyes are used in many industrial processes and they are, therefore, found in industrial wastewater, which poses a major environmental problem. One of the most commonly used methods for the removal of these compounds from the environment is photocatalytic degradation, in which a semiconductor is used as a catalyst [1]. This process has considerable advantages, since it can work with sunlight because the light required to activate the catalyst is low-energy UV- A [2], the use of dissolved oxygen (or air) is sufficient, which eliminates the need for expensive oxidizing chemicals (e.g. O<sub>3</sub>) and the catalysts most often used are inexpensive, nonhazardous, stable and reusable.

Degradations using heterogeneous catalysts involve at least two steps: physical adsorption and reaction on the catalyst surface followed by degradation upon illumination [3]. Therefore, analyzing the effect of the various process variables on the efficiency of photodegradation is of great interest [4-12]. The rate of photodegradation is the parameter used to measure this effect.

In the literature, two approaches are used to define the evolution of these processes: taking into account the value of adsorption and rate constants separately [5,9,10,13-15] or considering the process globally with a pseudo first-order kinetic model [4,6-8,16-22]. The methods used in the first approach often require a high number of experiments and/or a high instrumental cost. The second approach defines the whole process with a single step, which makes impossible to evaluate the specific influence of the adsorption in the global kinetics.

The objective of this work is to develop a rapid and simple method to calculate both kinetic and adsorption constants and to assess the effect of catalyst type, catalyst concentration and pH on the photocatalytic degradation efficiency of C.I. Acid Yellow 9. The strategy used involves an experimental design methodology, UV-visible monitoring of the photodegradation experiments and chemometric analysis of data in order to consider both the adsorption and the photodegradation steps. Specifically, the experiments were planned according to a full factorial 2<sup>3</sup> design. UV-visible spectra of all degradations were treated using

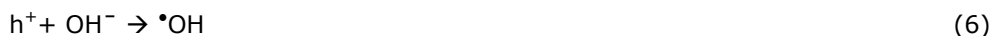
MCR-ALS [23]. The values of the adsorption and rate constants of the photocatalytic degradation were obtained by applying the hybrid hard- and soft-modelling MCR-ALS approach (HS-MCR-ALS) [24], incorporating the Langmuir-Hinshelwood model as a hard-modeling constraint [25,26]. This hybrid hard- and soft-modeling approach has been employed successfully in several fields [27-32].

The whole strategy presented above has been applied to study the photocatalytic degradation of C.I. Acid Yellow 9 and, at a low experimental cost, has allowed for the simultaneous determination of the adsorption and rate constants and the study of the effect of several factors on the process of interest. To our knowledge, no strategies of simultaneous determination of adsorption and rate constants in catalytic processes have been previously reported; therefore, this study represents an advance in the field of heterogeneous catalysis.

## 2. Theoretical background

### 2.1. Photocatalytic degradation

When catalyst (e.g. ZnO) particles are irradiated by means of UV light with an energy higher than its band gap energy, the following reactions can take place [9,18,33] (Eq 1-10):



Degradation starts when an electron ( $e^-$ ) on the catalyst surface is excited to the conduction band, leaving a positive hole in the valence band ( $h^+$ ) (Eq 1).

These electron-hole pairs can either recombine (Eq 2), react with the dye (Eq 3-4) or react with other molecules present in degradation medium (Eq 5-7). Photogenerated electrons might react to the dye (Eq 4) or to electron acceptors present in the water or adsorbed on the catalyst surface such as O<sub>2</sub> (Eq 7). On the other hand, photogenerated holes can oxidize dye (Eq 3) or react to OH<sup>-</sup> or H<sub>2</sub>O (Eq 5-6). The radicals that are formed are powerful oxidizing agents and attack the organic compounds (Eq 8-10) and intermediates to produce end products, such as H<sub>2</sub>O, CO<sub>2</sub> and small inorganic acids.

All these reactions take place through one of four possible situations: (a) the reaction occurs while both the radical and the substrate molecule are adsorbed, (b) the reaction takes place between a radical in solution and an adsorbed substrate molecule, (c) a radical linked to the surface reacts with a substrate molecule in solution or (d) the reaction takes place between a radical and a substrate molecule in solution [33-34].

It has been proved [3,9,10,13,33-34] that all these possible mechanisms give rise to the Langmuir-Hinshelwood model, commonly used to describe photocatalytic degradation kinetics, although it has not been possible to determine whether the process takes place on the surface of the solution or at the interface. This model is expressed as (Eq 11):

$$r = -\frac{dC}{dt} = \frac{k_r KC}{1 + KC} \quad (11)$$

where  $r$  is the rate of dye degradation,  $C$  is the concentration of the dye in mg·L<sup>-1</sup> at any time,  $k_r$  is the rate constant for photocatalysis and  $K$  the adsorption constant of the dye on the catalyst particles.

## **2.2. Hard and soft modeling (HS-MCR-ALS).**

Multivariate curve resolution-alternating least squares (MCR-ALS) is an iterative resolution algorithm based on the bilinear decomposition shown in Eq. (12):

---

$$\mathbf{D} = \mathbf{C}\mathbf{S}^T + \mathbf{E} \quad (12)$$

where the experimental matrix  $\mathbf{D}$  is decomposed into two new matrices:  $\mathbf{C}$ , which contains the process concentration profiles and  $\mathbf{S}^T$ , which contains the spectral profiles of the related pure process compounds. The resolution consists of finding the  $\mathbf{C}$  and  $\mathbf{S}^T$  matrices, which describe  $\mathbf{D}$  with an optimal fit, i.e., with the minimum sum of squares of all the elements in the error matrix  $\mathbf{E}$ , and with chemically meaningful profiles [23,24].

In soft-modeling MCR-ALS, natural constraints, such as unimodality or non-negativity are applied to the data sets during optimization [23]. The HS-MCR-ALS approach proposed includes a hard-modeling constraint during the optimization process that decreases the rotational ambiguity associated with the pure soft-modeling approach. The hard modelling constraint acts incorporating a physicochemical model, e.g., kinetic, equilibrium law, to give shape to the process profiles. Because of the flexibility of MCR-ALS regarding the application of soft and hard constraints, it is possible to force only some of the components in the  $\mathbf{C}$  matrix to obey a hard modelling constraint, while the other ones are soft modeled [24,27,32].

In this example, the hard-modeling constraint worked incorporating the Langmuir-Hinshelwood model to define the concentration profile related to the decay of the parental dye. As a result, this profile is shaped according to the model defined and the rate and adsorption constants are obtained as additional information. The concentration profiles of the photoproducts formed are soft-modelled.

### 3. Materials and methods

#### 3.1. Chemicals

The reagents used in this study were analytical-grade chemicals. C.I. Acid Yellow 9 (2-Amino-5-([4-sulfophenyl]azo)benzenesulfonic acid) (95%) was purchased from Sigma-Aldrich. ZnO powder with a particle size of less than 1 $\mu$ m



(99.9%) and  $\text{TiO}_2$  in anatase form (99.8%) were also purchased from Sigma-Aldrich and used as catalysts without further treatment. The pH was adjusted with NaOH and  $\text{H}_2\text{SO}_4$  from PROLABO. All solutions were prepared in ultrapure Milli-Q water from a system supplied by Millipore (USA). Degradation samples that contain catalyst were filtered through  $0.45 \mu\text{m}$  Teflon syringe filters before measuring the related UV spectra. We used Teflon filters instead of nylon filters to prevent the sulphonated azo dye from adsorbing into the filters.

### **3.2. Instruments and software**

Photodegradation studies were performed in a cylindrical annular batch reactor consisting of a Pyrex glass outer reactor with a capacity of 0.7 L and a quartz immersion tube (2.5 cm i.d. and 38 cm long) covered by a cooling quartz jacket. This tube contained a 47 W high-pressure mercury-vapor lamp (HPML) (Heraeus Noblelight, Germany). The light source emitted at 366 nm.

The spectrophotometric UV-visible data were acquired using a diode-array spectrophotometer (Shimadzu MultiSpec-1501) and Hyper-UV 1.51 software. The UV-visible spectra of the blank and dye degradation samples were recorded with a spectral resolution of 1 nm from 270 to 720 nm.

The UV-visible spectra were exported and converted in MATLAB binary files. The data matrix was first analyzed by MCR-ALS [35]. Hard and soft-modeling MCR routines in this work were designed in-house with a MATLAB 6.5 computer environment [36]. Experimental design calculations were performed using Statgraphics plus 5.0.

### **3.3. Samples and photodegradation procedure**

All samples contain 0.5 L solution of  $20 \text{ mg}\cdot\text{L}^{-1}$  of C.I. Acid Yellow 9 in Milli-Q water. Table 1 shows the design of the experiments performed, with the levels of the selected factors detailed. The concentrations of dye and catalyst were selected from those described in the literature and based on preliminary studies. ZnO and  $\text{TiO}_2$  were selected because they are the most commonly used photocatalysts for dye photodegradation [5,6,8-10,12,15,21]. pH is considered a qualitative factor, i.e., pH values selected were 1 unit above the zero point charge (high) when the

catalyst surface is negatively charged or 1 unit below the zero point charge (low) when the catalyst surface is positively charged. The pH value for the zero point charge corresponds to pH=6.5 for TiO<sub>2</sub> [13,37] and pH=9 for the ZnO [6].

**Table 1.** Experiments included in the full factorial 2<sup>3</sup> design.

Sample	Catalyst	Catalyst concentration (g·L <sup>-1</sup> )	pH
1	TiO <sub>2</sub>	1	low
2	ZnO	1	low
3	TiO <sub>2</sub>	2	low
4	ZnO	2	low
5	TiO <sub>2</sub>	1	high
6	ZnO	1	high
7	TiO <sub>2</sub>	2	high
8	ZnO	2	high

6 mL-samples of the degradation solution were taken at the beginning of the experiment (t=0 min), every minute until 10 min, every 2 min until 30 min, every 5 min until 60 min, every 10 min until 120 min and every 30 min until the end of the degradation, which can be seen by the complete discoloration of the solution. The total degradation time ranged from 150 to 240 min depending on the experiment. Samples were stored in the dark until they were filtered with Teflon syringe filters in order to separate the catalyst and record the spectra on a clean solution. All spectra were recorded the same day the degradation was performed. Moreover, a solution of 20 mg·L<sup>-1</sup> of C.I. Acid Yellow 9 without catalyst, used as the degradation blank, was introduced into the reactor and irradiated with the UV lamp for 180 minutes. The spectra of this solution were recorded every 30 min.

### 3.4. Chemometric procedure

All spectra recorded during the photodegradation of C.I. Acid Yellow 9 were arranged in a data matrix **D** ( $m \times n$ ) where  $m$  is the number of spectra recorded during the degradation process and  $n$  is the number of wavelengths. In our datasets,  $m$  can vary from 34 to 37 depending on the degradation time of each experiment and  $n$  is 451 in all cases.

The number of variability sources in the experimental data was determined by singular value decomposition (SVD). Evolving factor analysis (EFA) was applied

to obtain the evolution of the components throughout the degradation processes, i.e., when they emerge end when they decay [38]. The EFA solution was employed as an initial estimate of the concentration profiles in the first MCR-ALS analysis, where only the soft-modeling constraints of non-negativity for the concentration and spectral profiles and unimodality for the concentration profiles were applied. In a subsequent step, HS-MCR-ALS was performed including the hard-modeling constraint, which forced the concentration profile of C.I. Acid Yellow 9 to follow the Langmuir-Hinshelwood kinetic model (Eq. (11)). The spectral profiles obtained with the first MCR-ALS analysis were used in this case as initial estimates. The initial estimates for the adsorption and rate constants were obtained from the literature [5,10,13,14]. Spectral and concentration profiles and adsorption and rate constants were obtained from the resolution.

#### 4. Results and discussion

Fig. 1 shows the recorded spectra as a function of the degradation time for the blank (Fig. 1a), and for two experiments using  $\text{TiO}_2$  (Fig. 1b) and  $\text{ZnO}$  (Fig. 1c) as catalysts. These data show that the dye does not degrade in absence of catalyst, whereas degradation is almost complete when  $\text{ZnO}$  is added and only partial degradation occurs when  $\text{TiO}_2$  is used. The figure also shows that the value of maximum absorbance shifts slightly toward higher wavelengths during degradation. This variation suggests that the degradation process takes place through the formation of, at least, another chemical species that absorbs in the same UV-vis region of C.I. Acid Yellow 9.

When the spectral data matrices recorded throughout the monitored reactions were analyzed by singular value decomposition (SVD), two factors were found significant in all cases. The estimation of this number was done taking into consideration the second singular value obtained by SVD for the blank degradation ( $\lambda = 0.70$ ) as a threshold value. Therefore, two absorbing chemical species were assumed to be present during the dye degradation, i.e., the parental dye and an absorbing degradation product.

An evolving factor analysis (EFA) of the spectral data matrices recorded over the course of the monitored reaction was conducted to determine the evolution of the species involved in the degradation process, i.e., when they emerge (forward EFA) and when they disappear (backward EFA). Fig. 2 shows the EFA results obtained from the two first experiments listed in Table 1 (for the TiO<sub>2</sub> (Fig. 2a) and ZnO (Fig. 2b) catalysts). The red line indicates the noise threshold associated with the second singular value of the blank.

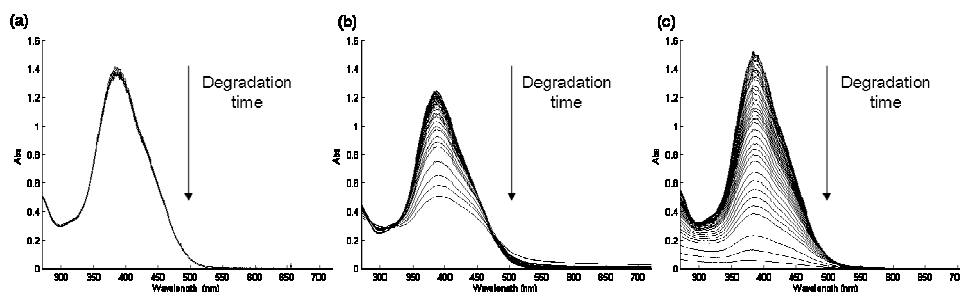


**Fig. 1.** Photodegradation spectra of C.I. Acid yellow 9: (a) dye solution in absence of catalysts, (blank), (b) with TiO<sub>2</sub> as catalyst (experiment 1) and (c) with ZnO as catalyst (experiment 2).

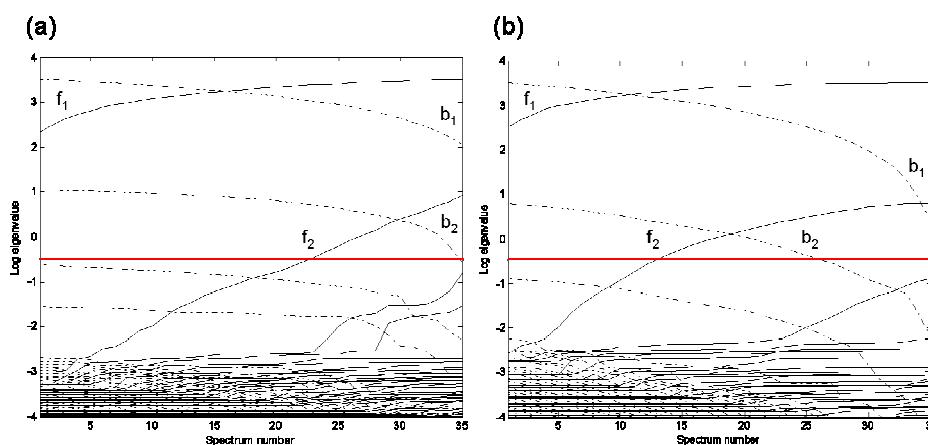


**Fig. 2.** Evolving factor analysis (EFA) plots in forward (continuous lines) and backward (dotted lines) directions. a) Results for experiments 1 and b) for experiment 2.

Analyzing the EFA plot in the forward direction (f), it can be seen that the first factor ( $f_1$ ) maintains a significant value from the beginning of the degradation process. The second factor ( $f_2$ ), which corresponds to the emergence of a new

species, achieves a significant value at the 22<sup>nd</sup> spectrum (35 min of degradation) when TiO<sub>2</sub> is employed as a catalyst, whereas this factor becomes significant at the 13<sup>th</sup> spectrum (14 min of degradation) when ZnO is used. This is a first sign of the faster degradation of the dye in the presence of ZnO. Complementary information is obtained in the backward analysis. When TiO<sub>2</sub> is used as a catalyst, two factors ( $b_1$  and  $b_2$ ) exist throughout the degradation process, whereas the second factor ( $b_2$ ) achieves a significant value at the 27<sup>th</sup> spectrum (60 min of degradation) when ZnO is used. This indicates that the parental dye disappears completely when ZnO is used, whereas a certain amount remains in the solution when TiO<sub>2</sub> is used for the same degradation process. This is consistent with the raw data shown in Fig. 1.

The first MCR-ALS was performed using the concentration profiles retrieved by EFA as initial estimates and soft-modeling constraints, such as non-negativity in the concentration and spectral direction and unimodality in the concentration direction. After this soft-modeling analysis, HS-MCR-ALS was performed using the resolved spectrum for the intermediate species and the pure UV-vis spectra of C.I. Acid Yellow 9 as initial estimates. As mentioned in section 3.4, the Langmuir-Hinshelwood kinetic model was applied as a hard-modeling constraint to model the decay profile of the parental dye. The resolution results obtained by HS-MCR-ALS for the photodegradation of the two experiments shown in Figures 1b and 1c are presented in Fig. 3. In all the experiments analyzed (see Table 1), the fitting error varied from 1 to 6% and the explained variance was always higher than 99.6%. These values indicate the satisfactory description of the variation of the raw data and support the appropriateness of the hard model applied.

Fig. 3a and 3b show the recovered spectral profiles by HS-MCR-ALS. The black spectrum is from the C.I. Acid Yellow 9, as shown by the correlation coefficient between the real C.I. Acid Yellow 9 spectrum and the spectrum retrieved by MCR-ALS, always higher or equal to 0.9999, whereas the grey spectrum is attributed to an intermediate whose spectrum is slightly shifted towards higher wavelengths. The correlation coefficient of the spectrum recovered for the parental dye, along with the high explained variance and the consistency of the spectral shapes recovered with the evolution of the raw spectra suggests that

the results obtained provide a good description of the real process of photocatalytic degradation.

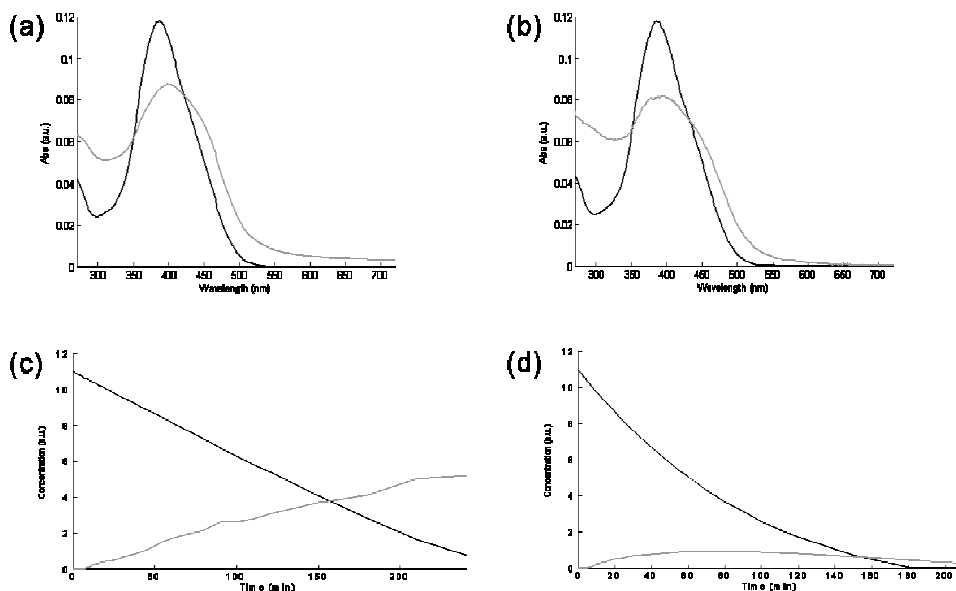
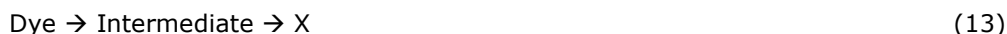


**Fig. 3.** HS-MCR-ALS resolution results. (a and c) correspond to experiment 1 (TiO<sub>2</sub>) and (b and d) to the experiment 2 (ZnO).

Fig. 3c and 3d show the concentration profiles recovered. When TiO<sub>2</sub> is used (Fig. 3c), the intermediate remains in solution at the end of the degradation process, whereas when ZnO is used (Fig. 3d), the intermediate is degraded over the course of the photodegradation period and no new photoproducts are generated. The evolution of these degradation profiles confirms the expected faster degradation of the dye in the presence of ZnO as compared with TiO<sub>2</sub> and suggests the following general degradation pathway (Eq 13):



where X may correspond to non-absorbing species in the wavelength range studied, such as CO<sub>2</sub> and H<sub>2</sub>O or small inorganic acids, which are typical products of photocatalytic degradation processes. Despite the fact that MCR-ALS solutions may incorporate certain degree of ambiguity [23], the solutions obtained in this

example lack this phenomenon for several reasons: first, the spectrum of the dye is unambiguously recovered because it is the only species present at the beginning of the reaction. Second, because of the application of the hard-modeling constraint, the concentration profile of the dye and the spectrum of the intermediate are also resolved without ambiguities, as proven in a recent work by Golshani et al. [39]. Therefore, the conclusions extracted related to the dye degradation process and the related adsorption and rate constants are highly reliable and unaffected by the uncertainty coming from ambiguity.

Table 2 shows the adsorption and rate constants for each analyzed experiment and the degradation rate calculated using Eq 11. It is important to note that the photodegradation processes carried out using  $\text{TiO}_2$  as a catalyst (Exp 1, 3, 5 and 7) always needed longer degradation times. In all cases, the degradations using this catalyst were measured until the fixed limit time value (240 min) and in all cases after this time the solution remained coloured. The degradations employing  $\text{ZnO}$  as a catalyst (Exp 2, 4, 6 and 8) were performed for 150-210 min and after this time, discoloration of the solution and, hence, complete degradation, was achieved.

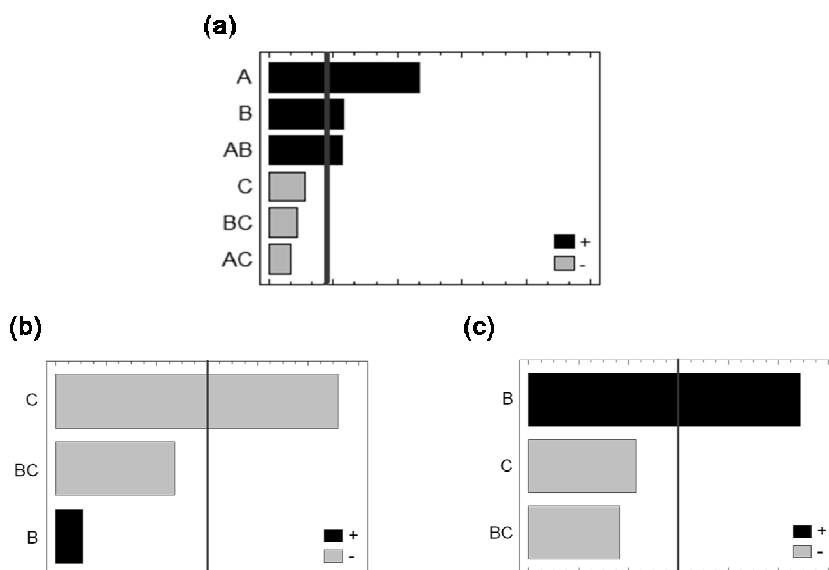
The degradation rate was always higher when  $\text{ZnO}$  was used as a catalyst, which is consistent with previous results. For this catalyst, the adsorption constant was lower than the rate constant, which suggests that this catalyst favours the adsorption of water molecules and/or  $\text{OH}^-$  ions (reactions 5 and 6 in section 2.1) and the generated  $\text{OH}^\bullet$  could be the species reacting with the dye molecules in solution (reaction 9, section 2.1). When  $\text{TiO}_2$  was used, the adsorption constant was higher than the rate constant, except in experiment 3, which suggests that reaction 3 and 4 in section 2.1, in which the degradation of dye is done on the surface of the catalyst, are important processes when this catalyst is employed.

Fig. 4a shows the Pareto chart obtained to evaluate the significance of the effects of the factors considered on the degradation rates. The vertical line indicates the value above which the effects are relevant for a significance level of  $\alpha = 0.05$ . The chart shows that there are two relevant factors - catalyst type and catalyst concentration - and that their interaction is significant. The most important

factor is catalyst type, and high values for this factor corresponding to the use of the ZnO catalyst are related to higher degradation rates, which is in agreement with the results shown in Table 2.

**Table 2.** Adsorption, rate constants and degradation rates for experiments in Table 1.

Exp	kr (mg·L <sup>-1</sup> ·min <sup>-1</sup> )	K (L·mg <sup>-1</sup> )	r (mg·L <sup>-1</sup> ·min <sup>-1</sup> )
1	0.065 ± 0.001	1.3 ± 0.2	0.06
2	0.5 ± 0.1	0.026 ± 0.008	0.18
3	0.17 ± 0.05	0.04 ± 0.02	0.07
4	1.4 ± 0.4	0.024 ± 0.008	0.4
5	0.06 ± 0.03	0.15 ± 0.01	0.05
6	0.3 ± 0.1	0.05 ± 0.03	0.16
7	0.05 ± 0.01	0.22 ± 0.08	0.04
8	1.5 ± 0.6	0.013 ± 0.001	0.3



**Fig. 4.** Pareto charts for (a) all experiments, (b) TiO<sub>2</sub> experiments and (c) ZnO experiments. A designs catalyst type, B catalyst concentration and C pH.

Because catalyst type was found to have the most pronounced effect, we decided to study the effect of concentration and pH separately for the set of experiments performed with each catalyst. Fig. 4b shows that the effect of pH is important when TiO<sub>2</sub> is used as catalyst and, in this case, the degradation is more efficient at lower pH values (pH 5.5). The Pareto chart for ZnO shown in Fig. 4c



demonstrates that only the effect of catalyst concentration is relevant with regard to this catalyst. This is not easy to interpret because pH plays multiple roles in photodegradation processes (reactions 5, 6 and 8, section 2.1), so it may be affecting the process in a confounded manner [7].

Fig. 5 shows the concentration profiles retrieved by HS-MCR-ALS for C.I. Acid Yellow 9 during the first 150 min in all eight experiments. It is clear from the figure that the shape of the kinetic profiles is consistent with the conclusions inferred from the Pareto charts of Fig. 4. The profiles are grouped according to catalyst type. Odd numbers refer to  $\text{TiO}_2$  catalyst and the degradation curves are always above those using ZnO as catalyst (even numbers), implying a lower degradation when the former catalyst is used. As seen in specific Pareto tables for each catalyst, the increase of catalyst concentration with ZnO leads to higher degradation (compare experiment pairs 2 and 4 and 6 and 8), whereas for  $\text{TiO}_2$  experiments, lowering the pH is the clearest option to favour degradation (compare pairs 1 and 5 and 3 and 7). When  $\text{TiO}_2$  was used, the best results were achieved in experience 1 (approximately 20% of the dye remained in the solution) in which low concentration values of  $\text{TiO}_2$  were used at a low pH. When ZnO was used as a catalyst in experiment 4, which corresponds to high concentration values of ZnO at a low pH, 100% of the dye was degraded.

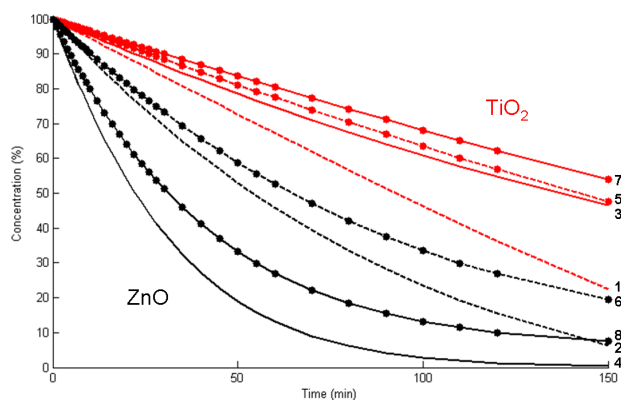


**Fig. 5.** Decay profiles for C.I. Acid yellow 9 retrieved by HS-MCR-ALS. Small numbers refer to experiments listed in Table 1. (-) high catalyst concentration, (--) low catalyst concentration, (●) high pH values.

---

## 4. Conclusions

The method proposed, which is based on the use of UV-vis spectroscopic monitoring and HS-MCR-ALS including the Langmuir-Hinshelwood model as a hard modeling constraint makes possible understanding the behavior of the photodegradation of C.I. Acid Yellow 9, establishing the reaction pathway and obtaining the adsorption and rate constant values defining this process.

Preliminary exploratory by EFA analysis and soft-modeling MCR-ALS suggested that the dye photodegradation takes place through the formation of an intermediate that is afterwards degraded to form non-absorbing species, which could be  $\text{CO}_2$ ,  $\text{H}_2\text{O}$  and small inorganic acids. HS-MCR-ALS allowed a better modeling of the photodegradation data by imposing the hard modeling constraint only onto the dye concentration profile. As straightforward results, the physical adsorption of the dye onto the catalyst was found to be more relevant when  $\text{TiO}_2$  was used as opposed to  $\text{ZnO}$ , where degradation took place without much effect of adsorption in the global degradation rate.

From the HS-MCR-ALS analysis of all experiments, process parameters could be derived that helped to understand better the effect of potential factors, such as catalyst type, catalyst concentration and pH onto the photodegradation evolution. The results showed that the most important factors in this process are catalyst type, catalyst concentration and their interaction. pH was only found to be relevant when  $\text{TiO}_2$  was used. Optimal conditions for photodegradation of C.I. Acid Yellow 9 involved using high concentration of  $\text{ZnO}$  as a catalyst.

## Acknowledgements

The authors would like to thank the Spanish Ministry of Science and Innovation for providing Cristina Fernández with a doctoral fellowship (AP2007-03788). A.de Juan acknowledges financial support from the Spanish government (grant CTQ2009-11572).

## References

- [1] C. Fernández, M.S. Larrechi, M.P. Callao, *Trends Anal. Chem.* 29 (2010) 1202-1211.
- [2] K. Mehrotra, G.S. Yablonsky, A.K. Ray, *Ind. Eng. Chem. Res.* 42 (2003) 2273-2281.
- [3] K.V. Kumar, K. Porkodi, A. Selvaganapathi, *Dyes Pigm.* 75 (2007) 246-249.
- [4] V.K. Gupta, R. Jain, A. Mittal, M. Mathur, S. Sikarwar, *J. Colloid Interface Sci.* 309 (2007) 464-469.
- [5] A.P. Toor, A.Verma, C.K. Jotshi, P.K. Bajpai, V. Singh, *Dyes Pigm.* 68 (2006) 53-60.
- [6] S.K. Kansal, M. Singh, D. Sud, *J. Hazard. Mater.* 141 (2007) 581-590.
- [7] M.M. Uddin, M.A. Hasnat, A.J.F. Samed, R.K. Majumdar, *Dyes Pigm.* 75 (2007) 207-212.
- [8] M.R. Sohrabi, M. Ghavami, *Desalination* 252 (2010) 157-162.
- [9] M.A. Behnajady, N. Modirshahla, R. Hamzavi, *J. Hazard. Mater.* B133 (2006) 226-232.
- [10] S. Chakrabarti, B. K. Dutta, *J. Hazard. Mater.* B112 (2004) 269-278.
- [11] M. Sleiman, D. Vildoza, C. Ferronato, J.M. Chovelon, *Appl. Catal., B* 77 (2007) 1-11.
- [12] C. Fernández, M.S. Larrechi, M.P. Callao, *Talanta* 79 (2009) 1292-1297.
- [13] K. Sahel, N. Perol, H. Chermette, C. Bordes, Z. Derriche, C. Guillard, *Appl. Catal., B* 77 (2007) 100-109.
- [14] J.P.S. Valente, P.M. Padilha, A.O. Florentino, *Chemosphere* 64 (2006) 1128-1133.
- [15] S. Dutta, S.A. Parsons, C. Bhattacharjee, P. Jarvis, S. Datta, S. Bandyopadhyay, *Chem. Eng. J.* 155 (2009) 674-679.
- [16] J.C. Garcia, J.L. Oliveira, A.E.C. Silva, C.C. Oliveira, J. Nozaki, N.E. de Souza, *J. Hazard. Mater.* 147 (2007) 105-110.
- [17] B. Mounir, M.N. Pons, O. Zahraa, A. Yaacoubi, A. Benhammou, *J. Hazard. Mater.* 148 (2007) 513-520.
- [18] W.Z. Tang, Z. Zhang, H. An, M. O. Quintana, D.F. Torres, *Environ. Technol.* 18 (1997) 1-12.
- [19] K. Tanaka, K. Padermpole, T. Hisanaga, *Water Res.* 34 (2000) 327-333.
- [20] C. Galindo, P. Jacques, A. Kalt, *J. Photochem. Photobiol., A* 130 (2000) 35-47.
- [21] M.G. Dias, E. B. Azevedo, *Water, Air, Soil Pollut.* 240 (2009) 79-87.
- [22] A.J. Julson, D.F. Ollis, *Appl. Catal., B* 65 (2006) 315-325.
- [23] R. Tauler, *Chemom. Intell. Lab. Syst.* 30 (1995) 133-146.
- [24] A. de Juan, M. Maeder, M. Martínez, R. Tauler, *Chemom. Intell. Lab. Syst.* 54 (2000) 123-141.
- [25] K.V. Kumar, K. Porkodi, F. Rocha, *Catal. Commun.* 9 (2008) 82-84.
- [26] A.V. Emeline, V.K. Ryabchuk and N. Serpone, *J. Phys. Chem., B* 109 (2005) 18515-18521.
- [27] C. Fernández, M.P. Callao, M.S. Larrechi, *J. Hazard. Mater.* 190 (2011) 986-992.
- [28] J. Diewok, A. de Juan, M. Maeder, R. Tauler, B. Lendl, *Anal. Chem.* 75 (2003) 641-647.

- 
- [29] A. de Juan, M. Maeder, M. Martínez, R. Tauler, *Anal. Chim. Acta.* 442 (2001) 337-350.
- [30] K.J. Molloy, M. Maeder, M.M. Schumacher, *Chemom. Intell. Lab. Syst.* 46 (1999) 221-230.
- [31] J.M. Amigo, A. de Juan, J. Coello, S. MasPOCH, *Anal. Chim. Acta.* 567 (2006) 245-254.
- [32] N. Mouton, A. de Juan, M. Sliwa, C. Ruckebusch, *Chemom. Intell. Lab. Syst.* 150 (2011) 74-82.
- [33] I.K. Konstantinou, T.A. Albanis, *Appl. Catal., B* 49 (2004) 1-14.
- [34] C.S. Turchi, D.F. Ollis, *J. Catal.* 122 (1990) 178-192.
- [35] J. Jaumot, R. Gargallo, A. de Juan, R. Tauler, *Chemom. Intell. Lab. Syst.* 76 (2005) 101. <http://www.mcrals.info/>. Last accessed october 2011
- [36] Matlab 6.5, The Mathworks, South Natick, MA, USA.
- [37] A. Aguedach, S. Brosillon, J. Morvan, E.K. Lhadi, *Appl. Catal., B* 57 (2005) 55-62
- [38] M. Maeder, A. Zuberbuehler, *Anal. Chem.* 62 (1990) 2220-2224.
- [39] A. Golshan, H. Abdollahi, M. Maeder. *Anal. Chim. Acta.* 709 (2012) 32-40.

UNIVERSITAT ROVIRA I VIRGILI

ANALYTICAL METHODOLOGIES BASED ON CHEMOMETRICS TO OPTIMIZE THE PHOTODEGRADATION OF DYES

Cristina Fernández Barrat

DL:T. 160-2012

---

### 3.4. Dye determination by sequential injection chromatography (SIC)

This section deals with objective (d) mentioned in chapter 1 and is related to one of the future proposals indicated in section 3.1: the development of rapid analytical methods for determining dyes with an economic use of reagents and little production of waste. The contribution of this thesis is presented in the paper: ***Multisyringe chromatography (MSC) using a monolithic column for the determination of sulphonated azo dyes***. In this study the experimental work was carried out in collaboration with the group of Analytical Chemistry, Automation and Environment of the University of the Balearic Islands (UIB).

In this paper, a versatile and low-cost methodology based on MSC is developed to determine Acid Yellow 23, Acid Yellow 9 and Acid Red 97 in real water samples. Sequential injection chromatography, which involves monolithic columns coupled to flow techniques is a promising technique for the analysis of simple mixtures.

UNIVERSITAT ROVIRA I VIRGILI

ANALYTICAL METHODOLOGIES BASED ON CHEMOMETRICS TO OPTIMIZE THE PHOTODEGRADATION OF DYES

Cristina Fernández Barrat

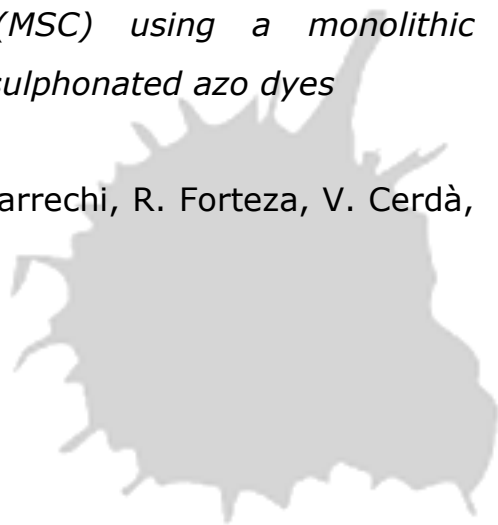
DL:T. 160-2012

### **3.4.1. Paper**

*Multisyringe chromatography (MSC) using a monolithic column for the determination of sulphonated azo dyes*

Cristina Fernández, M. Soledad Larrechi, R. Forteza, V. Cerdà,  
M. Pilar Callao

**Talanta 82 (2010) 137-142**





UNIVERSITAT ROVIRA I VIRGILI

ANALYTICAL METHODOLOGIES BASED ON CHEMOMETRICS TO OPTIMIZE THE PHOTODEGRADATION OF DYES

Cristina Fernández Barrat

DL:T. 160-2012

---

## Multisyringe chromatography (MSC) using a monolithic column for the determination of sulphonated azo dyes

Cristina Fernández<sup>a</sup>, M. Soledad Larrechi<sup>a</sup>, R. Forteza<sup>b</sup>, V. Cerdà<sup>b</sup>, M. Pilar Callao<sup>a</sup>

<sup>a</sup> *Department of Analytical and Organic Chemistry, Rovira i Virgili University, Marcel·lí Domingo s/n Campus Sescelades, E-43007 Tarragona, Spain*

<sup>b</sup> *Department of Chemistry, Faculty of Sciences, University of the Balearic Islands, Carretera de Valldemossa, Km 7.5, E-07122 Palma de Mallorca, Spain*

### Abstract

A methodology, based on multisyringe chromatography with a monolithic column was developed to determine three sulphonated azo textile dyes: Acid Yellow 23, Acid Yellow 9 and Acid Red 97. An ion pair reagent was needed because of the low affinity between the monolithic column and the anionic dyes. The proposed analytical system is simple, versatile and low-cost and has great flexibility in manifold configuration.

The method was optimized through experimentation based on experimental design methodology. For this purpose two blocks of full factorial  $2^3$  were done sequentially. In the first experimental plan, the factors studied were: the % of acetonitrile in organic phase, the % of H<sub>2</sub>O in the mobile phase and the kind of ion pair reagent. In this stage, a simple configuration was used which has only one syringe for the mobile phase.

After the first experimentation, we added a second syringe with a second mobile phase to the multisyringe module and performed a second full factorial  $2^3$ . The factors studied in this case were: the % of acetonitrile in the second mobile phase, the pH and the concentration of ion pair reagent in both mobile phases. After this design, the optimal conditions were selected for obtaining a good resolution between the peaks of yellow dyes (1.47) and the elution of red dye in less than 8 min.

The methodology was validated by spiking different amounts of each dye in real water samples, specifically, tap water, well water and water from a biological wastewater lagoon.

**Keywords:** Textile dyes; Low pressure chromatography; Multisyringe module; Experimental design; Full factorial design.

## 1. Introduction

Azo dyes are the main category of dyes used in the textile industry and many of them are highly soluble in water and resistant to microbial degradation. Consequently, these compounds can be found in wastewater as well as in surface water [1]. These dyes are of great environmental and toxicological concern, which mean that reliable methods are needed for their determination.

The most common methodologies for this purpose use separation techniques [2]. The most frequently applied technique for determining sulphonated azo dyes is ion pairing high-performance liquid chromatography (HPLC) with tetraalkylammonium salts. This technique is used because it fully ionizes anionic (poly)sulphonated dyes over a broad pH range without suppressing their dissociation in buffered mobile phases at a low pH [3-7]. Due to the ionic character of the analytes, electrophoresis has a great potential for determining this kind of compound [8-11]. Also, methodologies have been proposed that employ UV-visible spectrophotometry to make direct measurements; these methodologies have lower experimental costs and lower analysis times. In these cases, to solve the lack of selectivity, chemometric techniques are employed to obtain the concentration of the dyes [12-14]. In spite of the advantages, these kinds of methodologies are not usually used in routine analyses in laboratories.

The aim of our study is to develop a methodology using multisyringe ion pair chromatography with a monolithic column to determine three sulphonated azo dyes (Acid Yellow 23, Acid Yellow 9 and Acid Red 97) which are used jointly in the textile industry to obtain certain tonalities.

---

Monolithic columns offer the opportunity to perform separations in some flow-analysis manifolds that would not withstand the back-pressure from conventional packed columns. Monolithic columns are more tolerant of eluent switching and equilibrate more rapidly, which means they can work in multiisocratic mode. The applications of ion chromatography and ion-pair chromatography with C18 monolithic columns have been reviewed [15]. It has to be noticed that despite their advantages this kind of columns are not frequently used in typical HPLC configurations.

Sequential injection chromatography (SIC) used with a hybrid FIA/HPLC system with monolithic columns combines chromatographic techniques with the flow techniques of analysis and has been shown to be a good alternative to HPLC for quickly analyzing simple samples [16,17]. There are some examples in the literature that use SIC to determine pharmaceutical compounds [18-20], pesticides [21] or phenolic species [22]. Multisyringe chromatography (MSC) is a new combination of multisyringe flow injection analysis with low pressure chromatography, which allows the mobile phase to be managed in ways that are not possible with SIC. The main difference between SIC and MSC is that in SIC only one syringe is employed; this means that there can be only one mobile phase. In MSC, a multisyringe module is used which makes the system more versatile and allows to use more than one mobile phase in the process, as well as sample injection and derivatization strategies. Other features of the multisyringe module are its robustness and the use of aggressive fluids [23]. MSC has been used to determine different analytes such vitamins [24], phenolic pollutants [25], pharmaceutical residues [26,27].

In chromatographic processes, a large number of factors could be influential when separating analytes. Experimental designs are useful for optimizing processes involving a high number of factors [28]. In most of the papers consulted, the optimal conditions for separating the dyes were obtained by varying one factor at a time without taking into account the possible interactions between factors. Recently, experimental designs have been proposed for use in HPLC [29-32], but have only been used to optimize SIC or MSC methodologies in a few cases [24].

After determining the acceptable initial conditions that allow the elution of the three dyes, we have used experimental design methodologies to find the optimal conditions for separating these three dyes. The usual strategy, when there is an elevated number of factors to consider, is to design an experimentation to screen the various factors (Plackett-Burman or saturated fractionated factorial designs), these being the methodologies with the lowest experimental cost. Moreover, in these strategies it must be assumed that the interactions between two or more factors have no effect on the response. Consequently, these kinds of designs can lead to erroneous conclusions.

Confusion between the factors and the interactions can be avoided by optimizing the process through the performance of sequentially different full factorial designs. This experimentation determines the effect of each factor and each interaction. In this case a first full factorial design is built which contains 3 or 4 of the most basic factors. On the basis of the results obtained from this first design, a second design is constructed which uses other factors or which rescales some of the factors because they may have varied over inappropriate ranges.

To our knowledge, no studies have yet reported the use of SIC or MSC methodologies to determine sulphonated azo dyes.

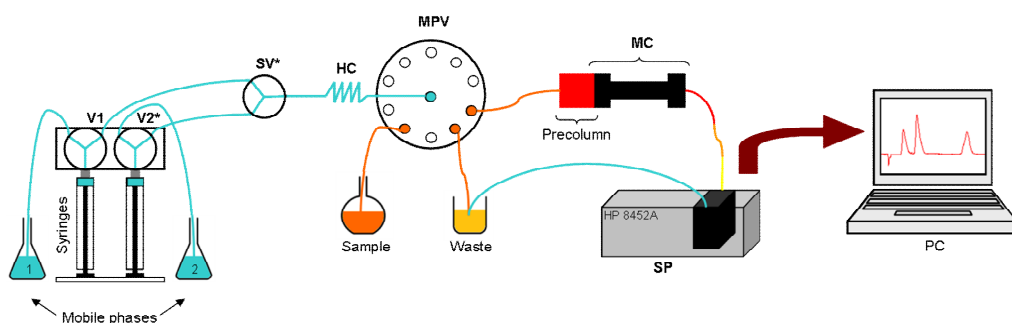
## **2. Experimental**

### **2.1. Apparatus**

The proposed multisyringe liquid chromatography (MSC) system (Fig. 1) used a multisyringe burette module (MSP; CRISON, Alella, Spain), equipped with two 5 mL high precision bidirectional syringes and one additional MTV-3-N1/4UKG solenoid valve (Takasago, Japan) that can endure pressures up to 600 kPa without damage. The manifold was constructed with 0.8 mm i.d. poly(tetrafluoroethylene) (PTFE) tubing. The chromatographic separation was done on a Phenomenex Onyx Monolithic C18 silica-based monolithic column (25 mm x 4.6 mm) protected with a guard cartridge Phenomenex Onyx C18 (5 mm x 4.6 mm). A Hewlett Packard 8453 diode array spectrophotometer equipped with a flow-through quartz cell (Hellma,

18  $\mu\text{L}$  inner volume, 10 mm path length) was used as detector. Measurements were recorded from 220 to 720 nm, with correction at 720 nm in order to minimize the effect of changes in the refractive index (Schlieren effect). The sample volume was of 50  $\mu\text{L}$ .

The software package AutoAnalysis 5 (Sciware, Spain) was used to control the instruments, to obtain the data and to process the chromatographic results. Statistical calculations have been performed by MS-Excel.



V1 and V2: Syringe valves; SV: external solenoid valve; HC: holding coil of 3 ml capacity; MPV: multiposition valve; Precolumn (5 x 4.6 mm); MC: Monolithic column (25 x 4.6 mm); SP: Spectrophotometer.

\* V2 and SV are added to the system when a second phase mobile is necessary.

**Fig. 1.** Multisyringe chromatography (MSC) system.

## 2.2. Reagents and samples

Acid Yellow 23 and Acid Yellow 9 were purchased from Sigma-Aldrich. Acid Red 97 was obtained from Trumpler Española, S.A. (Barberà del Vallès, Barcelona, España). Fig. 2 shows the molecular formula and the spectra at 30  $\text{mg}\cdot\text{L}^{-1}$  for each dye. All dyes were used without further purification. Stock solutions of 500  $\text{mg}\cdot\text{L}^{-1}$  were prepared in distilled water purified by passage through a Millipore system. Methanol Chromasolv® (HPLC grade, Sigma-Aldrich) and acetonitrile (HPLC-gradient grade PAI-ACS, Panreac) were used to prepare the required mobile phase. Other chemicals (acid orto-phosphoric and di-ammonium hydrogen phosphate) were obtained from Scharlau (Barcelona, Spain). Triethylamine hydrochloride and dodecyltrimethylammonium bromide were used as ion pair reagents and were obtained from Fluka and Across Organics respectively.

Mobile phases were filtered through 0.45  $\mu\text{m}$  Nylon membranes. Calibration standards and samples were filtered through 0.45  $\mu\text{m}$  Teflon syringe filters. We used Teflon filters instead of Nylon filters to prevent the sulphonated azo dyes from adsorbing in the filters. Mobile phases as well as standards and samples were degassed for 10 min in an ultrasonic bath. Spiked samples were prepared in tap water, well water and lagoon water from a biological wastewater treatment station.

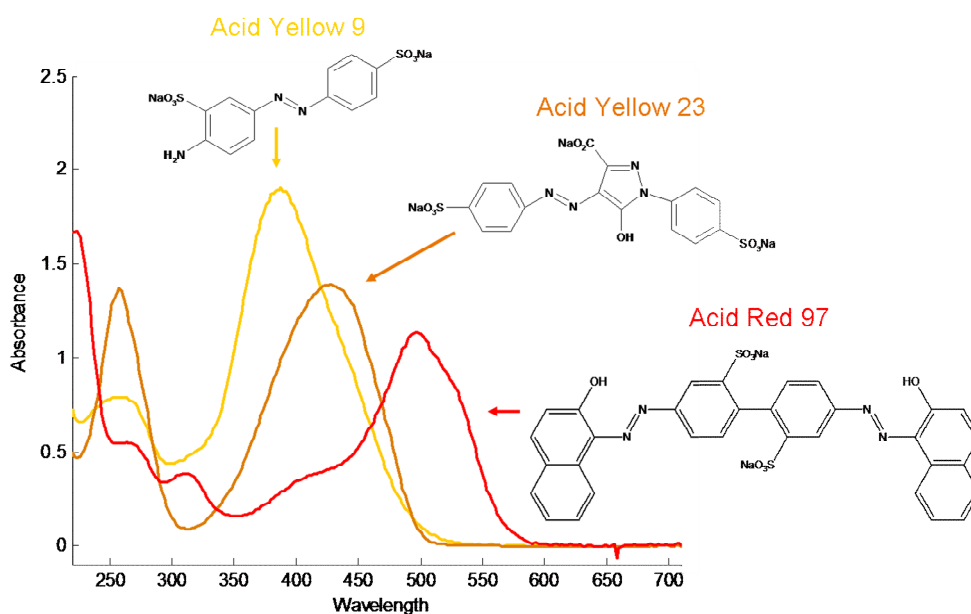


**Fig. 2.** Spectra and molecular formula of the studied dyes.

## 2.3. Procedure

### 2.3.1. Chromatographic aspects

Usually the chosen mobile phase in ion pairing chromatography is water/methanol, but methanol can cause overpressure problems with the monolithic column due its high viscosity (0.59 cP at 25°C, compared with 0.38 of acetonitrile or 0.894 cP of water), for this reason we used a mixture of acetonitrile/methanol as the organic part in the mobile phase in order to decrease the viscosity. We use a phosphate buffer (acid orthophosphoric and di-ammonium hydrogen phosphate) in order to control the pH of the mobile phase.

An ion pair reagent is needed to retain the compounds because of their ionic character and their low affinity with the C18 monolithic column. We have studied how the dye retention behaves with different amounts of a small ternary ammonium salt (triethylamine hydrochloride) and a voluminous quaternary ammonium salt (dodecyltrimethylammonium bromide).

Before starting the analysis of the factors with the experimental design, certain variables were fixed that were thought not to have a determinant effect on dye separation. Thus, the sample volume was fixed at 50  $\mu\text{l}$  because this provides enough sensitivity to determine the dyes and because smaller volumes are less reproducible when a multisyringe is employed to inject the sample. The flow rate was fixed at 1  $\text{mL}\cdot\text{min}^{-1}$ . Major fluxes produce problems of overpressure when the proportion of methanol is increased in the mobile phase.

Every day the column and precolumn were preconditioned with 5 mL of a 0.01% triethylamine solution in water to prevent the dyes irreversibly adsorbing to the residual silanol groups on the bonded silica surface [3].

### **2.3.2. Experimental design aspects**

Firstly, a  $2^3$  full factorial experimental design was built, in which the factors considered were the percentage of acetonitrile in the organic phase, the percentage of aqueous phase in mobile phase and the type of ion pair reagent. Multisyringe chromatography (MSC) with only one syringe and mobile phase were used because this is the simplest configuration.

The results obtained in the first experimental design showed that a second mobile phase was needed to elute red dye in a shorter time; for this reason a second syringe was added to the multisyringe with the aim of dispensing this second mobile phase. We decided to use a multiisocratic mode instead of a gradient mode due to the different composition of the two mobile phases. A second  $2^3$  full factorial design was created which included new factors as well as the most influential factors of the first design. Together these were the % of acetonitrile in mobile phase, the pH and the concentration of ion pair reagent. This design was used to finally select the best conditions for separating the three dyes.



In all the experiments of both experimental designs, a standard  $10 \text{ mg}\cdot\text{L}^{-1}$  solution of each dye was injected in the system. The chromatograms were showed at  $\lambda=460 \text{ nm}$  because at this wavelength, all of the studied dyes gave a signal with a correction wavelength of  $720 \text{ nm}$  that minimized the effect of changes in the refractive index (Schlieren effect).

### **2.3.3. Quantitative analysis**

In order to establish a calibration curve, 10 different standards were prepared in milli-Q water using different concentrations of each dye in each sample ( $5 - 50 \text{ mg}\cdot\text{L}^{-1}$ ). In this case the wavelength of maximum sensitivity for each dye ( $392 \text{ nm}$  for Acid Yellow 9,  $428 \text{ nm}$  for Acid Yellow 23,  $500 \text{ nm}$  for Acid Red 97) was used for quantification. The peak area was used as the analytical signal. Each dissolution was repeated twice and an ANOVA regression test was used to validate the resulting calibration curve [33]. The concentration values of the calibration standards are shown in the first 10 rows of Table 1. As can be seen, different concentrations of each dye have been selected in each standard, all within the linearity range, because the calibration curves include all possible circumstances, for example, dyes that are present in the same concentrations or dyes that are present in high or low concentrations. Repetitions of standard 1, which corresponds to the standard containing  $10 \text{ mg}\cdot\text{L}^{-1}$  of each dye, were done at different days in order to calculate the reproducibility and repeatability of the methodology.

All calibration standards were prepared from a concentrated standard of  $500 \text{ mg}\cdot\text{L}^{-1}$  of each dye in milli-Q water, the corresponding solutions being diluted with the first mobile phase used in the corresponding elution.

In order to validate the method, we used spiked real water samples (tap water, well water and lagoon biological wastewater). These samples were prepared in the same way as the standards, that is, different quantities of each dye were spiked in each kind of water sample instead of in milli-Q water. The real water was checked beforehand to ensure it did not contain any of the studied dyes. The spiked concentrations in the real samples are shown in the last three rows of Table 1. The concentration levels selected are in according to the dye concentrations obtained in industry during and after the tanning process. Usually, these

concentrations are higher from 30 to more than 100 mg·L<sup>-1</sup> [13] and a dilution step is necessary before analytical determination.

**Table 1.** Concentration of calibration standards and real samples (mg·L<sup>-1</sup>).

Number	Acid Yellow 9	Acid Yellow 23	Acid Red 97
1	10	10	10
2	40	20	20
3	10	5	40
4	30	30	10
5	20	40	25
6	5	5	50
7	10	40	5
8	50	30	40
9	25	25	30
10	30	50	20
S1 <sup>a</sup>	20	35	20
S2 <sup>a</sup>	25	10	10
S3 <sup>a</sup>	10	15	25

<sup>a</sup> Spiked concentration in real water samples

### 3 Results

#### 3.1. Experimental design

As has been stated, the first experiments were carried out using only one syringe in the multisyringe module working in isocratic mode. The factors studied in the first full factorial design were the percentage of water in the mobile phase, the percentage of acetonitrile in the organic phase formed by methanol and acetonitrile and the type of ion pair reagent (dodecyltrimethylammonium bromide or triethylamine hydrochloride). All of the experiments were carried out at pH = 7.5. The responses studied were qualitative (separation or not of the two yellow dyes and elution or not of red dye).

Table 2 shows the 8 experiments in this 2<sup>3</sup> experimental design. It can be seen that triethylamine hydrochloride as ion pair reagent does not allow to separate yellow dyes; instead, it is necessary to use dodecyltrimethylammonium bromide to favor the retention of these dyes in the monolithic column. Regarding experiments 3 and 4 in Table 2, it can be seen that when the mobile phase contains 50% H<sub>2</sub>O, 50% acetonitrile (100% of acetonitrile in organic phase) and

DTMA, the yellow dyes are not separated but the red dye is eluted; however, when the mobile phase contains 70% H<sub>2</sub>O, 30% acetonitrile (100% of acetonitrile in organic phase) and DTMA, the yellow dyes are completely separated but the red dye is not eluted. These results suggest that an intermediate mobile phase could separate yellow dyes and elute the red dye. We tested this hypothesis by using a mobile phase a mixture of 60% H<sub>2</sub>O and 40% acetonitrile (100% of acetonitrile in organic phase) and keeping dodecyltrimethylammonium bromide as the ion pair reagent; however, under these conditions yellow dyes were not separated and the red dye were not eluted.

**Table 2.** Experimental plan and responses of the first experimental design 2<sup>3</sup>.

Experiment	H <sub>2</sub> O	%ACN in organic phase <sup>a</sup>	Ion pair reagent	Separation of yellow dyes	Presence of red dye peak
1	50	50	DTMA	YES	NO
2	70	50	DTMA	NO	NO
3	50	100	DTMA	NO	YES
4	70	100	DTMA	YES	NO
5	50	50	TEA	NO	YES
6	70	50	TEA	NO	NO
7	50	100	TEA	NO	YES
8	70	100	TEA	NO	YES

<sup>a</sup> organic phase = methanol and acetonitrile

DTMA = Dodecyltrimethylammonium bromide

TEA = Triethylamine hydrochloride

The main conclusion of this additional experiment was that the mobile phases which allow the two yellow dyes to be separated are different from the mobile phases which elute the red dye in a reasonable time. This means that the dyes studied cannot be separated and eluted in a reasonable time if only one syringe or mobile phase is used. The use of multisyringe chromatography (MSC) allows two syringes to be used, that is, two mobile phases working in multiisocratic mode. First, we can employ one mobile phase to separate the two yellow dyes and then another different mobile phase to elute the red dye without stabilization between the two phases because monolithic columns are more tolerant of eluent switching and equilibrate more rapidly than the particle-packed columns used in HPLC.

In order to find the optimum conditions, a second full factorial 2<sup>3</sup> design was performed. According to the results obtained in the previous step, the initial

factors were fixed as follows: 50% water, 25% acetonitrile and 25% methanol in the first mobile phase and dodecyltrimethylammonium bromide as the ion pair reagent. The factors studied in this case were the % of acetonitrile in mobile phase 2 formed by a mixture of water/acetonitrile, the pH of both mobile phases, and the concentration of ion pair reagent in both mobile phases. This second design is described in Table 3, which shows the experimental plan in its three first columns and the quantitative responses obtained (the resolution between two peaks corresponding to yellow dyes and the analysis time) in its last two columns.

**Table 3.** Experimental plan and responses of the second experimental design 2<sup>3</sup>.

Experiment	% ACN in phase 2	pH	Ion pair concentration (mM)	Resolution between yellow dye peaks	Retention time of red dye (s)
1	50	4	5	0.78	345
2	70	4	5	0.29	234
3	50	7.5	5	0.29	357
4	70	7.5	5	0.44	242
5	50	4	15	1.47	468
6	70	4	15	1.14	256
7	50	7.5	15	1.34	487
8	70	7.5	15	1.04	244

This experimental design allowed us to select the best conditions for separating and determining these dyes. Table 3 shows that experiments 5 and 7 give good resolution values between the peaks corresponding to yellow dyes and the analysis time is similar in both experiments. Any of these experiments could be used to separate the three dyes but in our case we chose experiment 5 because it has the highest resolution value between the two first peaks, specifically 1.47, and because the red dye was eluted in a shorter analysis time, specifically 468 s. A chromatogram obtained from this is shown in Fig. 3. This figure shows that the three dyes could be completely and perfectly separated in less than 8 min. The first dye to elute to the monolithic column is Yellow 9, followed by Yellow 23 in second place and Acid Red 97 last of all.

The operating sequence for multisyringe liquid chromatographic separation is summarized in Table 4, where details of multisyringe burette motion, positions of the selection valve, syringe valves and the external solenoid valve are given along with the corresponding consumption of the mobile phases and the sample.

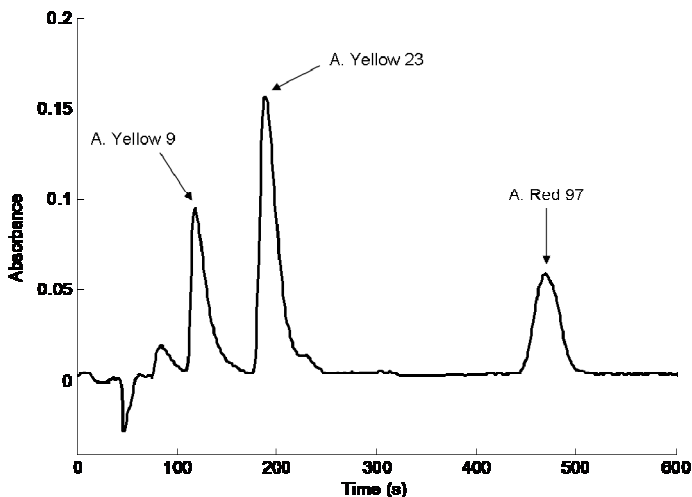


**Fig. 3.** Chromatogram obtained with the optimal conditions.

**Table 4.** Operating sequence for MSC separation.

Operation		Flow rate (mL·min <sup>-1</sup> )	V1	V2	VS	Observations
MSP	Dispense 4000 µl	1	On	Off	Off	Pre-conditioning of the system
SP	Measure Blank					
MSP	Aspirate 3000 µl	2,5	Off	Off	Off	
MPV	Move to position 8					
MSP	Aspirate 200 µl	2,5	On	Off	Off	Loading of sample
MPV	Move to position 3					
MSP	Dispense 1000 µl	2,5	On	Off	Off	
MSP	Aspirate 1750 µl	2,5	Off	Off	Off	
MPV	Move to position 8					
MSP	Aspirate 50 µl	1	On	Off	Off	
MPV	Move to position 1					
SP	Get spectral range from 220 to 720 nm					Data Acquisition
MSP	Multicommutation protocol HC*	1	On	Off	Off	
	500 µl phase 1 + 9500 µl phase 2	1	Off	On	On	
SP	Stop measurement					

V1: syringe valve corresponding to mobile phase 1; V2: syringe valve corresponding to mobile phase 2; VS: external solenoid valve; MSP: multisyringe pump; MPV: multiposition valve; SP: spectrophotometer; Position 8 corresponds to the sample; Position 3 corresponds to waste; Position 1 corresponds to monolithic column.

\*HC: Holding coil contains 3 mL of phase A

### 3.2. Calibration and validation in real samples

Table 5 shows the figures of merit for the calibration curves obtained for each dye. All of the curves pass the ANOVA regression test. The detection limit was calculated with 95% of confidence whilst taking into account the uncertainty in the regression line [33]. The repeatability, as standard deviation, was evaluated by performing ten replicate measurements in a mixture of 10 mg·L<sup>-1</sup> of each dye. Reproducibility was calculated as the standard deviation of a solution with 10 mg·L<sup>-1</sup> of each dye on 8 different days (3 replicates per day). The values of reproducibility and repeatability are satisfactory taking into account the simply configuration employed (a syringe) to inject the sample.

**Table 5.** Figures of merit for the calibration curves of each dye.

	Acid Yellow 9	Acid Yellow 23	Acid Red 97
Interval range (mg·L <sup>-1</sup> )	5 – 50	5 – 50	5 – 50
Wavelength	392	428	500
Slope (sd <sup>a</sup> )	0.55 (0.01)	0.43 (0.01)	0.3
Intercept (sd <sup>a</sup> )	0.69 (0.28)	0.01 (0.29)	0.04 (0.20)
Standard deviation of residuals	0.64	0.65	0.43
R	0.9969	0.9954	0.9957
N	20	20	20
ANOVA, F <sub>cal</sub> <sup>b</sup>	1.48	2.41	2.38
Detection limit (mg·L <sup>-1</sup> )	1.75	2.30	2.19
Reproducibility <sup>c</sup> (RSD%, 10 mg·L <sup>-1</sup> )	4.0	2.7	3.3
Repeatability <sup>d</sup> (RSD%, 10 mg·L <sup>-1</sup> )	3.7	2.4	3.0

<sup>a</sup> sd: standard deviation

<sup>b</sup> F<sub>tab</sub>(0.05,8,18) = 3.03

<sup>c</sup> 8 days

<sup>d</sup> 10 repetitions

To validate this methodology in real samples, we used tap water, well water and lagoon biological wastewater spiked with different concentrations of the selected dyes. Specifically, we determined these dyes in nine samples, three for each kind of water, spiked with different concentrations of Acid Yellow 9, Acid Yellow 23 and Acid Red 97 (see Table 1).

In order to validate the results obtained with the real samples a regression line was established representing the spiked concentrations versus the concentrations predicted with the MSC methodology. This line was then compared

using a join test with the following line of identity: regression slope=1, regression intercept=0 [33].

All the dyes passed the test for all the water samples with a significance level  $\alpha=0.05$  except Acid Yellow 23 in lagoon biological wastewater, which passed the test with a significance level  $\alpha=0.015$ . Fig. 4 shows the spiked concentration versus the predicted concentration of the studied dyes in the well water samples.

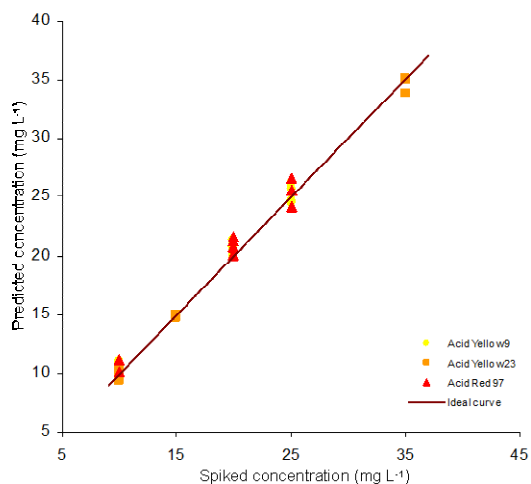


Fig.4. Validation curve for well water samples.

#### 4. Conclusions

The proposed MSC system is simpler, more versatile and cheaper than HPLC when the samples are fairly simple, as is the case in our study. It can be regarded as a low pressure alternative to HPLC and it could be a very attractive technique for improving selectivity in flow analytical systems (FIA and SIA). Moreover, back-pressure was not a limiting factor in MSC.

MSC allowed us to use similar flow-rates to those in HPLC under the same conditions. Therefore, special benefit can be derived from combining flow techniques with monolithic columns when carrying out low-cost chromatographic separations of azo dyes in polluted water samples. Another significant advantage of using MSC is its great flexibility in manifold configuration. If necessary in the

future, an on-line pretreatment of the sample can be carried out using a multisyringe with a solid phase extraction cartridge to extract and preconcentrate sulphonated azo dyes from water samples.

The application of experimental designs allowed us to use a smaller number of experiments and qualitative responses to optimize the separation of the three sulphonated azo dyes (Acid Yellow 9, Acid Yellow 23 and Acid Red 97). The use of this strategy can determine the influence of each factor (pH, mobile phase, ion pair reagent, etc.) and thus simplify the experiment because the separation behaviour could be predicted when the value of the factors is changed. This provides a collection of quality chromatograms that can be used for the further quantification of the analytes.

Using the experimental design has clearly proven that the three target compounds cannot be separated with one single syringe or mobile phase. These compounds can, nevertheless, be completely separated using ion pair multiisocratic MSC with two mobile phases. This methodology has been validated in real samples (tap water, well water and water from a lagoon in a biological wastewater treatment station) and in all cases good results were obtained.

### Acknowledgements

The authors would like to thank Trumpler Española, S.A., for supplying the Acid Red 97 dye and the Spanish Ministry of Science and Innovation (Project CTQ2007-61474/BQU) for economic support and for providing Cristina Fernández with a doctoral fellowship (AP2007-03788).

### References

- [1] T. Storm, T. Reemtsma, M. Jekel, *J. Chromatogr. A* 854 (1999) 175–185.
- [2] J. Riu, I. Schönsee, C. Ràfols, D. Barceló, *Trends Anal. Chem.* 16 (1997) 405-419.
- [3] A.P. Bruins, L.O.G. Weidolf, J.D. Henion, *Anal. Chem.* 59 (1987) 2647-2652.
- [4] D. Vanerková, P. Jandera, J. Hrabica, *J. Chromatogr. A* 1143 (2007) 112-120.
- [5] M.R. Fuh, K.J. Chia, *Talanta* 56 (2002) 663-671.
- [6] M. Pérez-Urquiza, M.D. Prat, J.L. Beltrán, *J. Chromatogr. A* 871 (2000) 227-234.



- [7] M. Holcapek, P. Jandera, P. Zderadicka, *J. Chromatogr. A* 926 (2001) 175-186.
- [8] J. Riu, I. Schönsee, D. Barceló, *J. Mass. Spectrom.* 33 (1998) 653-663.
- [9] M. Pérez-Urquiza, R. Ferrer, J.L. Beltrán, *J. Chromatogr. A* 883 (2000) 277-283.
- [10] E.R. Cunha, M.F. Alpendurada, *J. Liq. Chromatogr. Relat. Technol.* 25 (2002) 1835-1854.
- [11] T. Poiger, S.D. Richardson, G.L. Baughman, *J. Chromatogr. A* 886 (2000) 271-282.
- [12] Y.S. Al-Degs, A.H. El-Sheikh, M.A. Al-Ghouti, B. Hemmateenejad, G.M. Walker, *Talanta* 75 (2008) 904-915.
- [13] V. Gómez, J. Font, M.P. Callao, *Talanta* 71 (2007) 1393-1398.
- [14] C. Fernández, M.S. Larrechi, M.P. Callao, *Talanta* 79 (2009) 1292-1297.
- [15] S.D. Chambers, K.M. Glenn, C.A. Lucy, *J. Sep. Sci.* 30 (2007) 1628-1645.
- [16] J. L. Adcock, P.S. Francis, K.M. Agg, G.D. Marshall, N.W. Barnett, *Anal. Chim. Acta* 600 (2007) 136-141.
- [17] P. Chocholous, P. Solich, D. Satínský, *Anal. Chim. Acta* 600 (2007) 129-135.
- [18] P. Chocholous, P. Holík, D. Satínský, P. Solich, *Talanta* 72 (2007) 854-858.
- [19] P. Chocholous, D. Satínský, P. Solich, *Talanta* 70 (2006) 408-413.
- [20] J. Huclová, D. Satínský, R. Karlíček, *Anal. Chim. Acta* 494 (2003) 133-140.
- [21] P. Chocholous, D. Satínský, R. Sladkovský, M. Pospíšilová, P. Solich, *Talanta* 77 (2008) 566-570.
- [22] V. Gómez, M. Miró, M.P. Callao, V. Cerdà, *Anal. Chem* 79 (2007) 7767-7774.
- [23] M. Fernandez, H.M. González-San Miguel, J.M. Estela, V.Cerdà, *Trends Anal. Chem.* 28 (2009) 336-346.
- [24] M. Fernandez, M. Miró, H.M. González, V. Cerdà, *Anal. Bioanal. Chem.* 391 (2008) 817-825.
- [25] H.M. Oliveira, M.A. Segundo, J.L.F.C. Lima, V. Cerda, *Talanta* 77 (2009) 1466-1472.
- [26] M.A. Obando, J.M. Estela, V. Cerda, *J. Pharm. Biomed. Anal.* 48 (2008) 212-217.
- [27] H.M. González-San Miguel, J.M. Alpizar-Lorenzo, V. Cerdà, *Talanta* 72 (2007) 296-300.
- [28] D.C. Montgomery, *Design and Analysis of Experiments*, John Wiley&Sons, New York, 1997.
- [29] J.F. Huertas-Pérez, A.M. García-Campaña, *Anal. Chim. Acta* 630 (2008) 194-204.
- [30] P. Barmpalexis, F.I. Kanaze, E. Georganakis, *J. Pharm. Biomed. Anal.* 49 (2009) 1192-1202.
- [31] R. Gheshlaghi, J.M. Scharer, M. Moo-Young, P.L. Douglas, *Anal. Biochem.* 383 (2008) 93-102.
- [32] K. Vuievi, G. Popovi, K. Nikolic, I. Vovk, D. Agbaba, *J. Liq. Chromatogr. Relat. Technol.* 32 (2009) 656-667.
- [33] D.L. Massart, B.G.M. Vandeginste, et al., *Handbook of Chemometrics and Qualimetrics Part A*, Elsevier, Amsterdam, 1997.

## **4. GENERAL CONCLUSIONS**



UNIVERSITAT ROVIRA I VIRGILI

ANALYTICAL METHODOLOGIES BASED ON CHEMOMETRICS TO OPTIMIZE THE PHOTODEGRADATION OF DYES

Cristina Fernández Barrat

DL:T. 160-2012

## 4. CONCLUSIONS

This chapter summarizes the general conclusions of the work presented in this doctoral thesis. Specific conclusions have been drawn at the end of each of the papers in chapter 3.

Experimental designs and chemometric treatment of UV-visible spectra obtained by the photodegradation of azo dyes gave rise to analytical methodologies that are in agreement with the principles that define green chemistry. These methodologies can be extrapolated to solve other problems pertaining to the removal of other contaminants from the same or different samples.

The specific objectives described in chapter 1 and the conclusions that can be drawn are the following:

*(a) To prepare a critical overview of the processes that are currently available for removing organic dyes and of the most common techniques for monitoring these processes.*

This bibliographic work made it possible to detect the weak and strong points of research into the removal of organic dyes from industrial wastewater samples. The aspects that needed to be developed and which were related to our field of research were identified, a necessary first step if the remaining objectives were to be achieved.

*(b) To establish methodologies that use second order data treatment for the simultaneous analysis of more than one component throughout photodegradation processes.*

The application of MCR-ALS to the data obtained with UV-visible spectrophotometry during simultaneous photodegradation processes of various components allows their quantitative control along the time. This methodology is an alternative to separation techniques because it is quick

and cheap. It can provide information about the behavior of each dye and the reaction intermediates, which is not provided when such simpler approaches as univariate monitoring are used in this kind of study.

*(c) To use experimental design methodologies to study the influence of the variables in photodegradation processes and to optimize these processes.*

A experimental strategy was established that consists of screening variables, which made it possible to study a high number of variables at little experimental cost. From the screening results, a few of the most influential variables were selected and the experimental domain was adapted to the optimal response zone (high degradation efficiency). Finally a response surface was established that enabled the response for a selected value of the variables to be predicted and/or the value of particular experimental conditions to be decided for a pre-set response.

*(d) To establish methodologies for studying the degradation kinetics (degradation constants and/or degradation intermediates) that are based on the multivariate data obtained throughout dye photodegradation processes.*

Two different methodologies based on hybrid hard- and soft- multivariate curve resolution with alternating least squares (HS-MCR-ALS) were developed to study the kinetics of photodegradation processes. It can be concluded that:

- By comparing the degradation rate values of the steps involved in this process, the risk of assuming that the kinetics of the dye photodegradation can be analyzed without taking the pathway of the process into account can be evaluated. In our particular study the intermediates degraded at a degradation rate that was similar to that of the initial dye, but this may not occur in other cases. This shows that multivariate approaches need to be considered if the conditions of the photodegradation process are to be optimal.

- Although the adsorption constant is lower than the rate constant, it needs to be taken into account in the analysis of the influence of the process variables and in the study of the photocatalytic degradation mechanism.

*(e) To develop rapid methodologies based on sequential injection chromatography (SIC) for determining dyes.*

A methodology based on multisyringe chromatography (MSC) was developed to determine three sulphonated azo dyes. This methodology is an advance for dye determination because it can be a good alternative to high-pressure chromatographic techniques: it consumes few reagents and generates little waste, and is, therefore, low-cost and environmentally friendly.

UNIVERSITAT ROVIRA I VIRGILI

ANALYTICAL METHODOLOGIES BASED ON CHEMOMETRICS TO OPTIMIZE THE PHOTODEGRADATION OF DYES

Cristina Fernández Barrat

DL:T. 160-2012

## **APPENDIX**





UNIVERSITAT ROVIRA I VIRGILI

ANALYTICAL METHODOLOGIES BASED ON CHEMOMETRICS TO OPTIMIZE THE PHOTODEGRADATION OF DYES

Cristina Fernández Barrat

DL:T. 160-2012

---

### List of papers by the author presented in this thesis

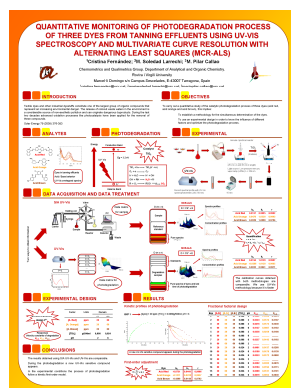
1. Cristina Fernández, M. Soledad Larrechi, M. Pilar Callao. *Study of the influential factors in the simultaneous photocatalytic degradation process of three textile dyes*, Talanta 79 (2009) 1292-1297.
2. Cristina Fernández, M. Soledad Larrechi, M. Pilar Callao. *Modelling of the simultaneous photodegradation of Acid Red 97, Acid Orange 61 and Acid Brown 425 using factor screening and response surface strategies*, Journal of Hazardous Materials 180 (2010) 474-480.
3. Cristina Fernández, M. Soledad Larrechi, R. Forteza, V. Cerdà, M. Pilar Callao, *Multisyringe chromatography (MSC) using a monolithic column for the determination of sulphonated azo dyes*, Talanta 82 (2010) 137-142.
4. Cristina Fernández, M. Soledad Larrechi, M. Pilar Callao. *An analytical overview of processes for removing organic dyes from wastewater effluents*, Trends in Analytical Chemistry 29 (2010) 1202-1211.
5. Cristina Fernández, M. Pilar Callao, M. Soledad Larrechi, *Kinetic analysis of C.I. Acid Yellow 9 photooxidative decolorization by UV-visible and chemometrics*, Journal of Hazardous Materials 190 (2011) 986-992.
6. Cristina Fernández, Anna de Juan, M. Pilar Callao, M. Soledad Larrechi, *The evaluation of the adsorption and rate constants of the photocatalytic degradation of C.I. Acid Yellow 9 by means of HS-MCR-ALS: a study of process variables*, Submitted.

### List of papers by the autor not presented in this thesis

Cristina Fernández, J. M. Amigo, R. Bro, M. Pilar Callao, M. Soledad Larrechi, *Study of the concentration effect on the efficiency of the simultaneous photodegradation of three azo dyes by PARAFAC*.

In preparation

## Contributions to international meetings



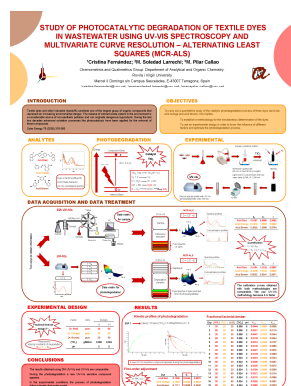
*Quantitative monitoring of photo-degradation process of three dyes from tanning effluents applying MCR-ALS to the UV-visible spectra obtained using a SIA methodology*

Cristina Fernández, M. Soledad Larrechi, M. Pilar Callao

11th International Conference on Chemometrics for Analytical Chemistry (CAC)

Montpellier (France, 2008)

Poster communication



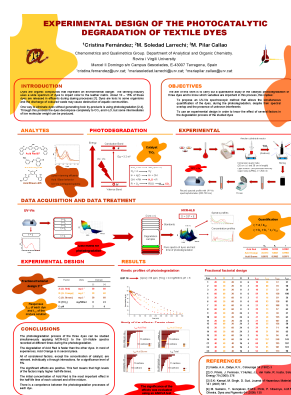
*Study of photocatalytic degradation of textile dyes in wastewater using UV-Vis spectroscopy and multivariate curve resolution - alternating least squares (MCR-ALS)*

Cristina Fernández, M. Soledad Larrechi, M. Pilar Callao

III Workshop de Quimiometría

Burgos (Spain, 2008)

Poster and Flash communication

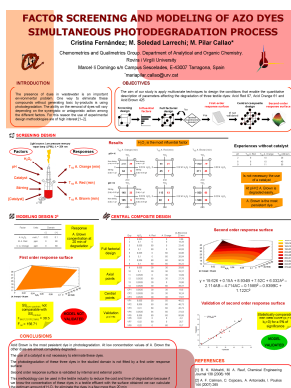


*Experimental design of the photocatalytic degradation of textile dyes*

Cristina Fernández, M. Soledad Larrechi, M. Pilar Callao

XII Jornadas de Análisis instrumental (JAI) Barcelona (Spain, 2008)

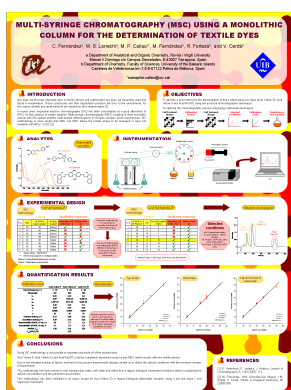
Poster communication



*Factor screening and modeling of azo dyes simultaneous photodegradation process*

Cristina Fernández, M. Soledad Larrechi, M. Pilar Callao

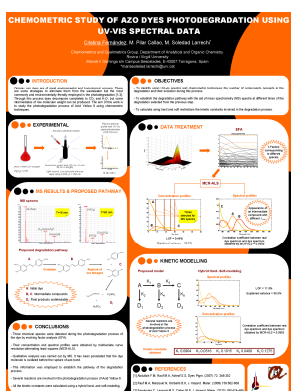
XV Reunión de la Sociedad Española de Química Analítica  
San Sebastián (Spain, 2009)  
Poster Communication



*Multi-syringe chromatography (MSC) using a monolithic column for the determination of textile dyes*

Cristina Fernández, M. Soledad Larrechi, M. Pilar Callao,  
M. Fernández, R. Forteza, V. Cerdà

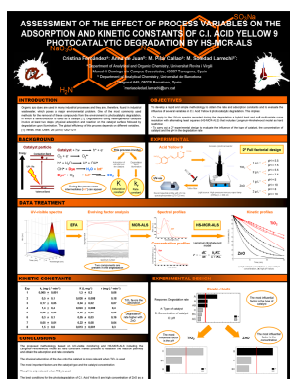
XI Flow análisis  
Pollença (Spain, 2009)  
Poster Communication



*Chemometric study of azo dyes photodegradation using UV-Vis spectral data*

Cristina Fernández, M. Pilar Callao, M. Soledad Larrechi

VII Colloquium Chemiometricum Mediterraneum  
Granada (Spain, 2010)  
Poster communication



*Assessment of the effect of process variables on the adsorption and kinetic constants of C.I. Acid Yellow 9 photocatalytic degradation by HS-MCR-ALS*

Cristina Fernández, Anna de Juan, M. Pilar Callao, M. Soledad Larrechi

XIII Jornadas de Análisis instrumental (JAI)

Barcelona (Spain, 2011)

Poster communication

*The evaluation of the adsorption and rate constants of the photocatalytic degradation of C.I. Acid Yellow 9 by means of HS-MCR-ALS: a study of process variables process variables*

Cristina Fernández, Anna de Juan, M. Pilar Callao, M. Soledad Larrechi

IV Workshop de Quimiometría

A Coruña (Spain, 2011)

Oral communication

## Research stays

### 1. Palma de Mallorca (May – July 2009)

Objective: To develop analytical methodologies based on sequential injection chromatography (SIC) to determine organic azo dyes in wastewater samples.

Analytical Chemistry, Automation and Environment group

Department of Chemistry

Faculty of Sciences

University of the Balearic Islands (UIB)

Supervised by Dr. Victor Cerdà and Dr. Rafel Forteza

### 2. Copenhagen (April – June 2011)

Objective: To develop analytical methodologies to study degradation processes of different azo dyes based on the application of PARAFAC to the UV-visible data obtained throughout these processes.

Quality and Technology group

Department of Food Science

Faculty of Life Sciences

University of Copenhagen

Supervised by Dr. Rasmus Bro

UNIVERSITAT ROVIRA I VIRGILI

ANALYTICAL METHODOLOGIES BASED ON CHEMOMETRICS TO OPTIMIZE THE PHOTODEGRADATION OF DYES

Cristina Fernández Barrat

DL:T. 160-2012